Aneuploidy in pancreatic intraepithelial neoplasia.

Morhan, Alina Raluca

Aneuploidy in pancreatic intraepithelial neoplasia

Alina Raluca Morhan MD MRCSEd

Submitted to the University of Wales
in fulfilment of the requirements
for the Degree of Doctor of Medicine

Swansea University

2015

Abstract

Pancreatic ductal adenocarcinoma has one of the most unfavourable prognoses and survival patterns. Pancreatic intraepithelial ductal neoplasias (PanINs) 1-3 are microscopic precursors which display genetic and epigenetic changes leading to adenocarcinoma. We investigated the chromosomal numeric changes for chromosomes 1, 6, 9 and 18 using fluorescence in situ hybridization in the progressing intraepithelial neoplasias and the corresponding tumours. We also assessed the protein levels for mitotic checkpoint proteins Mad2 and BubR1 using immunohistochemistry and applied correlation models to derive potential significant correlations to chromosome numeric anomalies and clinicopathological parameters. The results revealed that, for the chromosomes included in the study, the average numeric anomalies (aneuploidy) increases with the advancing histological stage. Moreover, the extra copy anomalies (amplifications) were significantly higher in the final precancerous stage (PanIN 3) and/or the cancer stage (p-value<0.05). The protein levels for Mad2 and BubR1 did not show a direct correlation to the aneuploidy levels but that could be due to the diversity of the individual tumour makeup and the limited specimens included in the analysis. In the current trend towards personalized genetic therapy for aggressive tumours, the aneuploidy levels and the mitotic checkpoint protein levels could potentially be incorporated in a panel of biomarkers used to predict prognoses and survival patterns.

Acknowledgments

I would like to thank The College of Medicine at Swansea University for approving this project and providing part of the funding. I am also grateful to The Research and Development department at the ABMU Health Board Swansea for their financial support. I extend my special thanks to Professor Gareth Jenkins for his unfailing patience and expert guidance, to Mr. Bilal Al-Sarireh, Consultant Hepatobiliary Surgeon, for making this project a launching pad for further pancreatic work, to Dr. Paul Griffiths, Consultant Histopathologist, for his inspiring dedication and precision and to Dr. Shareen Doak, Senior Lecturer, for her expert insight and practical tutoring. Also, I would like to thank Mrs. Margaret Clatworthy and Mrs. Sally James, laboratory technicians for their guidance and support and the team in The Institute of Science, floor 4, for inspiring team values and high standards. Special thanks go to Mrs. Lynda Hopkins, Senior Manager, Cellular Pathology, NHS Wales, and her team in the Graduate Entry Pathology Laboratory, Singleton Hospital, for overseeing the laboratory work and for allowing me to use their facilities and benefit from their expertise. I also thank Dr. Owen Bodger for his guidance on advanced statistical analysis. Last but not least, heartfelt thanks go to my brother, Codrin Morhan, Computer Science graduate of Swansea University, for his hard work and dedication towards the typesetting of this thesis.

Contents

List of Tables

List of Figures

List of Abbreviations

17-AAG	17-N-allylamino-17-demethoxygeldanamycin
AICAR	5-Aminoimidazole-4-carboxamide ribonucleotide
AJCC	The American Joint Committee on Cancer
AMPK	AMP-dependent-protein-kinase
ANOVA	analysis of variance between groups
APC/C	anaphase-promoting complex / cyclosome
BIC	Bayesian information criterion
BubR1	budding uninhibited by benomyl related-1
CA19-9	cancer antigen 19-9
Cdc 20	cell-division cycle protein 20
CEA	carcinoembryonic antigen
CEP	chromosome enumeration probes
CGH	comparative genomic hybridization
CIN	chromosomal instability
CISH	chromogenic in situ hybridization
CI	confidence interval
DAPI	4′, 6-diamidino-2-phenylindole
DNA	deoxyribonucleic acid
EGFR	epithelial growth factor receptor
ERCP	endoscopic retrograde cholangiopancreatography
EUS	endoscopic ultrasound

FFPE	formalin-fixed paraffin embedded
FISH	fluorescence in situ hybridization
G1	Gap Stage 1
G2	Gap Stage 2
GTP	guanosine triphosphate
HCl	hydrogen chloride
Her2	human epidermal growth factor receptor 2
HE	haematoxylin and eosin
HR	hazard ratio
Hsp90	heat shock protein 90
IHC	immunohistochemistry
IMS	Industrial Methylated Spirits
IPMN	intraductal pancreatic mucinous neoplasm
ITPN	intraductal tubulopapillary neoplasm
KRAS	v-Ki-ras2 Kirsten rat sarcoma viral oncogene homolog
LMM	Linear Mixed-Effect models
LNR	lymph node ratio
LOH	loss of heterozygosity
LSI	locus-specific indicator probes
M-FISH	multiplex fluorescence in situ hybridization
Mad2	mitotic arrest deficient 2
MCC	mitotic checkpoint complex
MCN	mucinous cystic neoplasm
microRNA	micro (small non-encoding) Ribonucleic acid
MRCP	magnetic retrograde cholangiopancreatography
NCCN	The National Comprehensive Cancer Network

p16/CDKN2A	cyclin-dependent kinase inhibitor 2A
PanIN	pancreatic intraepithelial neoplasia
PDAC	pancreatic ductal adenocarcinoma
PET-CT	positron emission tomography-computer tomography
PTC	percutaneous transhepatic cholangiography
RT	room temperature
SAC	spindle assembly checkpoint
SKY	spectral karyotyping
SMAD4/DPC4	SMAD family member 4
SSC	saline-sodium citrate
S	Synthesis Stage
TGF-β	transforming growth factor beta
TP53	tumour protein p53
UICC	The Union for International Cancer Control

Chapter 1

General Introduction

1.1 Pancreatic ductal adenocarcinoma

1.1.1 Epidemiology

Pancreatic cancer is currently the 5^{th} most common cause of cancer death and represents 5% of all deaths from cancer in the UK (2011), with equal distribution between males and females. 8320 deaths from pancreatic cancer were recorded in the UK in 2011, with a male to female ratio of 1:1. The crude mortality rate associated with pancreatic cancer is the same for the male and female population (13 cancer deaths per every 100 000 males/females). Age-specific mortality rates increase significantly for the >55 age group (11 cancer deaths per every 100 000 females and 16 cancer deaths per every 100 000 males), with the highest rates in the >85 age group (94 cancer deaths per every 100 000 females and 110 cancer deaths per every 100 000 males). The male to female ratio varies with the age group and the widest difference in age-specific mortality is for the 45-49 age group (15:10). Worldwide, pancreatic cancer is the 7^{th} most common cause of cancer death, with more than 330 000 deaths in 2012 (4% of total) (Cancer Research UK 2014). On average, 4.1 new cases are diagnosed per year per 100 000 people worldwide (Ferlay J et al., 2010). The 5-year survival rate is less than 4%. This is due to the failure to diagnose early curable disease, a pattern of aggressive dissemination and resistance to available systemic therapeutic regimens (Carpelan-Holmstrom M et al., 2005, Benson AB, 2007).

The main known risk factors are tobacco smoking, chronic pancreatitis, late-onset diabetes mellitus and increased body mass index (Ghaneh P, 2008). 10% of cases are associated with an inherited predisposition based on familial clustering (Hezel A et al., 2006).

Several genetic syndromes are associated with an increased risk for pancreatic cancer, which include:

- Hereditary breast and ovarian cancer syndrome, associated with mutations in the

BRCA2 gene.

- Familial melanoma, associated with mutations in the p16/CDKN2A gene.
- Familial pancreatitis, associated with mutations in the PRSS1 gene.
- Hereditary non-polyposis colorectal cancer (HNPCC), commonly associated with mutations in the MLH1 or MSH2 genes, but also in MLH3, MSH6, TGBR2, PMS1 and PMS2 genes.
- Peutz-Jeghers syndrome, associated with mutations in the STK11 gene.
- Von Hippel-Lindau syndrome, associated with mutations in the VHL gene (Wolfgang CL et al., 2013).

There is no population screening programme for pancreatic cancer but surveillance is recommended for patients with a strong family history, certain genetic syndromes (Peutz-Jeughers syndrome, familial atypical multiple mole melanoma, ataxia telangiectasia syndrome) and hereditary pancreatitis (Brand RE et al., 2007).

1.1.2 Anatomy and physiology

The pancreas lies posteriorly to the stomach on the posterior abdominal wall. It is divided in head, neck, body and tail. It lies obliquely, with the head towards the right side, in contact with the duodenum and the tail towards the spleen. The main pancreatic duct runs longitudinally in the organ and drains the pancreatic juice into the duodenum through the major duodenal papilla (ampula of Vater) alongside the common bile duct which drains the bile from the liver and the gallbladder. When the main pancreatic duct is accompanied by an accessory pancreatic duct, the latter drains into the duodenum through the minor duodenal papilla (Fig. 1.1). (Beger HG et al. ed, 2008:52).

The pancreas has an endocrine and an exocrine function. The endocrine tissue is represented by endocrine cells grouped in the islets of Langerhans. Specialised cells (α, β, γ and PP) express insulin, glucagon, somatostatin and pancreatic polypeptide respectively, which are transported via the blood flow.

The exocrine tissue is represented by the acinar exocrine cells grouped in acini. They express digestive enzymes like trypsin and lipase which are transported via a ductal system leading to the main pancreatic duct draining into the duodenum. The ducts are lined with epithelial cells. Connective tissue forms a supportive matrix for the ducts as well as the blood vessels, lymphatic vessels and nerves which provide functional support (Dockman DE, 2008:50).

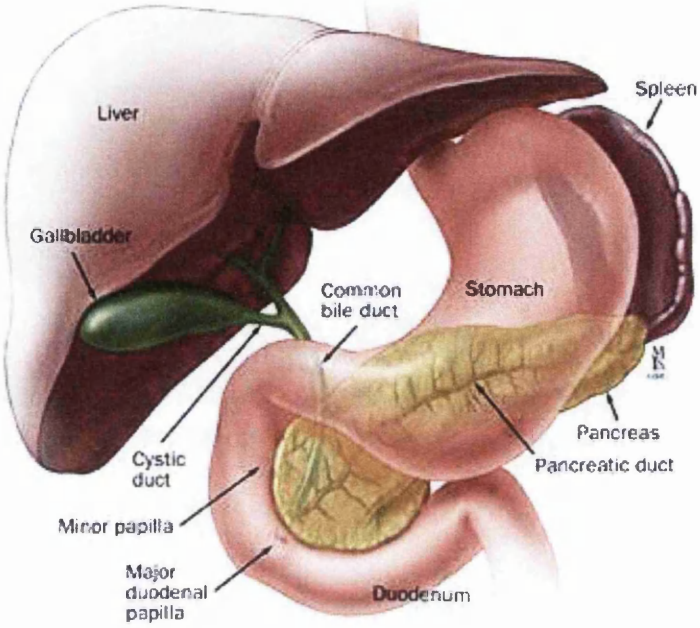

Figure 1.1: Anatomy of the pancreas, illustrating the position of the pancreas related to the stomach, spleen, liver, gallbladder and duodenum. The main pancreatic duct drains into the duodenum through the major duodenal papilla alongside the common bile duct. The accessory pancreatic duct drains into the duodenum through the minor duodenal papilla (The pancreas and adjacent anatomy, 2014).

1.1.3 Histopathology

Over 85% of pancreatic tumours are ductal adenocarcinomas. Other types of tumours include: acinar cell carcinoma, acinar cell cystadenocarcinoma, fibrosarcoma, pancreatoblastoma (Williams NA ed, 2013:1129).

The carcinogenesis process in ductal adenocarcinoma is initiated in the ductal cells and extends to the rest of the tissue as the process advances (Hruban RH et al., 2004). The tissue architecture in such cancer specimens appears distorted compared to normal specimens (Fig. 1.2).

Pancreatic ductal adenocarcinoma progression leads to local invasion to adjacent structures like regional lymph nodes, gastro-intestinal blood vessels, duodenum and stomach, and to distant metastases most commonly to lung, brain and peritoneum (Wolfgang CL et al., 2013).

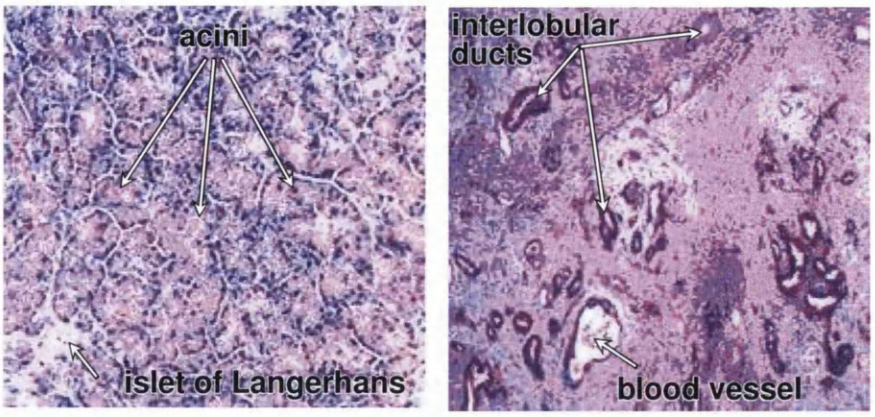

(a) Normal pancreas with islet of Langerhans (endocrine structure) and acini (exocrine component) (arrows).

(b) Pancreatic ductal adenocarcinoma with distorted tissue architecture; interlobular ducts and blood vessel (arrows).

Figure 1.2: Photomicrographs $\times 10$ of HE sections of normal pancreatic tissue and pancreatic ductal adenocarcinoma, respectively.

1.1.4 Premalignant lesions

The premalignant lesions in PDAC are: pancreatic intraepithelial neoplasia (PanIN), mucinous cystic neoplasm (MCN), intraductal mucinous papillary neoplasm (IPMN) and intraductal tubulopapillary neoplasm (ITPN) (de Wilde RF et al., 2012, Brosens LAA et al., 2013, Distler M et al., 2014). Even though adenocarcinomas may be a result of any of the precursor lesions, the ones associated with PanINs are far more common (13 to 100-fold) in pancreatectomy specimens (Winter JM, 2006). One of the reasons for this is the higher frequency of early diagnosis for non-invasive IPMNs and MCNs (Gaujoux S, 2011).

IPMNs are macroscopically visible mucin-producing cystic tumours located in the main pancreatic duct or one of its branches (Shi C et al., 2012). The associated symptoms include abdominal or back pain, nausea, vomiting, or recurrent episodes of pancreatitis and are caused by a dilated main pancreatic duct due to an increase in the production of mucin (Ghaneh P et al., 2006). IPMNs can be associated with invasive PDAC and in such cases the 5-year survival is 30-60% compared to 90-100% for the cases without invasive PDAC (Crippa S et al., 2010).

MCNs are macroscopically visible cystic tumours, most frequently located in the body and tail of pancreas and which do not communicate with the pancreatic ductal system. They can cause non-specific symptoms like abdominal discomfort (Zamboni G et al., 2010). When associated with invasive PDAC, the 5-year survival rate is 50-60% compared to 90-100% when not associated with invasive PDAC (de Wilde RF et al., 2012).

ITPNs are rare macroscopically large (average 6 cm diameter) solid nodular tu-

mours found in the pancreatic duct. In contrast to the cystic precursors, there is no overt mucin producing component (Yamaguchi H et al., 2009). About 40% cases can be associated with invasive PDAC. The 5-year survival is likely more than 30% but not enough data is currently available to differentiate between the cases with / respectively without invasive PDAC (Adsay NV et al., 2010).

IPMNs, MCNs and ITPNs are managed according to the "Sendai" criteria which are based on size, symptoms and evidence of associated malignant changes (Tanaka M et al., 2012).

PanINs are microscopic intraductal lesions that include several different stages: PanIN 1A, PanIN 1B, PanIN 2 and PanIN3.

The prevalence of PanINs increases with age. PanIN 2 is three times more prevalent in pancreatic tissue with associated PDAC while PanIN 3 is only found associated with PDAC. PanINs are more common in pancreatic tissue with PDAC (82%) than with pancreatitis (60%) or normal tissue (16%). PanINs 1 and 2 are considered low risk lesions for the development of PDAC and they can be seen in normal pancreatic tissue as well as associated with non-malignant lesions. PanINs 3 can be considered fully developed neoplastic lesions and they display multiple genetic similarities to invasive PDAC (de Wilde RF et al., 2012).

PanINs are asymptomatic and, at present, cannot be detected by imaging techniques, including endoscopic ultrasound (Distler M et al., 2014). They are most frequently located in the head of the pancreas compared to the body and tail. They measure less than 5 mm in size and arise in the smaller pancreatic ducts. Histologically, PanINs are lined by columnar mucinous epithelium instead of the normal cuboidal pancreatic duct epithelium (Hruban RH et al., 2004). PanIN 1A have a flat epithelial structure with the nuclei basally aligned and supranuclear mucin. PanIN 1B have a papillary structure, while PanIN 2 display more complexity with pseudostratification, nuclear hyperchromasia and loss of nuclear polarity. PanIN 3 are characterized by a papillary structure, with cribriform growth. They show significant atypia, with complete loss of nuclear polarity, nuclear hyperchromasia and atypical mitotic figures (Hruban RH et al. 2004, de Wilde RF et al., 2012).

A step wise progression model for the carcinogenesis process has been suggested based on research into the natural history of PanINs (Fig. 1.3) (Ottenhof NA et al., 2011).

It was noted that some of the early genetic events occur at the PanIN 1 stage and include telomere shortening and the activation of the K-ras oncogene. K-ras mutations can initiate PanIN development and they were identified in >90% of both low - and high - grade PanIN lesions. The K-ras mutant clone expands during PanIN progression (Kanda M et al., 2012). Other significant events occur at PanIN 2 and PanIN 3 stages, like the inactivation of tumour supressor genes p16 and p53, respectively

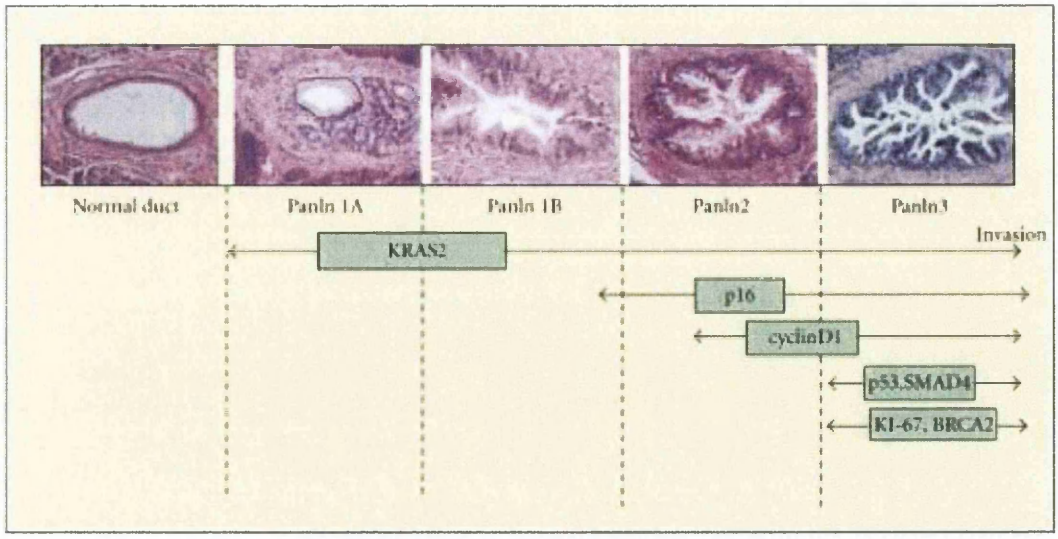

Figure 1.3: Progression model for pancreatic intraepithelial neoplasia (PanIN). The progressive histological changes are shown in the top row photomicrographs (hematoxylin and eosin (HE) staining, $\times 40$). The stepwise accumulation of genetic mutations is illustrated below the pictures (Ottenhof NA et. al., 2011)

(Hruban HR et al., 2000). p16 mutations were found in 11% of early PanIN lesions and more often in lesions without K-ras mutation (Kanda M et al., 2012). Loss of p16 protein expression was shown to increase with PanIN grade (Wilentz RE et al., 1998). Inactivation of p53 is a late event and is found in 30-50% cases with PanIN 3 and invasive PDAC. Inactivation of SMAD4 gene is found in 30% PanIN 3 lesions and 50% cancer cases (Hruban RH et al., 2000). Epigenetic inactivation of tumour supressor genes by hypermethylation occurs early and increases with PanIN grade (Sato M et al., 2008). Overexpression of oncogenes involved in EGFR, Notch and Hedgehog signaling occurs in PanINs associated with invasive PDAC (Miyamoto Y et al., 2003). Also, PanIN lesions display aberrant expression of many microRNAs, which may be used as diagnostic markers (Yu J et al., 2012).

Research studies investigating specimens of pancreatic tissue with chronic pancreatitis isolated premalignant lesions (PanIN 1-3) and demonstrated similar genetic changes seen in the PanINs from cancer specimens: p53 protein overexpression and loss of expression for p16 and DPC4 protein in PanIN 3, increasing aneuploidy from PanIN 1A to PanIN 3 (Baumgart M et al., 2010).

It was calculated using a computerised model that the time interval between the initiating tumour cell and the parental clone could be 10 years and that 5 more years could lead to fully metastatic disease (Yachida S et al., 2010).

1.1.5 Genetic pathways

Current knowledge based on extensive experimental and epidemiological data indicates that pancreatic cancer is a genetic disease. PDAC is characterized by the accumulation of a high number of gene deletions, mutations and amplifications.

The genes most commonly involved in pancreatic cancer are: KRAS2, p16/CDKN2A, TP53 and SMAD4/DPC4.

The KRAS2 oncogene is activated in virtually all cases of pancreatic cancer and is the most common genetic abnormality seen in this type of cancer (Almoguera C et al., 1988). Ras is a membrane-bound GTP-binding protein with a role in the growth factor-mediated signaling pathways. KRAS mutations lead to an activated form of Ras, locked in the GTP-bound state and able to stimulate a variety of downstream signaling pathways (Malumbres M et al., 2003). Mutations of this gene occur early in the progression model, namely in the PanIN 1A stage (Moskaluk CA et al., 1997). KRAS mutations can also be seen in nearly 25% of cases with chronic pancreatitis and even in healthy elderly population (Guerra et al., 2007).

The inactivation of the CDKN2A (p16) tumour suppressor gene is seen in up to 90% of all pancreatic cancers (Caldas C et al., 1994) and it can occur through homozygous deletion, mutation with loss of the second allele or epigenetic silencing of the locus on chromosome 9 (Schutte M et al., 1997). The p16 tumour suppressor pathway plays a vital role in cell proliferation by regulating entry into the S-phase of cell cycle (Sherr CJ, 2004, Liu H et al., 2004). p16 can be inactivated as early as the PanIN 2 stage (Moskaluk CA et al., 1997).

The TP53 gene is inactivated in a large proportion of pancreatic cancers (50-75%) (Redston MS et al., 1994), usually by mutation with loss of the second allele (Vogelstein B et al., 2000). The TP53 protein becomes activated and increases as a result of the oncogenic mutations, regulating a transcription response towards cell-cycle arrest or apoptosis (Sherr CJ, 2004). TP53 mutations are seen starting in the PanIN 3 lesions (DiGiuseppe JA et al., 1995).

The SMAD4 gene is inactivated in approximately 55% of the pancreatic cancers by homozygous deletion or mutation with loss of the second allele (Hahn SA et al., 1996). The MADH4 locus on chromosome 18 (18q21.1) encodes SMAD4 and it undergoes loss of heterozygosity in 90% of tumours (Rane SG et al., 2006). The loss of SMAD4 has significant effects on tumour microenvironment and tumour invasion (Schwarte-Waldhoff I et al., 2000, Duda DG et al., 2003) through its role in signal transmission for the TGF-β superfamily of cytokines (Bierie B et al., 2006). The inactivation can occur from the PanIN 3 stage (Wilentz RE et al., 2000).

Two of the most important pathways involved in pancreatic carcinogenesis are the Notch and the Hedgehog pathways.

The Notch pathway is instrumental in the processes of apoptosis, differentiation

and proliferation in pancreatic cancer initiation and invasion (Leach SD et al., 2005, Lomberk G et al., 2005). The Notch pathway also promotes tumour vascularisation (Rehman RO et al., 2006) which prompts advanced research into possible drug targets. The genes involved in this pathway are upregulated in the precursor lesions as well as in the invasive tumour (Miyamoto M et al., 2003).

The Hedgehog signaling pathway includes three different members: sonic, desert and Indian hedgehog, which coordinate the development of the gastrointestinal tract in association with other ligands (Thayer SP et al., 2003, Prasad NB et al., 2005, Kayed H et al., 2006). The Hedgehog signaling pathway mainly coordinates the development of the gastrointestinal tract. Upregulation of the genes involved in the Hedgehog pathway is initiated in the early premalignant stages (Prasad N et al., 2005). The Sonic hedgehog is believed to be involved in the development of the pancreatic cancer stem cells which are presumed potential precursor cells for pancreatic cancer. One study identified a specific phenotype (CD44 CD24 ESA) from primary pancreatic cancer cells that has a 100-fold increased malignant potential but detailed characterization of the molecular signature and progression pathway is still in research (Li C et al., 2007).

A variety of other genes are involved but with a lower frequency. The gene sets have been linked to 12 core signaling pathways and processes relevant to pancreatic carcinogenesis (Fig. 1.4). Only one gene from a pathway is usually involved in a specific carcinoma specimen while a wide range of genes is connected to different specimens (Iacobuzio-Donahue CA, 2012).

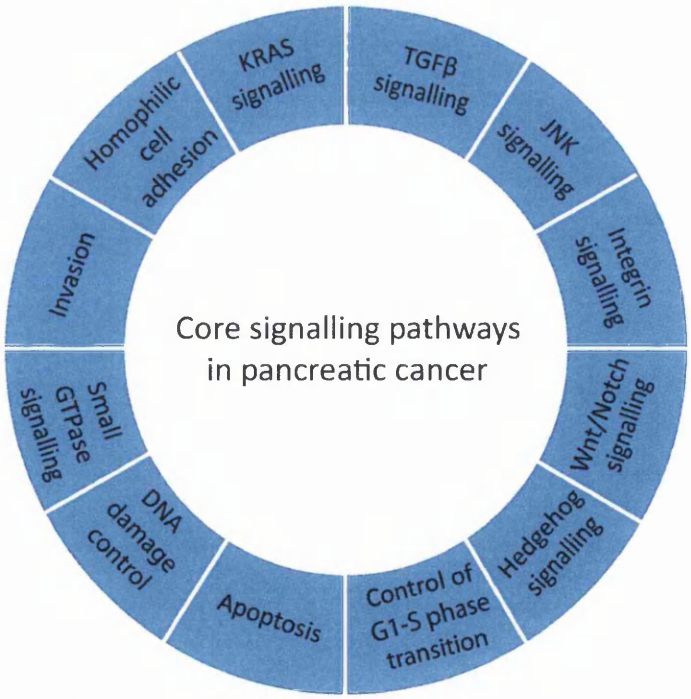

Figure 1.4: The main signaling pathways involved in pancreatic cancer (Iacobuzio-Donahue CA, 2012)

Each of the premalignant stages in the PanIN progression is associated with other less frequent genetic changes that contribute to the carcinogenesis process (Table 1.1) (Ghaneh P et al., 2008).

Table 1.1: Genetic alterations in the pre-malignant stages PanIN 1, PanIN 2 and PanIN 3 (Ghaneh P et al., 2008)

PanIN 1	PanIN 2	PanIN 3
K-ras	Cyclin D1	p53
Telomere shortening	Cyclo-oxygenase 2 (COX 2)	SMAD4
p21 (WAF1/CIP1)	Hes1 (Hair and enhancer of split 1)	BRCA2
Human epidermal growth factor receptor 2 (Her2 / neu)	Notch 1	S100P
Mucin 1 (MUC1)	Pepsinogen C	SHH
MUC6	Kruppel-like factor 4 (KLF4)	SialyT (mucin-associate carbohydrate antigen)
Trefoil factor 1 (TFF1)	HOXA5	Maspin
p16 (INK4a)	GATA5	MUC4
S100A11	Gastrin	Tumour suppressor in-lung cancer-1 (TSLC 1)
MUC5AC	Villin 1	Familial adenomatous polyposis (FAP)
S100A6	Villin 2	
	Cellular retinoic acid binding protein 4 (CRABP 4)	

Despite advances in studying cancer tissue the survival rates have not improved therefore major emphasis is currently placed on studying the premalignant stage in view of identifying and validating potential biomarkers for early detection. Currently there is no validated diagnostic method able to detect PanINs but the ongoing progress

in state-of-the-art radiology remains promising. The PanINs described by research studies come from surgical specimens resected for benign or malignant conditions or from mouse models. Genetically engineered mouse models, where one or more genes (KRAS, SMAD4) known to be involved in pancreatic carcinogenesis have been inactivated, can display the full route to cancer and metastasis as seen in humans (Bardessy N et al., 2006, Hingorani SR et al., 2005, Skoulidis F et al., 2010).

Increasing evidence from work carried out on pancreatic cancer specimens obtained at autopsy on patients with end stage disease suggests that a personalized approach to therapy could lead to improved outcome. For example, the status of the DPC4 gene in the tissue could direct treatment: patients with borderline resectable tumours and loss of DPC4 expression may indicate a high risk for distant spread and therefore be treated with systemic rather than locoregional therapy; if the DPC4 gene is retained, the patient could have adjuvant chemoradiotherapy. This is early stage retrospective data but there is an outstanding potential in this approach as genetic and targeted therapy advance (Iacobuzio-Donahue CA, 2012).

1.1.6 Biomarkers

The definition of a tumour marker is "a naturally occurring molecule that is measured in serum or plasma, or other body fluids or in tissue extracts or paraffin-embedded tissue to identify the presence of cancer, to assess patient prognosis, or to monitor a patient's response to therapy with the overall goal of improving the clinical management of the patient" (Fleisher M et al., 2002).

Biomarkers are classified in:

1. pre-disposition biomarkers, designed to identify at risk cases
2. screening biomarkers, used for early detection in general or at risk populations;
3. diagnostic biomarkers, for defining the tumour type, stage and grade;
4. prognostic biomarkers, used to identify the likely clinical disease course;
5. predictive biomarkers, designed to illustrate patient likelihood to benefit from individual therapies;
6. pharmacological biomarkers, used to monitor drug effects;
7. surrogate response biomarkers, for early prediction of ultimate clinical efficiency (Cancer Research UK, 2014).

There are no established pre-disposition or screening biomarkers in pancreatic cancer.

The only marker used in clinical practice for pancreatic cancer is CA 19-9 which has 90% specificity and 80% sensitivity (Steinberg H, 1990). However, CA 19-9 is a prognostic biomarker only relevant in monitoring for response to adjuvant therapy and for recurrence. Increased values can be seen in obstructive jaundice of non-malignant origin, chronic pancreatitis, cholangitis, cirrhosis and other gastrointestinal cancers therefore its independent diagnostic power is limited (Duffy MJ et al., 2010). Furthermore, CA 19-9, a syalilated antigen of the MUC1 protein, cannot be detected in patients with certain blood types who cannot express the antigen recognized by it (Steinberg H, 1990).

A wide range of potential diagnostic and predictive biomarkers relevant to pancreatic cancer are under investigation but so far they failed to be translated into clinical use (Buxbaum JL et al., 2010).

A systematic review on immunohistochemistry-based tissue biomarkers relevant in pancreatic cancer found a limited panel of promising markers for the prediction of overall survival: BAX (HR=0.31, 95% CI: 0.71-0.56), Bcl-2 (HR=0.41, 95% CI: 0.27-0.63), survivin (HR=0.46, 95% CI: 0.29-0.73), Ki-67 (HR=2.42, 95% CI: 1.8-3.14), COX-2 (HR=1.39, 95% CI: 1.13-1.71), E-cadherin (HR=1.80, 95% CI: 1.33-2.42) and S100A2 calcium-binding protein (HR=3.23, 95% CI: 1.58-6.62) (Jamieson NB et al., 2011).

CA242, CAM17.1 and TPS are candidate serum protein diagnostic markers under evaluation. MIC-1, osteopontin and TIMP-1 are candidate serum protein diagnostic markers in the research phase (Goggins M, 2010).

Pancreatic juice analysis could yield a panel of markers relevant in early detection. Thus, mutant K-ras, mutant p53, methylated DNA and mithocondrial DNA mutations are under evaluation as part of pancreatic juice analysis (Goggins M, 2010).

In other types of cancer molecular markers are already used in tailoring therapy: Kras sequencing (Van Cutsem E et al., 2009) and microsatellite instability (Jover R et al., 2009, Ribic CM et al., 2003) in colorectal cancer; hormone receptor status (Collab group, 1998) and Her2 expression (Perez EA et al., 2011) in breast cancer and similarly for melanoma (Chapman PB et al., 2011), lung cancer (Shedden K et al., 2008) and prostate cancer (Cheville JC et al., 2008).

1.1.7 Diagnosis

In the sections for diagnosis, staging and standard therapy the term pancreatic cancer refers to pancreatic ductal adenocarcinoma only, unless stated otherwise. Most frequently, pancreatic cancer is asymptomatic until late stage. The symptoms are usually non-specific like anorexia, weight loss, upper abdominal discomfort. Painless jaundice is associated with pancreatic cancer and is the symptom which draws medical attention. The first line of investigations includes blood tests and abdominal ultrasound

scan. If there is a suspicion of pancreatic cancer, the next test is a contrast-enhanced helical computerised tomography (CT) scan specific for the pancreas which is used for diagnosis and staging. Also, endoscopic ultrasound (EUS) is used to characterize the tumour and its extent and, potentially, to obtain biopsy. If surgery is appropriate based on the information obtained from CT and EUS and after assessing patient fitness, surgical resection is planned without delay. Another potential investigation is endoscopic retrograde colangiopancreatography (ERCP) which can be accompanied by biopsy and / or insertion of a stent to relieve the jaundice. Biopsies are important especially in palliative cases, to help tailor palliative therapy. For the cases which undergo radical surgery biopsy is not mandatory. Only in the cases where imaging of a pancreatic lesion is ambigous biopsy is peformed via EUS (Seufferlein T et al., 2012). Magnetic resonance cholangiopancreatography (MRCP) is non-invasive and can be used to gather information about the tumour and the adjacent bile ducts but cannot be used for biopsy. Percutaneous transhepatic cholangiography (PTC) is used for stent placement in the cases where ERCP is not feasible (Williams NA ed, 2013:1128-29). Positron emission tomography - computer tomography (PET-CT) is indicated for staging in potentially operable cases where other imaging is equivocal for metastatic disease and a positive PET-CT would lead to a decision not to operate (The Royal College of Physicians and Royal College of Radiologists, 2013). Tumour markers like CA 19-9 have limited diagnostic value. CA 19-9 is not specific for pancreatic cancer and can increase in non-malignant disease (Seufferlein T et al., 2012).

1.1.8 Staging

The staging system in pancreatic cancer is provided by the TNM staging system from The American Joint Committee on Cancer (AJCC) and The Union for International Cancer Control (UICC). The TNM staging system is determined by details on the primary tumour, regional lymph nodes and distant metastases (Seufferlein T et al., 2012) (Table 1.2).

Based on the TNM system, pancreatic cancer is divided into stage 0, IA, IB, IIA, IIB, III and IV (Seufferlein T et al., 2012) (Table 1.3).

Table 1.2: TNM classification for pancreatic cancer (Seufferlein T et al., 2012)

Primary Tumour	
Tx	Primary tumour cannot be assessed
T0	No evidence of primary tumour
Tis	Carcinoma in situ
T1	Tumour limited to the pancreas, $\leqslant$2cm in greatest dimension
T2	Tumour limited to the pancreas, >2cm in greatest dimension
T3	Tumour extends beyond the pancreas but without involvement of the celiac axis or the superior mesenteric artery
T4	Tumour involves the celiac axis or the superior mesenteric artery (unresectable primary tumour)
Regional lymph nodes	
Nx	Regional lymph nodes cannot be assessed
N0	No regional lymph node metastasis
N1	Regional lymph node metastasis
Distant metastases	
M0	No distant metastasis
M1	Distant metastasis

Table 1.3: Stage grouping of pancreatic cancer (Seufferlein T et al., 2012)

Stage	T	N	M
0	Tis	N0	M0
IA	T1	N0	M0
IB	T2	N0	M0
IIA	T3	N0	M0
IIB	T1	N0	M0
IIB	T2	N1	M0
IIB	T3	N1	M0
III	T4	Any N	M0
IV	Any T	Any N	M1

1.1.9 Standard therapy

The therapy in pancreatic cancer is guided by the staging system (Seufferlein T et al., 2012, Wolfgang CL, 2013). Most patients (50-60%) present with metastatic disease. 25-30% patients present with locally invasive/unresectable tumours. 15-20% patients present with resectable/borderline resectable tumours (Mauro LA et al., 2014). The only curable therapy is radical surgery. This is suitable for patients with stage I disease and some with stage II. The standard surgical intervention for tumours of the pancreatic head is partial pancreato-duodenectomy. Distal pancreatectomy is performed for tumours located in the body or the tail of the pancreas. In some cases, total pancreatectomy is required (Seufferlein T et al., 2012). The resectability/iresectability criteria are governed by The National Comprehensive Cancer Network (NCCN) Guidelines for pancreatic adenocarcinoma and are based on the extent of vascular invasion (NCCN, 2011). A raised level of CA 19-9 post resection, a positive circumferential resection margin and a lymph node ratio (LNR) >0.2 (number of positive lymph nodes/total number of lymph nodes excised) are negative prognostic factors (Riediger H et al., 2009). Adjuvant chemotherapy is standard and uses gemcitabine or 5-Fluorouracil for a period of 6 months (Neoptolemos JP et al., 2010). Adjuvant chemoradiation is

controversial. Neoadjuvant chemotherapy, radiotherapy or chemoradiation is used as part of clinical trials in resectable cases or in selected cases with borderline resectable tumours to downsize the tumour prior to resection. If the tumour is not resectable, the aim is to prolong survival by controlling local symptoms and metastatic growth. The standard therapy for stages III and IV is chemotherapy alongside symptom control. Regimens with gemcitabine or FOLFIRINOX (5-Fluorouracil, irinotecan and oxaliplatin) are used in this setting. A combined regimen of gemcitabine and erlotinib (epithelial growth factor receptor (EGFR) tyrosine kinase inhibitor) can be used in selected cases. Other combinations of chemotherapy agents have not showed any survival benefits. Palliative therapy includes symptom control (pain, nausea) as well as stenting in cases with jaundice or duodenal obstruction (Seufferlein T et al., 2012).

1.2 Aneuploidy

Chromosomal instability (CIN) is defined as an increased rate of chromosome missegregation in mitosis. The main mechanisms leading to chromosomal instability include an underactive or overactive mitotic spindle assembly checkpoint, defects of cohesion between sister chromatids, increased microtubule-kinetochore attachments or the presence of extra centrosomes. CIN can manifest itself as gains or losses of whole chromosomes (aneuploidy) or gross chromosomal rearrangements.

Aneuploidy is a chromosomal abnormality resulting from either an excess or deficit of a chromosome or several chromosomes so that the chromosome number is not an exact multiple of the typical haploid set (23).

Stable aneuploidy can occur without chromosomal instability (e.g. Down syndrome-trisomy 21) and it is antiproliferative but the aneuploidy seen in cancers is frequently caused by CIN. It is usually seen early in carcinogenesis and is associated with a poor prognosis (Yuen K et al., 2010).

The cell cycle is divided into interphase and mitosis. The interphase has 3 distinct stages: G1 (Gap Stage1), S (Synthesis Stage) and G2 (Gap Stage 2). Mitosis is organised in 4 steps: prophase, metaphase, anaphase and telophase. The mitotic cell division is designed to ensure proper chromosome segregation through the coordinated activities of the cyclin-dependent kinases and spindle assembly checkpoint (SAC).

In G1 there is an increase in protein synthesis so that the cell doubles in size, thus the daughter cells have the same function as the original cell. During the S phase the DNA is replicated by semi-conservative replication, producing two identical copies of each chromosome. The chromosomes get wrapped around proteins called histones and together they represent the chromatin. After the DNA replication, two identical chromosomes named sister chromatids are held together at a point named centromere. The DNA replication is governed by mechanisms that ensure exact copying in order to avoid mutations. During G2 there is further cell growth and rapid protein synthesis in preparation for mitosis.

During prophase the chromosomes become short and thick and can be visualised with a light microscope. The organelle called centriole divides in two and starts to form protein threads named spindle (microtubule) fibres. These attach to the centromeres on the sister chromatids. In prometaphase the nuclear envelope disappears and the sister chromatids individualize along the chromosome arms. In metaphase the chromosomes align themselves towards the centre of the cell (equatorial plate of the spindle), held by the spindle fibres. During anaphase, the spindle fibres contract separating the sister chromatides at the centromere and pulling them towards the opposite poles of the cell. In telophase the spindle fibres break down and a nuclear envelope forms around the two sets of sister chromatids at the poles of the cell. The cell divides into two (cytokinesis) generating two identical daughter cells.

The SAC acts in prometaphase and its role is to control the timing of anaphase. It delays sister chromatids separation until all the chromosomes are attached to the spindle (bipolar attachment). It is formed by the products of the MAD (mitotic arrest deficient) and BUB (budding uninhibited by benzimidazole) genes, of the Mps1 and Aurora B/Ipl1 kinases and additional accessory factors. The main proteins of the spindle assembly checkpoint are: Mad1, Mad2, Mad3, Bub1, Bub3, Mps1 and Cdc20. The depletion of Mad2 and BubR1 proteins leads to a premature anaphase with misaligned chromosomes (Silk AD et al., 2013, Lampson MA et al., 2004). The depletion of other SAC proteins including Mad1, Bub1 and Bub3 produces a premature exit from mitosis for the cells whose chromosomes are not properly aligned (Varetti G et al., 2008).

Several mechanisms of chromosomal instability have been identified in aneuploid human tumour cells: cohesion defects, SAC defects, supernumerary centrosomes, defects in kinetochore-microtubule attachment dynamics and defects in cell cycle regulation (Thompson S et al., 2010).

Aneuploid cells usually occur in most normal tissues due to errors in cell division but do not proliferate to produce abnormal clones (Sandberg AA et al., 1961). However, increased aneuploidy in tumour cells gives a poor prognosis through accelerated tumour progression and metastatic potential.

Aneuploidy could represent a biomarker of real value for the personalized approach to therapy in pancreatic cancer when correlated with relevant proteomics (i.e. CA19-9, CEA), transcriptomics (i.e. microRNA), metabolomics (i.e. glucose, creatine) and other genomics (i.e. mutant KRAS, p16, TP53).

The aberrations seen in pancreatic cancer involve gains or losses of whole-arm chromosomes as well as subchromosomal alterations. A wide panel of chromosomes are involved as demonstrated by multiple studies using different methods to investigate the genome for pancreatic cancer. Comparative genome hybridization (CGH), karyotype analysis and loss of heterozygosity (LOH) studies indicated that frequent gains are found in 3q, 5p, 7p, 8q, 11q, 12p, 17q and 20q and frequent losses in 3p, 4q, 6q, 8p, 9p, 10q, 12q, 13q, 17p, 18q, 21q and 22q (Hahn SA et al., 1995, Seymour AB et al., 1994, Fuji H et al., 1997, Mahlmaki EH et al., 1997, Sugio K et al., 1997). Correlations between the chromosomal anomalies and tumour dissemination proved that lymph node metastasis and vascular invasion is related to the genetic signature of the specimen (Aguirre AJ et al., 2004). Genome-wide array CGH on pancreatic ductal adenocarcinoma specimens revealed losses and gains in multiple different loci, most frequently located on 1p, 11q, 17p, 10q, 8p, 18q, 22q, 6q, 9p, 14q and 17q for losses and 7q, 12p, 1p, 8q, 12q and 14 q for gains (Loukopoulos P et al., 2007). This illustrates the diversity of the genetic material involved in pancreatic carcinogenesis but also the variation between the abnormalities reported in different studies and between individual cases.

1.3 Mitotic checkpoint proteins

The normal mitosis process (Fig. 1.5) is regulated by intricate mechanisms, among which the spindle assembly checkpoint plays a central role.

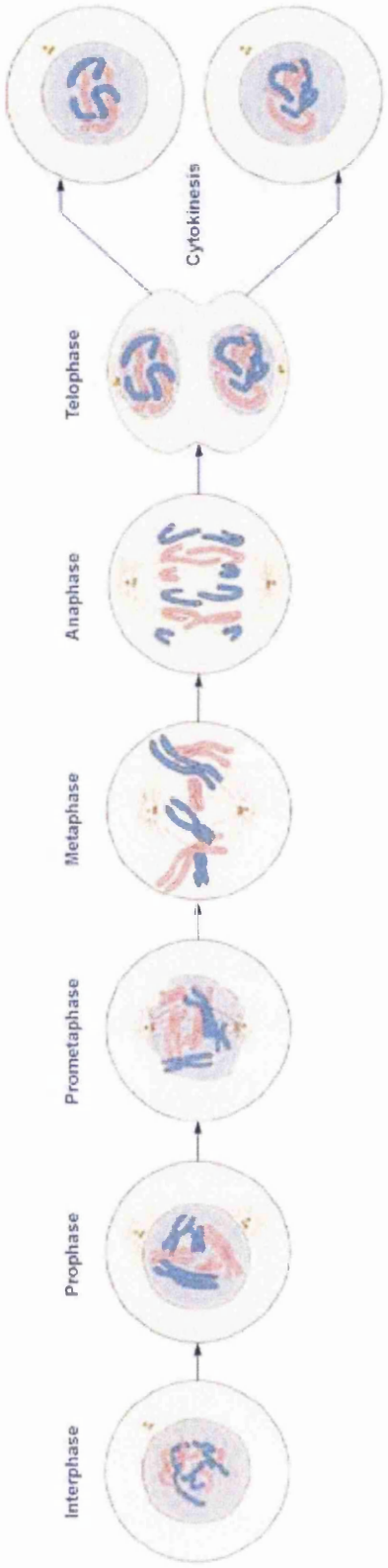

Figure 1.5: The normal mitosis process includes 4 distinct phases: prophase, metaphase, anaphase and telophase during which the cell components undergo specific modifications in preparation for division. The result of a normal mitosis is the division of the cell into two identical daughter cells (`http://www.nigms.nih.gov`)

The spindle assembly checkpoint is a feedback control that prevents cells with incompletely assembled spindles from continuing to mitosis (Fig. 1.6).

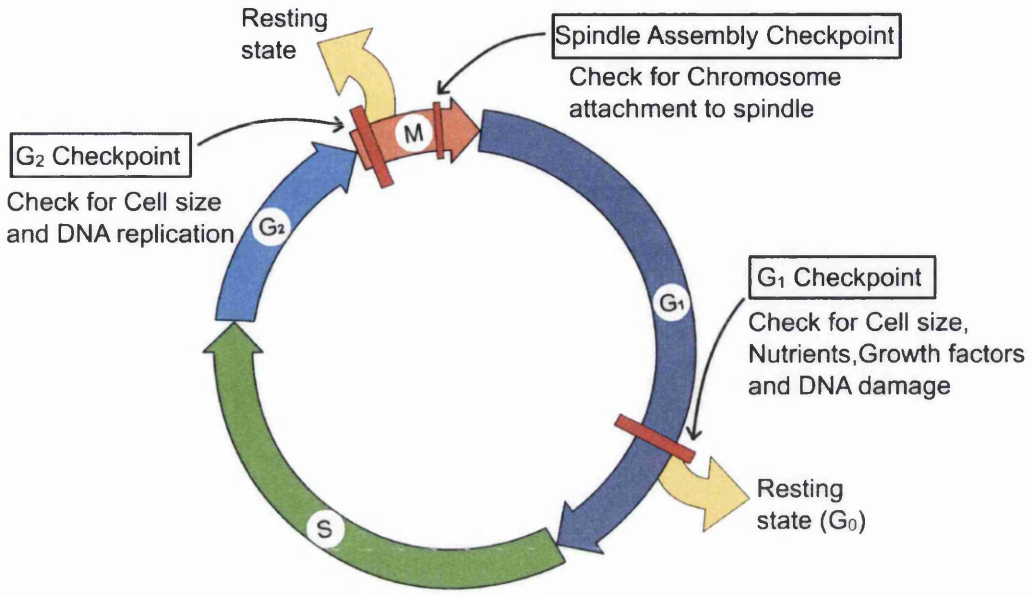

Figure 1.6: The cell cycle includes G1 (synthesis of RNA proteins for DNA replication), S (synthesis of DNA) and G2 (synthesis of more RNA proteins) before proceeding to mitosis. The spindle assembly checkpoint controls the exit from the mitosis ensuring that all cells underwent a normal division of their DNA material (`http://oncogenesandcancer.wordpress.com/`)

The molecular components of the checkpoint include Mad1, Mad2, Mad3/BubR1, Bub1, Bub3, Mps 1 and Aurora B among other proteins (Musachio A et al., 2002, Yu H, 2002, Bharadwaj R et al., 2004).The checkpoint is activated when chromatids are not properly attached to both poles of the mitotic spindle. This leads to the inhibition of the ubiquitin ligase activity of the anaphase-promoting complex or cyclosome (APC/C) and the delay of the onset of anaphase (Yu H, 2006)(Fig. 1.7).

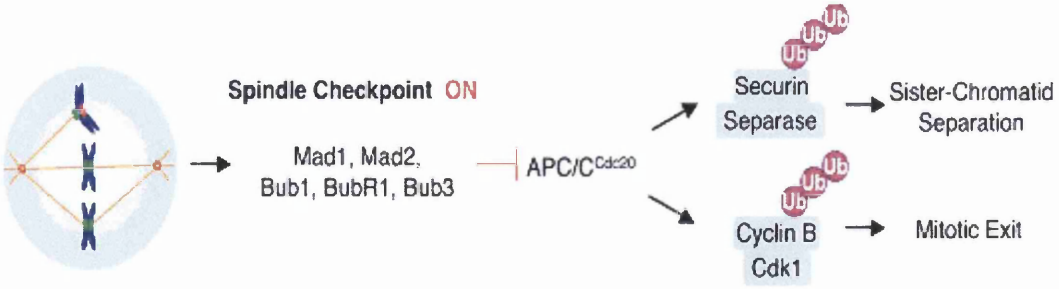

Figure 1.7: The mitotic spindle checkpoint which, when activated, inhibits the APC/C and delay sister chromatid separation (Yu H, 2006)

Mad2 (mitotic arrest deficiency 2) is recruited to the unattached kinetochores by

Mad1. When the checkpoint is active, Mad2 is relayed from the Mad1-Mad2 complex to the mitotic checkpoint complex (MCC), a tetramer composed of BubR1, Bub3 and Mad2 bound to Cdc20. It then inhibits the APC/C through binding to its mitotic-specific activator, Cdc20. BubR1 (budding uninhibited by benomyl related-1) also binds directly to Cdc20 and together with Mad2 are downstream components of the spindle checkpoint.

The genes that control Mad2 and BubR1 are part of the genetic pathways involved in controlling the cell cycle and thus genetic defects at this level can lead to chromosome instability and tumorigenesis (Jallepalli P et al., 2001). Complete inactivation of the Mad2 and Bub3 leads to embryonic death in experiments with mice (Dobles M et al., 2000, Kalitsis P et al., 2000). Tissue cultures using cells where one allele of Mad2 has been inactivated show high rates of chromosome loss per generation and a high degree of aneuploidy (Michel L.S et al., 2001). One study observed that mice with heterozygous mutations in Mad2 develop normally but display lung tumour in adulthood, indicating a potential quantitative effect of Mad2 expression on tumorigenesis (Michel L.S et al., 2001). Mad2 mutations were also demonstrated in breast and bladder cancers (Percy et al., 2000, Hernando et al., 2001) while Mad1 mutations were seen in lung cancer (Nomoto et al., 1999) and Bub1 mutations in lung and colorectal cancers (Gemma et al., 2000, Sato et al., 2000, Cahill et al., 1998).

BubR1 mutations have been identified in human cancers like colon cancer (Weaver BA et al., 2006, Cahill DP et al., 1998) while studies on mice demonstrated that decreased levels of BubR1 increase tumour incidence and progression (Babu JR et al., 2003, Baker DJ et al., 2004, Dai W et al., 2004, Rao CV et al., 2005).

The abnormal proliferation of tumours results from the alteration of the genetic mechanisms responsible for the cell cycle checkpoints. Therefore the proteins linked to the mitotic checkpoint mechanism become potential molecular biomarkers for the invasive potential of a type of tumour.

As the carcinogenesis process involves abnormal changes in several mechanisms that control normal cell apoptosis and mitosis, the significance of a certain pathway varies from tumour to tumour. Chromosomal instability is one mechanism that defines carcinogenesis and it is closely linked to aberrations of the mitotic checkpoint mechanism. Aneuploidy, in particular, as a direct result of abnormal mitosis, is correlated to changes in the levels of checkpoint proteins. Studies using mouse models have shown that decreased levels of Mad1, Mad2, Bub1 and BubR1 and overexpression of Mad2 result in increased rates of abnormal chromosome segregation (Dobles et al., 2000, Babu et al., 2003, Baker et al., 2004, Iwanaga et al., 2007, Jeganathan et al., 2007, Perera et al., 2007, Sotillo et al., 2007, Weaver et al., 2007).

Mad2 and BubR1 proteins were included in this study as recognised major players in the checkpoint mechanism. Also the quantification and interpretation of their levels

is well documented in the literature and clearly linked to the carcinogenesis process in different types of tumours: Mad2 in breast and bladder cancers (Percy et al., 2000, Hernando et al., 2001) and BubR1 in lung and colorectal cancers (Gemma et al., 2000, Sato et al., 2000, Cahill et al., 1998). The time-limiting design of this pilot study did not allow the inclusion of other proteins involved in controlling the mitotic checkpoint mechanism.

Multiple different genetic pathways are involved in pancreatic carcinogenesis. Abnormalities seen in the chromosomal number set represents a contributing aspect to the overall tumour progression. Aneuploidy levels have the potential to become part of the individual tumour signature and part of the specific individual genetic profile increasingly employed in discovering personalized targeted therapies.

For the purposes of this study four chromosomes have been selected to investigate the levels of aneuploidy they display along the process of pancreatic carcinogenesis: chromosome 1, 6, 9 and 18. The rationale behind this selection lies with the evidence from the pancreatic cancer genome which includes these chromosomes but also with the known hypothesis that aneuploidy is, to some extent, a random event, therefore it can be illustrated in an extensive panel of chromosomes. The selected chromosome probes provided satisfactory fluorescent results in pancreatic cancer tissue compared to a larger panel trialled initially. Furthermore, 9p 21 is the locus for the p16 gene and 18q21 is the locus for the SMAD4 gene, both proved to have a significant role in pancreatic cancer (Feldman G et al., 2007). However, the current study was not designed to investigate specific gene pathways.

1.4 Objectives and Study plan

1.4.1 Objectives

1. Retrospectively assess aneuploidy levels in pancreatic intraepithelial lesions associated with pancreatic ductal adenocarcinoma. This would help establish a potential critical progression stage in carcinogenesis and allow the use of aneuploidy in genotyping individual tumours.
2. Retrospectively assess the levels of mitotic checkpoint protein levels Mad2 and BubR1.
3. Correlate the aneuploidy and the mitotic checkpoint protein levels Mad2 and BubR1 to patient data.

1.4.2 Study plan

1. Use fluorescence in situ hybridization to evaluate the aneuploidy levels in different PanIN grades.
2. Use immunohistochemistry to evaluate the levels of mitotic checkpoint proteins Mad2 and BubR1 in a panel of pancreatic intraepithelial lesions.
3. Use statistical correlation models to test for potential significant correlations between the aneuploidy levels and mitotic checkpoint proteins Mad2 and BubR1 levels.

Chapter 2

Aneuploidy in pancreatic intraepithelial lesions

2.1 Introduction

The method employed to score the chromosomal copy numbers was fluorescence in situ hybridization (FISH). FISH is a technique that uses fluorescently labelled DNA probes to detect chromosomal alterations in cells. It involves the preparation of short sequences of single-stranded DNA called probes, which are complementary to the DNA sequences to be investigated. These probes hybridize to the complementary DNA and, because they are labelled with fluorescent tags, they allow the quantification of chromosome copy numbers. There are two types of chromosome probes: chromosome enumeration probes (CEP), used to detect chromosomal number anomalies, and locus-specific indicator probes (LSI) used to investigate deletion or amplification of specific genes. FISH allows visualization of chromosomes in metaphase or interphase with numerical or structural anomalies with high sensitivity and specificity (Ried T et al., 1998).

The diagnostic applications include detecting gene amplifications (Her2 in breast cancer) (Bartlett J et al., 2001), gene rearrangements (BCR-Abl in leukemia) (Nolte M et al., 1996), viral infections (human papilloma virus) (Bartlett J, 2006). The advantages of the method are that it has a high specificity and sensitivity for the selected chromosome(s), that the chromosome probes used are widely available, that it is a validated diagnostic tool and that the automated method is time saving allowing for large numbers of specimens to be processed. The disadvantages are related to its use in tissues that present difficulties for optimizing the method, to intraobserver and interobserver variation, to sectioning bias and to the limited number of probes used on the same tissue sample. FISH can be used for diagnostic cytology in bladder, lung, oesophagus and bile duct cancers (Halling K et al., 2007).

FISH can only detect a known genetic aberration, provided the specific probe is

available, in other words FISH cannot be used as a generic screening tool for unknown chromosome rearrangements (Speicher MR et al., 2005, Ried T et al., 1998), however advanced types of FISH can be used for 24-colour karyotyping: multiplex FISH (M-FISH) or spectral karyotyping (SKY). Both methods allow painting of the whole chromosome complement in a single hybridization by utilising different fluorophores. The fluorescence microscope used to capture the images has filter sets specific for particular fluorochromes and uses an algorithm to separate and identify the chromosomes which are visualized in characteristic colours. The difference between M-FISH and SKY lies in the method used to differentiate the labelled probes (Speicher MR et al., 2005).

This validated method of detecting aneuploidy levels is already used in the base laboratory for detecting chromosome number changes in premalignant stages of oesophageal and gastric cancer (Hilling K et al., 2007, Doak S et al., 2003, Cronin J et al., 2011, Williams L et al., 2005, Williams L et al., 2009).

This part of the study was designed to:

1. Identify pancreatic intraepithelial lesions (PanINs 1-3) associated with PDAC in archival pancreatic tissue stored after pancreatic resection.

2. Quantify the levels of aneuploidy displayed by chromosomes 1, 6, 9 and 18 in different histological stages.

3. Demonstrate how aneuploidy changes with the PanIN grade.

2.2 Materials and method

2.2.1 Sample characteristics

The specimens included in the study were obtained from the archive of the Histopathology department in Morriston Hospital, ABMU Health Board Swansea where they were stored after elective surgical resection in the local Pancreatic Unit, tertiary referral centre for South Wales. Ethical approval for the project was granted by the South West Wales Research Ethics Committee on the 17^{th} November 2010.

30 patients were included in this study, 21 males and 9 females, median age 68.5 years, range 53-82 years. All patients underwent pylorus-preserving pancreatico - duodenectomy between 2010 - 2012. Specimens with any PanIN 1-3 in the resected PDAC specimen in 4 consecutive sections needed for the FISH treatment were included. The tissue sections displayed at least one type of PanIN lesion and often more than one type. Specimens with peripheral ducts with PanIN lesions which would not allow sequential sectioning and specimens from patients who underwent neoadjuvant therapy were excluded.

Positive and negative controls for pancreatic tissue were provided by the manufacturer together with the FISH reagents on request (Vysis, UK).

3 patients who underwent distal pancreatectomy for multiple congenital cysts, lymphoepithelial cyst and peritoneal pseudocyst, respectively, were included as normal controls (Table 2.1).

Table 2.1: Patient demographics selected for the aneuploidy study.

Patient no.	Age	Sex	Diagnosis	Date of surgery	Tumour size (cm)	Histology	TNM	Stage	Survival (months)
1	64	M	IPMN	20/02/2009	n/a	normal duct, PanIN 1, PanIN 2	n/a	n/a	n/a
2	72	M	pancreatic cancer	30/12/2010	3.7	normal duct, PanIN 1	pT3N1	IIB	12
3	74	M	pancreatic cancer	13/08/2010	3.3	normal duct, PanIN 1, PanIN 3	pT3N1Mx	IIB	11
4	74	M	pancreatic cancer	16/06/2011	4.1	normal duct, PanIN 1	pT3N1	IIB	20
5	68	M	pancreatic cancer	10/06/2011	4.6	normal duct, PanIN 2	pT3N1	IIB	12

TNM - tumour staging system; **IPMN** - intraductal pancreatic mucinous neoplasm; **PanIN** - pancreatic intraepithelial neoplasia

Patient no.	Age	Sex	Diagnosis	Date of surgery	Tumour size (cm)	Histology	TNM	Stage	Survival (months)
6	69	M	pancreatic cancer	28/10/2010	n/a	normal duct, PanIN 1	pT3N1	IIB	10
7	80	M	pancreatic cancer	01/07/2011	4	normal duct, PanIN 2, invasive cancer, lymph node with metastasis	pT3N1M1	IV	13
8	60	M	pancreatic cancer	08/07/2010	3	normal duct, PanIN 1, PanIN 3	pT3N1	IIB	10
9	75	M	pancreatic cancer	15/07/2011	4.6	normal duct, PanIN 1, PanIN 2	pT3N1	IIB	18

TNM - tumour staging system; **IPMN** - intraductal pancreatic mucinous neoplasm; **PanIN** - pancreatic intraepithelial neoplasia

Patient no.	Age	Sex	Diagnosis	Date of surgery	Tumour size (cm)	Histology	TNM	Stage	Survival (months)
10	65	F	pancreatic cancer	24/06/2011	3.3	normal duct, PanIN 1	pT3N1	IIB	14
11	70	M	pancreatic cancer	17/06/2011	4.1	normal duct, PanIN 1, PanIN 3	pT3N1	IIB	3
12	81	M	pancreatic cancer	14/07/2011	2	normal duct, PanIN 1	pT3N0	IIA	15
13	80	M	pancreatic cancer	30/06/2011	2.5	normal duct, PanIN 1	pT3N1	IIB	23
14	58	M	pancreatic cancer	13/10/2011	4.7	normal duct, PanIN 1, PanIN 2	pT3N1	IIB	4

TNM - tumour staging system; **IPMN** - intraductal pancreatic mucinous neoplasm; **PanIN** - pancreatic intraepithelial neoplasia

Patient no.	Age	Sex	Diagnosis	Date of surgery	Tumour size (cm)	Histology	TNM	Stage	Survival (months)
15	54	M	lympho-epithelial cyst	11/02/2010	n/a	normal duct	n/a	n/a	n/a
16	67	F	pancreatic cancer	14/10/2011	3.5	normal duct, PanIN 1	pT3N0	IIA	12
17	62	F	chronic pancreatitis	07/10/2011	3.7	normal duct, PanIN 1	n/a	n/a	n/a
18	60	M	well differentiated endocrine tumour	03/11/2011	n/a	normal duct	n/a	n/a	n/a
19	61	F	pancreatic cancer	29/09/2011	3	normal duct, PanIN 1, PanIN 2, PanIN 3	pT3N1	IIB	17

TNM - tumour staging system; **IPMN** - intraductal pancreatic mucinous neoplasm; **PanIN** - pancreatic intraepithelial neoplasia

Patient no.	Age	Sex	Diagnosis	Date of surgery	Tumour size (cm)	Histology	TNM	Stage	Survival (months)
20	74	F	pancreatic cancer	24/11/2011	n/a	normal duct, PanIN 1	pT2N0	IB	18
21	67	F	multiple congenital cysts	09/12/2011	n/a	normal duct, PanIN 1	n/a	n/a	n/a
22	68	M	pancreatic cancer	27/01/2012	6	PanIN 3, invasive cancer	pT3N1	IIB	6
23	82	M	pancreatic cancer	24/02/2012	4	invasive cancer	pT3N1	IIB	20
24	70	M	pancreatic cancer	01/03/2012	4.9	invasive cancer	pT3N1	IIB	9

TNM - tumour staging system; **IPMN** - intraductal pancreatic mucinous neoplasm; **PanIN** - pancreatic intraepithelial neoplasia

Patient no.	Age	Sex	Diagnosis	Date of surgery	Tumour size (cm)	Histology	TNM	Stage	Survival (months)
25	63	F	benign peritoneal pseudocyst	26/01/2012	n/a	normal duct	n/a	n/a	n/a
26	72	M	pancreatic cancer	30/03/2012	5.5	invasive cancer	pT3N1	IIB	7
27	53	F	pancreatic cancer	08/03/2012	2.8	invasive cancer	pT3N1	IIB	9
28	77	M	pancreatic cancer	12/04/2012	3.5	PanIN 2, invasive cancer	pT3N1	IIB	6
29	58	F	multiple small epithelial cysts	29/03/2012	n/a	normal duct	n/a	n/a	n/a

TNM - tumour staging system; **IPMN** - intraductal pancreatic mucinous neoplasm; **PanIN** - pancreatic intraepithelial neoplasia

Patient no.	Age	Sex	Diagnosis	Date of surgery	Tumour size (cm)	Histology	TNM	Stage	Survival (months)
30	77	M	IPMN	23/12/2011	n/a	normal, PanIN 2, invasive cancer	pT3N0	IIA	18

TNM - tumour staging system; **IPMN** - intraductal pancreatic mucinous neoplasm; **PanIN** - pancreatic intraepithelial neoplasia

A total number of 68 histological lesions were identified including 3 normal ducts from non-malignant specimens, 22 normal ducts from PDAC specimens, 11 ducts with PanIN 1A, 12 ducts with PanIN 1B, 7 ducts with PanIN 2, 7 ducts with PanIN 3 and 8 ducts with PDAC. One lymph node metastasis noted on a PDAC specimen was included in one case analysis but excluded from the overall data analysis.

All the specimens included in this study had ductal adenocarcinoma but the aneuploidy was not scored in the areas with adenocarcinoma, but in ducts away from the tumour to ensure that the premalignant stages were clearly not intraductal carcinoma.

The PanIN lesions were identified and graded by a Consultant Histopathologist with a special interest in pancreatic cancer into PanIN 1A, PanIN 1B, PanIN 2 and PanIN 3 using standard histological criteria previously described in the literature (Hruban RH et al., 2004). The opinion of a second expert was requested and the results of both gradings are detailed in Table 2.2.

Table 2.2: Observer 1 and 2 grading of the histological stages in the specimens included in the study, the differences noted by observer 2 highlighted in red

#	Main Pathology	Observer 1 grading	Observer 2 grading
1	Ductal adenocarcinoma head pancreas		
		PanIN 1B	PanIN 1B + CA in duct
		Squamous metaplasia	PanIN 1B + focus CA in duct
		N	N
2	IPMN no invasion		
		PanIN 1B ?2	LGD in IPMN
		PanIN 1B	LGD IN IPMN
		N	N
3	IPMN no invasion		
		? PanIN 2	PanIN 1A
		PanIN 1B	PanIN 1B and LGD in IPMN
		N	N

N = normal (duct); **PanIN** = pancreatic intraepithelial neoplasia; **CA** = carcinoma; **IPMN** = intraductal pancreatic mucinous neoplasia; **LGD** = low grade dysplasia

#	Main Pathology	Observer 1 grading	Observer 2 grading
4	Ductal adenocarcinoma head pancreas		
		N	N
		PanIN 1A/1B	PanIN 1B
		PanIN 1B	PanIN 1B ?2
5	Ductal adenocarcinoma head pancreas		
		PanIN 1B	PanIN 3
		N	N
		PanIN 2	PanIN 3
6	Ductal adenocarcinoma head pancreas		
		N	N
7	Ductal adenocarcinoma head pancread		
		N	N
		N	PanIN 1B
8	Ductal adenocarcinoma head pancreas		
		PanIN 2	PanIN 2
		N	N and PanIN 1A
9	Cholangiocarcinoma		
		PanIN 1B	PanIN 1B
10	Cholangiocarcinoma		
		N	N
11	Ductal adenocarcinoma head pancreas		
		PanIN 3	CA
12	Ductal adenocarcinoma head pancreas		
		PanIN 1A	PanIN 1A

N = normal (duct); **PanIN** = pancreatic intraepithelial neoplasia; **CA** = carcinoma; **IPMN** = intraductal pancreatic mucinous neoplasia; **LGD** = low grade dysplasia

#	Main Pathology	Observer 1 grading	Observer 2 grading
13	Ductal adenocarcinoma head pancreas		
		PanIN 2 ?1B	PanIN 2
		N	N
		CA metastasis	CA metastasis
14	Adenocarcinoma arising in IPMN		
		N	N
		PanIN 2	PanIN 2 + 3
15	Ampullary carcinoma		
		N	N
		PanIN 2	PanIN 1B and 2
16	Ductal adenocarcinoma head pancreas		
		N	N
		PanIN 3/CA	CA in duct
		PanIN 1A	PanIN 1B
17	Ductal adenocarcinoma head pancreas		
		PanIN 1A	PanIN 1B
		N	N
18	Ductal adenocarcinoma head pancreas		
		N	N
		Squamous metaplasia	PanIN 1A/Squamous metaplasia
19	Ductal adenocarcinoma head pancreas		
		PanIN 1A	PanIN 1B
		N	N
20	Ductal adenocarcinoma head pancreas		
		PanIN 2	CA in duct

N = normal (duct); **PanIN** = pancreatic intraepithelial neoplasia; **CA** = carcinoma; **IPMN** = intraductal pancreatic mucinous neoplasia; **LGD** = low grade dysplasia

#	Main Pathology	Observer 1 grading	Observer 2 grading
21	Ductal adenocarcinoma head pancreas		
		PanIN 1B	PanIN 1B
		N	N
22	Lympho-epithelial cyst		
		N	N
23	Ampullary carcinoma. Deep pancreas invasion		
		N	N
		PanIN 2	PanIN 1B
		PanIN 3/CA	CA in lymph duct
24	Ductal adenocarcinoma head pancreas		
		PanIN 2	CA in lymph duct?
		PanIN 1B	PanIN 1B
		N	N
25	Ductal adenocarcinoma head pancreas		
		PanIN 2	PanIN 2
		PanIN 1B	PanIN 1B
		N	N + PanIN 1B
26	Ductal adenocarcinoma head pancreas		
		N	N
		PanIN 2	PanIN 1B and 2
		PanIN 3	CA in duct
		CA	CA
27	Duodenal carcinoma		
		PanIN 2 ?1B	PanIN 2
		N	N
28	Endocrine tumour		
		N	N

N = normal (duct); **PanIN** = pancreatic intraepithelial neoplasia; **CA** = carcinoma; **IPMN** = intraductal pancreatic mucinous neoplasia; **LGD** = low grade dysplasia

#	Main Pathology	Observer 1 grading	Observer 2 grading
29	Ampullary carcinoma		
		N	N
		PanIN 1A	PanIN 1B
30	Ampullary carcinoma		
		PanIN 1B	PanIN 1B
31	Multiple congenital cysts		
		N	N
32	Multiple congenital cysts		
		PanIN 1A	PanIN 1B
33	Adenocarcinoma arising in IPMN		
		PanIN 2	Intermediate grade dysplasia
		CA	CA
34	Multiple congenital cysts		
		N	N
35	Ductal adenocarcinoma		
		CA	CA
36	Ductal adenocarcinoma		
		PanIN 2	PanIN 2 + CA in duct
		CA	CA
37	Ductal adenocarcinoma		
		CA	CA
38	Peritoneal pseudocysts		
		N	N

N = normal (duct); **PanIN** = pancreatic intraepithelial neoplasia; **CA** = carcinoma; **IPMN** = intraductal pancreatic mucinous neoplasia; **LGD** = low grade dysplasia

#	Main Pathology	Observer 1 grading	Observer 2 grading
39	Ductal adenocarcinoma		
		PanIN 3	CA in duct
		PanIN 2	CA
		PanIN 3	CA in duct
40	Ductal adenocarcinoma		
		CA	CA
41	Multiple epithelial cysts (? acinar cell cystadenoma)		
		N	N
42	Neuroendocrine carcinoma		
		PanIN 3	CA
		CA	CA
43	Ductal adenocarcinoma		
		CA	CA

N = normal (duct); **PanIN** = pancreatic intraepithelial neoplasia; **CA** = carcinoma; **IPMN** = intraductal pancreatic mucinous neoplasia; **LGD** = low grade dysplasia

There was agreement in all but one case for the normal ducts, in 84.2% for the PanIN 1, in 46.6% for the PanIN 2, in no case for the PanIN 3 and in all cases for the carcinoma stage. 5 out of 6 PanIN 1A lesions were classed by the second observer as PanIN 1B. One PanIN 1B was graded as PanIN 3 which highlights the fact that not only the macroscopic characteristics but also the topography related to the main tumour has to be included in the grading criteria. Over 50% of the PanIN 2 received a different or a mixed grading from the second observer, with some ducts displaying a lower or higher grade or even carcinoma. Noteworthy, most of the PanIN 3 lesions were classed by the second observer as intraductal carcinoma, which highlights the difficulties in isolating with confidence the late premalignant stages in a specimen with carcinoma. Only by surveying areas as distant as possible from the main tumour the grading of these premalignant lesions could be confidently done. Another method of differentiation would be by using molecular markers which could allow for confident grading. In this study, the final analysis was based on the grading provided by the first observer to ensure consistency with other linked studies. It is worth mentioning that in studies on dysplasia the concordance between experts is poor as measured by the inter-observer

kappa values (κ) and that there is no study of observer agreement between experts for PanINs. κ values higher than 0.60 indicate good and very good strength of agreement. Montgomery demonstrated the existing poor agreement in assessing Barrett's dysplasia amongst a panel of international experts (κ=0.15-0.32) (Montgomery et al., 2001).

2.2.2 Optimization

The protocol used in this study was optimized for pancreatic tissue starting from the validated FISH protocol used for diagnostic human epidermal receptor type 2 (Her2/neu) gene status in breast cancer. The FISH assay is based on the gene copy number and the ratio between the numbers of Her2 and Chromosome 17 sequences (Wolff AC et al., 2007).

The mentioned protocol is a validated diagnostic protocol and has been used routinely for several years in the Graduate Entry Pathology Laboratory, Singleton Hospital, Abertawe Bro Morgannwg University Health Board Swansea. The senior staff in the Pathology Laboratory demonstrated the protocol then supervised the first independent run and was available for troubleshooting when needed throughout the project work. The final protocol used for pancreatic tissue followed the exact same steps with few adjustments highlighted in the description below.

The protocol consisted of the following steps:

1. The 4 μm paraffin-embedded tissue sections on glass slides (Menzel-Glaser Superfrost, Fisher Scientific UK Ltd) were baked overnight at 65°C.

2. De-waxing was achieved by placing the slides in two consecutive Xylene washes (Fisher Scientific UK Ltd) at room temperature (RT) for 10 minutes.

3. The slides were immersed in two consecutive 100% Industrial Methylated Spirit (IMS) washes (Fisher Scientific UK Ltd) for 5 minutes at RT.

4. Air dry stage.

5. The slides were immersed in consecutive solutions 100% IMS, 85% IMS and 70% IMS for 1 minute each at RT.

   The 85% IMS solution was prepared by mixing 85 mL 100% IMS and 15 mL distilled water (H_2O_2). The 70% IMS solution was prepared by mixing 70 mL 100% IMS and 30 mL H_2O_2. Between uses, the solutions were kept tightly covered at room temperature. The unused stock was discarded after 6 months (`www.abbottmolecular.com`).

6. The slides were immersed in H_2O_2 for 1 minute at RT.

7. Acid permeabilisation was achieved by placing the slides in 0.2N hydrogen chloride (HCl) solution (Sigma-Aldrich Co UK) for 20 minutes at RT.

8. The slides were immersed in H_2O_2 for 3 minutes at RT.

9. The slides were immersed in wash buffer (Vysis Paraffin Pretreatment IV & Post-Hybridization Wash Buffer Kit, Abbott Molecular England) for 3 minutes at RT.

   The wash buffer solution was provided by the manufacturer (Abbott Molecular England) and represented a 2X SSC/0.1% NP-40 Wash Solution. It can be prepared by mixing vigorously 100 mL 20X SSC (pH 5.3) and 850 mL H_2O_2 and then adding 1 mL NP-40. The solution pH was adjusted to 7.0 $\pm$ 0.2 using sodium hydroxide (NaOH). H_2O_2 was added to bring the final volume to 1L. The solution was stored in a covered container at room temperature. The unused solution was discarded after 6 months or earlier if it appeared cloudy or contaminated.

10. The slides were placed in glass Coplin jars (Thermo Scientific, Fisher Scientific UK Ltd) containing the pre-treatment solution (8% sodium thiocyanate) (Vysis Paraffin Pretreatment IV & Post-Hybridization Wash Buffer Kit, Abbott Molecular England) in a water bath (VWR 1229 Water Bath, VWR International UK) at 80°C for 30 minutes. The glass Coplin jars (Thermo Scientific, Fisher Scientific UK Ltd) containing the solution were placed in the cold water bath and the temperature was increased gradually to avoid the glass cracking/breaking before the slides were added.

11. The slides were immersed in H_2O_2 for 1 minute at RT.

12. The slides were immersed in wash buffer (Vysis Paraffin Pretreatment IV & Post-Hybridization Wash Buffer Kit, Abbott Molecular England) twice for 5 minutes at RT.

13. The slides were placed in glass Coplin jars containing a protease solution with 0.005% pepsin enzyme (Vysis Paraffin Pretreatment IV & Post-Hybridization Wash Buffer Kit, Abbott Molecular England) added approximately 5 minutes to the protease buffer (Vysis Paraffin Pretreatment IV & Post-Hybridization Wash Buffer Kit, Abbott Molecular England) before introducing the slides. The slides were kept in the jars in a water bath (VWR 1229 Water Bath, VWR International UK) at 37°C for 30 min. This represented the digestion phase required to allow probe access by opening up the cytoplasm. It was one of the critical stages as suboptimal digestion impacts on the final scoring.

    When a new protease batch was used, the protocol included an additional stage to ensure optimal digestion: the product used for nuclear staining (in this case, DAPI III Counterstain, Abbott Molecular England) was added to the slides and cover slips were applied; the slides were examined under the microscope – usually, optimal digestion was illustrated by homogeneously stained nuclei which

looked slightly swollen compared to under-digested tissue; suboptimal digestion could appear as heterogeneous nuclear staining while over-digestion was demonstrated by damaged nuclear membranes. In case of insufficient digestion, the cover slips could be removed and the slides added to the protease buffer for extra time until optimal digestion was achieved. In case of over-digestion, the slides could not be reliably scored so they were discarded and fresh tissue sections were used to restart the protocol using a reduced digestion stage until optimal digestion was achieved.

The time interval for the digestion stage was readjusted repeatedly in the optimization phase until an optimal time of 30 min for PDAC tissue digestion was reached.

14. The slides were dipped in wash buffer (Vysis Paraffin Pretreatment IV & Post-Hybridization Wash Buffer Kit, Abbott Molecular England) for 5 times at RT.

15. The slides underwent fixation in neutral buffered formol saline solution (Sigma-Aldrich Co UK) for 10 minutes at RT.

16. The slides were immersed in wash buffer (Vysis Paraffin Pretreatment IV & Post-Hybridization Wash Buffer Kit, Abbott Molecular England) for 5 minutes at RT.

17. The slides were immersed consecutively in 70% IMS, 85% IMS and 100% IMS for 1 minute each at RT.

18. Air dry stage.

19. The slides were placed in glass Coplin jars containing 70% Formamide solution in a water bath (VWR 1229 Water Bath, VWR International UK) at 72°C for 7 min. The glass Coplin jars (Thermo Scientific, Fisher Scientific UK Ltd) containing the solution were placed in the cold water bath and the temperature was increased gradually to avoid the glass cracking/breaking before the slides are added. After use, the solution was discarded using the toxic products handling protocol in the toxic waste container which was collected regularly for disposal as per toxic waste protocol. This stage represented the denaturation of DNA stage whereby the DNA double strand was separated into single strands to allow hybridization with the probe in the hybridization stage. The 70% Formamide solution was prepared in a fume hood using the toxic products handling protocol, by mixing 49 mL ultrapure formamide (Fisher Scientific UK Ltd) stored in the toxic products compartment, 7 mL 20X SSC (pH 5.3) and 14 mL H_2O_2 in a glass Coplin jar (Thermo Scientific, Fisher Scientific UK Ltd). The pH was measured using a pH meter with a glass electrode to ensure pH was 7.0-8.0. The

solution was stored between uses in a secured container in the toxic products compartment at 2-8°C. It was discarded after 7 days.

The time interval for the denaturation stage was readjusted repeatedly in the optimization phase until an optimal time of 5 min for PDAC tissue was reached.

20. The slides were dipped in H_2O_2 x 5 times at RT in the fume hood. After use, the H_2O_2 was discarded using the toxic products handling protocol in the toxic waste container.

21. The slides were immersed consecutively in 70% IMS, 85% IMS and 100% IMS for 1 minute each at RT in the fume hood. After use, the 70% IMS and 85% IMS solutions were discarded using the toxic products handling protocol in the toxic waste container.

22. Air dry in the fume hood.

23. The chromosome probe mixture was added to each slide in the fume hood, ensuring minimal exposure to light to prevent degradation of the fluorescence. Also, uniform coverage of the relevant area of the tissue section was vital.

    The probes used were centromeric enumeration probes (CEP) (fluorophore-labeled enumerator probe and blocking DNA in Tris-EDTA buffer) for chromosomes 1 (band region 1p11-q11, locus D1Z5, Orange), 6 (band region 6p11.1-q11, locus D6Z1, Green), 9 (band region 9p11-q11, Green) and 18 (band region 18p11.1-q11.1, locus D18Z1, Orange) (Vysis, UK).

    The composition of the probe mixture was repeatedly readjusted during the optimisation phase until an optimal formula was reached to ensure satisfactory scoring. We used 2 μl of each CEP probe and 6 μl of CEP hybridization buffer (Dextran sulphate, Formamide, SSC)(Vysis, UK). They were stored at –20°C prior to use.

24. Cover slips were applied, most commonly 22 x 30 mm (Menzel-Glaser, Fisher Scientific UK Ltd) but occasionally of a different size depending on the size of the relevant tissue section.

25. The cover slips were sealed in place using commercial rubber solution (Halfords Group plc) applied in a thin layer on the margins and on the adjacent area of the glass slide. Minimal exposure to light was ensured during this stage.

26. The slides were then placed in a pre-warmed Hybrite (Vysis Slide Stainer, Abbott Molecular England) and incubated for 16 hours overnight at 37°C.

27. The slides were removed from the Hybrite promptly after the 16 hours and the rubber seal was gently removed to prevent any movement of the cover slip and with minimal exposure to light.

28. The slides were immersed in posthybridization wash buffer (Vysis Paraffin Pretreatment IV & Post-Hybridization Wash Buffer Kit, Abbott Molecular England), protected from direct light, until the cover slips became loose and were removed.

29. The slides were placed in glass Coplin jars containing posthybridization wash buffer (Vysis Paraffin Pretreatment IV & Post-Hybridization Wash Buffer Kit, Abbott Molecular England) in a water bath (VWR 1229 Water Bath, VWR International UK) at 72°C for 2 minutes in the fume hood. The glass Coplin jars (Thermo Scientific, Fisher Scientific UK Ltd) containing the solution were placed in the cold water bath and the temperature was increased gradually to avoid the glass cracking / breaking before the slides were added.

30. The slides were rinsed vigorously for 10-15 seconds in the hot fluid from the previous stage which had been transferred to a wash pot. This stage was important to ensure any redundant superfluous chromosome probe was washed off.

31. The slides were immersed in fresh posthybridization wash buffer (Vysis Paraffin Pretreatment IV & Post-Hybridization Wash Buffer Kit, Abbott Molecular England) for 2 minutes at RT, protected from direct light.

32. The slides were dipped in 70% IMS at RT.

33. Air dry in the dark.

34. 10 μl DAPI III Counterstain (Abbott Molecular England) was added to each slide as a contrast media for the nucleoplasm, ensuring uniform coverage of the relevant tissue area and minimal exposure to light.

    We used 10 μl of Vectashield Antifade 4′, 6-diamidino-2-phenylindole (DAPI) 125 μg/ml (Vector Laboratories, Inc. Burlingame, CA 94010) for each section with satisfactory results.

35. Cover slips were applied, most commonly 22 $\times$ 30 mm (Menzel-Glaser, Fisher Scientific UK Ltd) but occasionally of a different size depending on the size of the relevant tissue section. They were fixed in place using commercial adhesive products (i.e. clear nail varnish).

36. The slides were stored in the dark until scoring.

Negative and positive control sections were included in the treatment algorithm with each set of tissue sections. The negative control was represented by a tissue section from one of the breast cancer specimens included in the treatment which did not have the fluorescent probe added to it. The positive control was represented by a tissue section from a breast cancer specimen which had previously been treated and scored according to the manufacturer's instructions.

2.3 Results

The work for the present study was performed on formalin-fixed paraffin embedded (FFPE) archival tissue sections from tissue blocks obtained after elective surgical resection for malignant or benign pancreatic disease and stored in the Histopathology Department, Morriston Hospital, ABMU Health Board Swansea.

Each set of sections was accompanied by a haematoxylin and eosin stained section from the same tissue block which was used to identify and match the relevant histopathological structures with the sections used for FISH (Fig. 2.1-2.6).

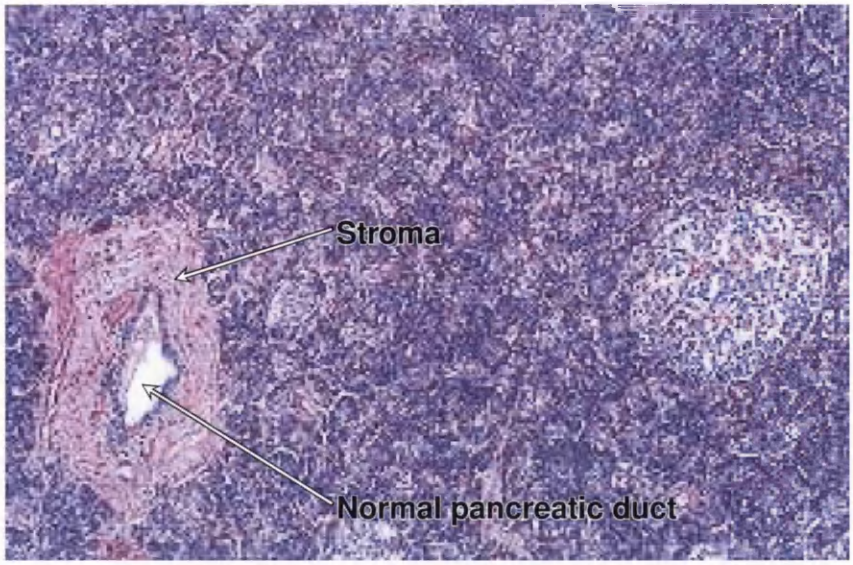

(a) Haematoxylin-eosin (HE) section $\times 10$ showing the ductal cells in a single layer

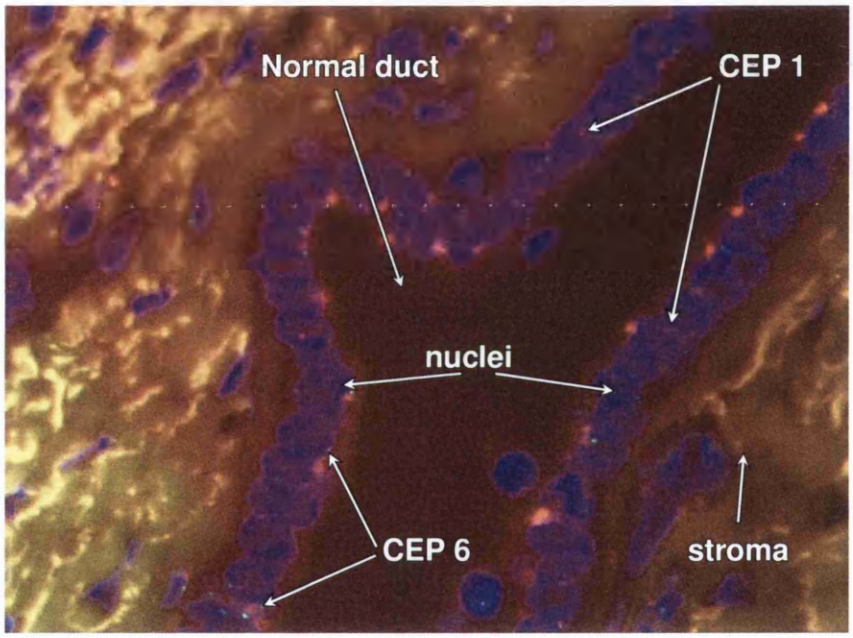

(b) FISH section $\times 60$ seen with DAPI filter showing a fragment of the duct with CEP 6 green signals, CEP 1 orange signals, DAPI blue cells nuclei and non-specific cytoplasmic uptake in the stromal layer .

Figure 2.1: Tissue section from a normal specimen; the relevant duct and the surrounding stroma highlighted on the HE section; the CEP signals and relevant histological structures highlighted on the FISH section.

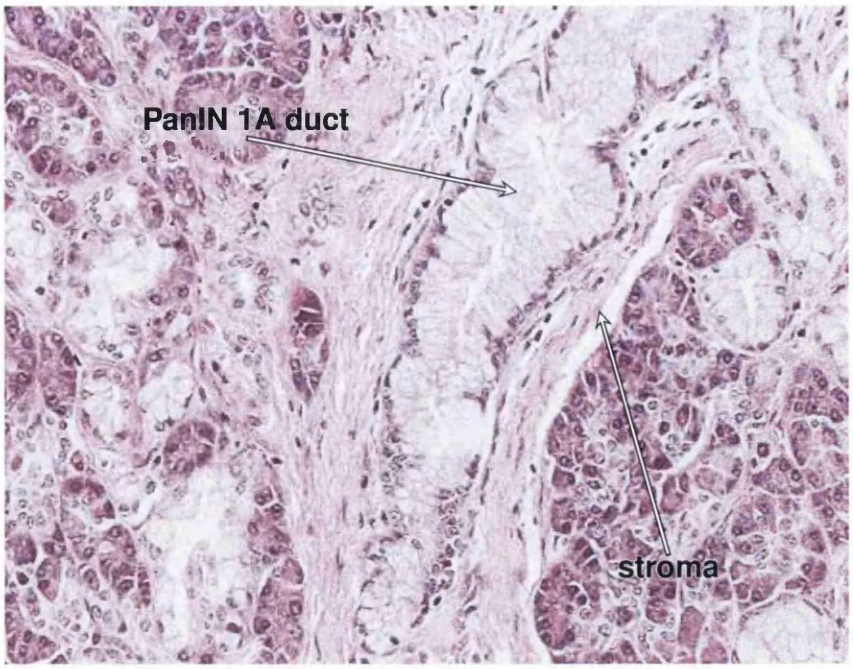

(a) Haematoxylin-eosin (HE) section ×10 showing the ductal cells in a single layer with mucin accumulation at the apical pole.

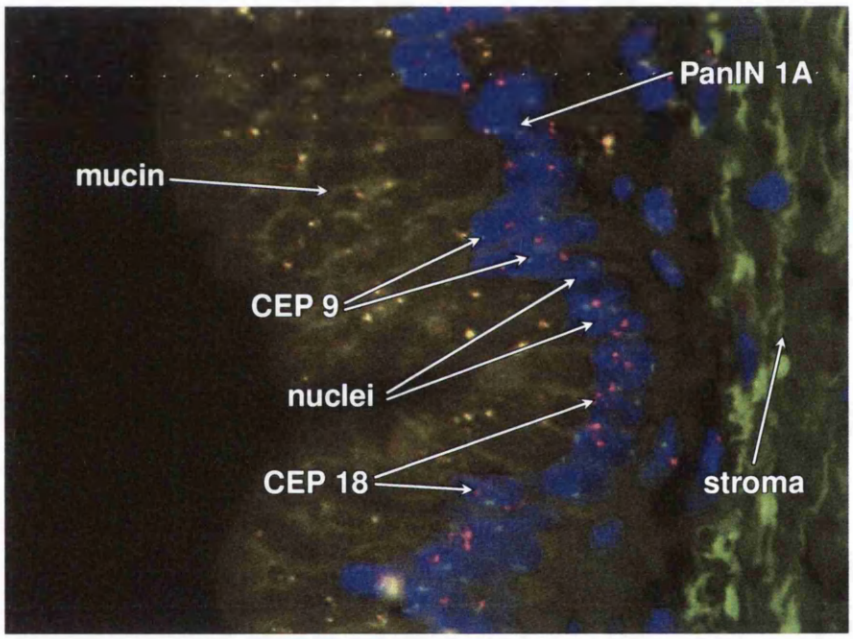

(b) FISH section ×60 seen with DAPI filter showing a fragment of the duct with CEP 9 green signals, CEP 18 orange signals, DAPI blue cells nuclei and non-specific cytoplasmic uptake in the stromal layer as well as the mucin layer.

Figure 2.2: Tissue section from a specimen with PanIN 1A; the relevant duct and the surrounding stroma highlighted on the HE section, ; the CEP signals and relevant histological structures highlighted on the FISH section.

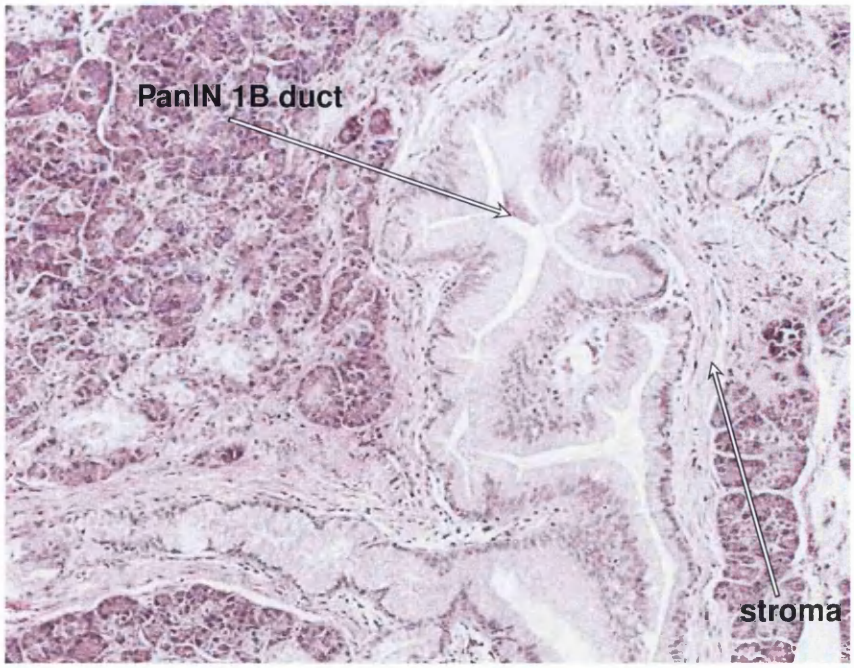

(a) Haematoxylin-eosin (HE) section ×10 showing the duct with areas of multilayered cells with mucin accumulation at the apical pole.

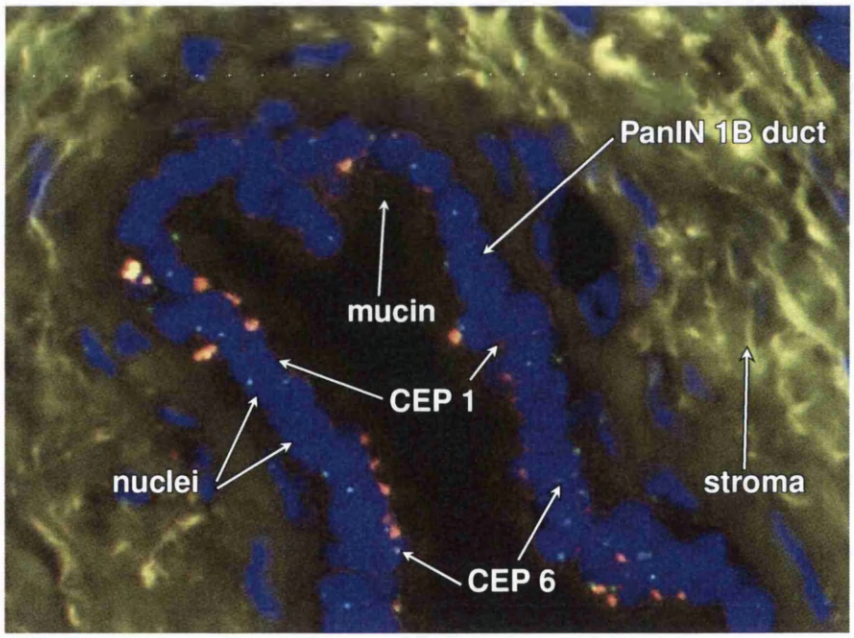

(b) FISH section ×60 seen with DAPI filter showing a fragment of the duct with CEP 6 green signals, CEP 1 orange signals, DAPI blue cells nuclei and non-specific cytoplasmic uptake in the stromal layer.

Figure 2.3: Tissue section from a specimen with PanIN 1B; the relevant duct and the surrounding stroma highlighted on the HE section, ; the CEP signals and relevant histological structures highlighted on the FISH section.

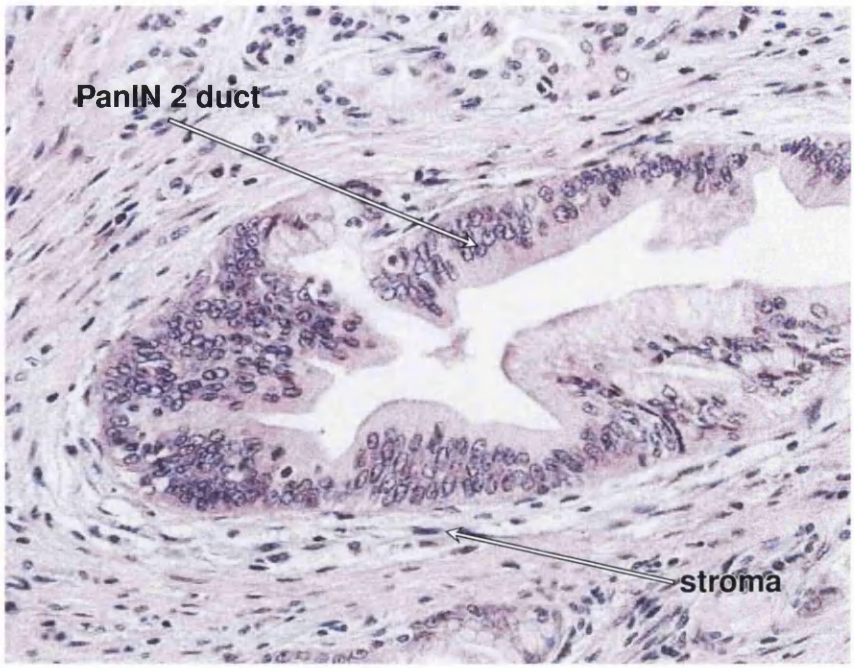

(a) Haematoxylin-eosin (HE) section ×10 showing the multilayered ductal cells with mucin accumulation at the apical pole

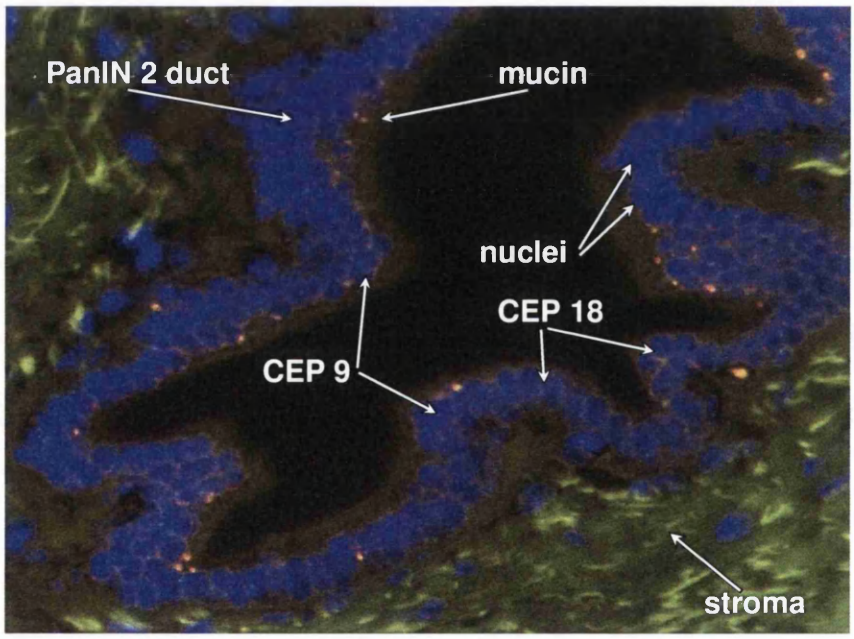

(b) FISH section ×60 seen with DAPI filter showing a fragment of the duct with CEP 9 green signals, CEP 18 orange signals, DAPI blue cells nuclei and non-specific cytoplasmic uptake in the stromal layer as well as the mucin layer.

Figure 2.4: Tissue section from a specimen with PanIN 2; the relevant duct and the surrounding stroma highlighted on the HE section, ; the CEP signals and relevant histological structures highlighted on the FISH section.

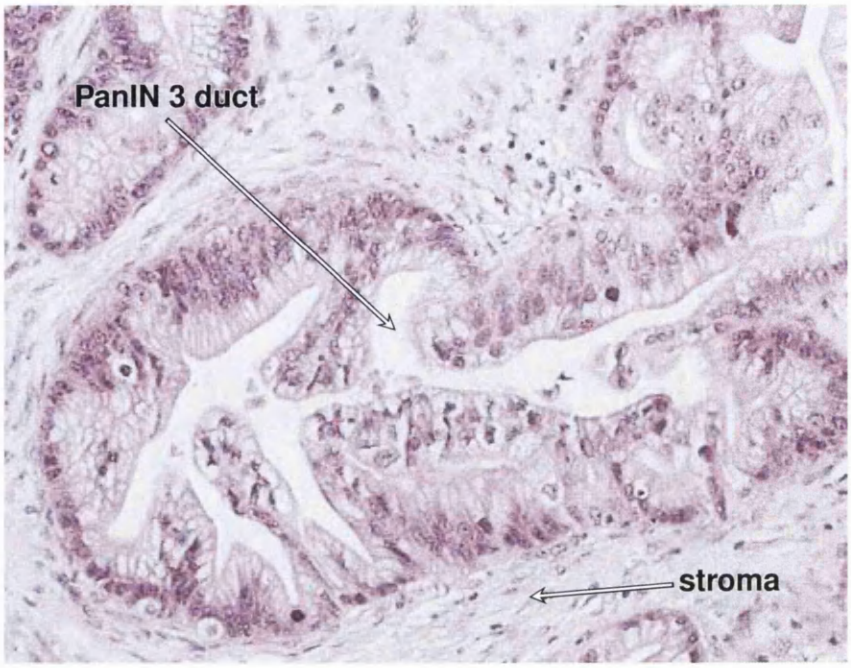

(a) Haematoxylin-eosin (HE) section ×10 showing the multilayered ductal cells with some desquamation from the top layer and mucin accumulation at the apical pole.

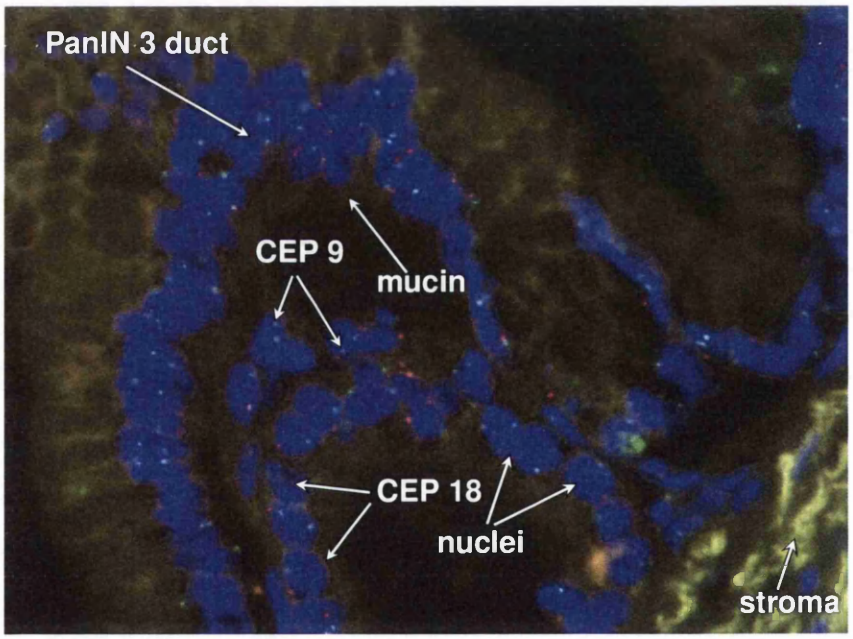

(b) FISH section ×60 seen with DAPI filter showing a fragment of the duct with CEP 9 green signals, CEP 18 orange signals, DAPI blue cells nuclei and non-specific cytoplasmic uptake in the stromal layer as well as the mucin layer.

Figure 2.5: Tissue section from a specimen with PanIN 3; the relevant duct and the surrounding stroma highlighted on the HE section, ; the CEP signals and relevant histological structures highlighted on the FISH section.

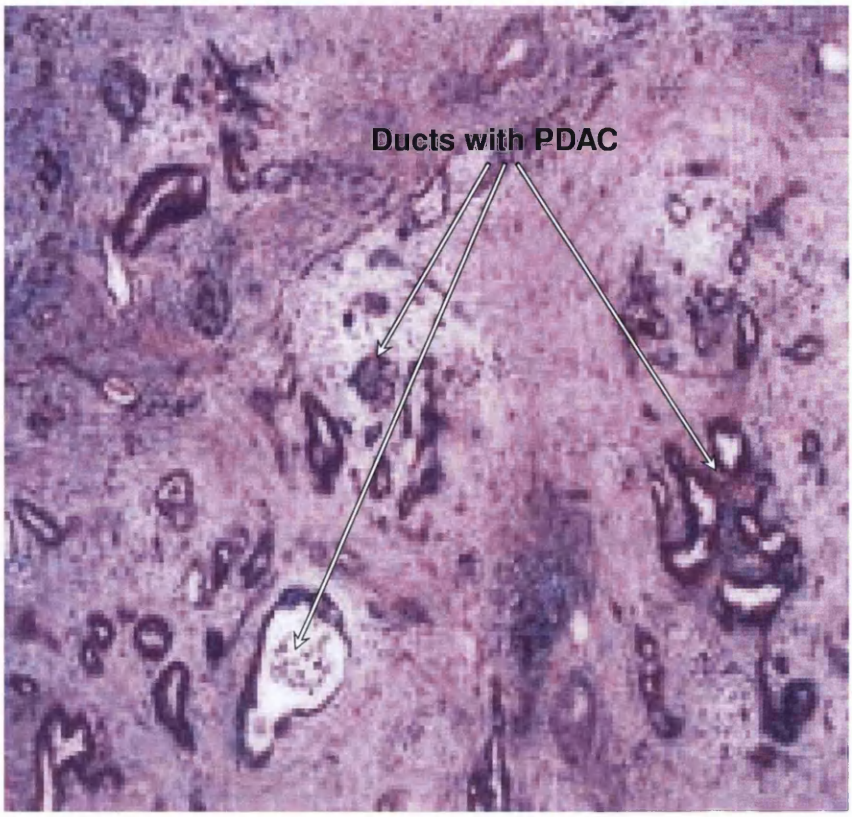

(a) Haematoxylin-eosin (HE) section ×10 showing multiple ducts with distorted architecture.

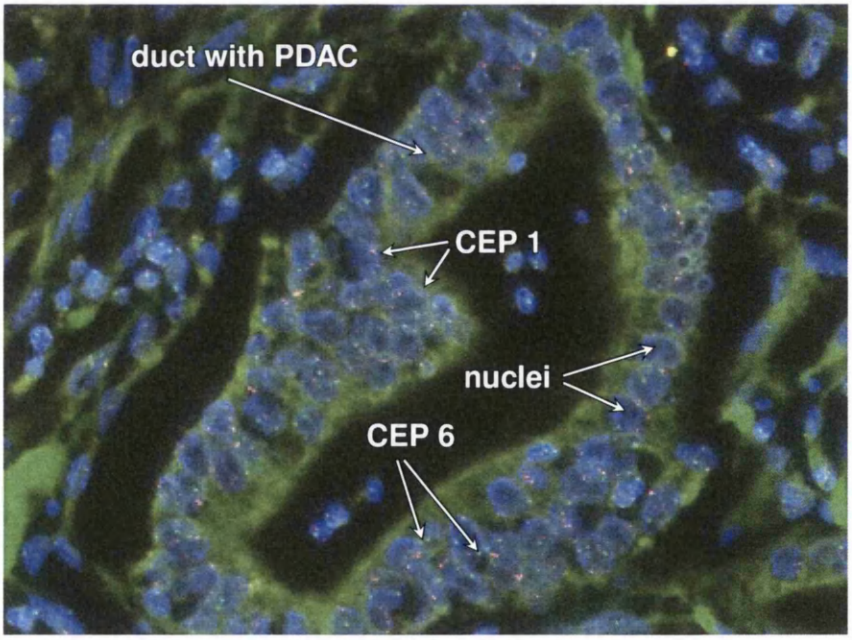

(b) FISH section ×60 seen with DAPI filter showing one duct with CEP 6 green signals, CEP 1 orange signals, DAPI blue cells nuclei and non-specific cytoplasmic uptake.

Figure 2.6: Tissue section from a specimen with PDAC; the relevant ducts highlighted on the HE section; the CEP signals and relevant histological structures highlighted on the FISH section.

After completing the treatment the sections were assessed to ensure adequate digestion and hybridization. If suitable, they were then scored manually for aneuploidy using a Zeiss Axio Imager Z1 Fully Motorised Upright microscope with MetaSystems Isis FISH imaging software, equipped with DAPI, Spectrum Green and Spectrum Orange filters.

The principal investigator performed all the steps in the manual protocol for FISH treatment and underwent training for manual scoring using the fluorescent microscope. 200 nuclei were scored, on average, in each histological area of interest and the number of chromosome copies was documented in different categories: one copy (deletion), two copies (diploid), more than two copies (amplification). The scoring was done for each of the four chromosome probes.

The main end points in the study were the overall aneuploidy score (mean percentage of aneuploid cells in a pancreatic duct displaying a certain histological stage), the level of deletions (mean percentage of cells with chromosomal deletions in a pancreatic duct displaying a certain histological stage) and the level of amplifications (mean percentage of cells with chromosomal amplifications in a pancreatic duct displaying a certain histological stage). The results for each category were entered into statistical analysis to uncover potential significant variations between different histological stages. A total of 146000 cells have been scored. Occasionally the architecture of the pancreatic ducts with advanced premalignant lesions precluded confident scoring because of overlapping of the nuclei and those areas have been excluded to avoid overscoring for amplifications (Fig. 2.7).

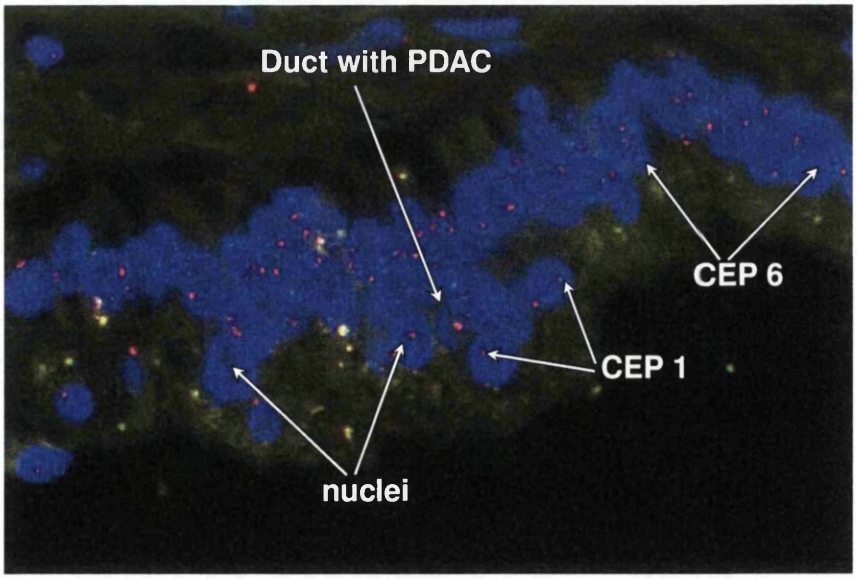

Figure 2.7: Area with overlapping nuclei in a pancreatic duct with adenocarcinoma after hybridization with dual probe CEP 1 (Orange signals) and CEP 6 (Green signals); the blue staining is the result of nuclear staining with DAPI; the green internuclear staining represents non-specific cytoplasmic uptake.

2.3.1 Statistical analysis

The final results were divided into overall, average and individual levels of chromosomal abnormalities (aneuploidy, amplifications and deletions, respectively) for chromosomes 1, 6, 9 and 18.

The final results were processed using Microsoft Excel 2007 and IBM SPSS Statistics version 2011. The Student paired t-test was used to uncover potential significant differences between paired histological stages as reflected in the levels of overall aneuploidy, deletions and amplifications. The one-way analysis of variance (ANOVA) was used to determine the differences across all the histological groups. Significance was attributed to a p-value less than 0.05.

Several case studies were included to illustrate individual patterns for aneuploidy progression in individual tumours.

The scoring results for overall aneuploidy, overall amplifications and overall deletions for each chromosome in different histological stages were introduced respectively in statistical analysis using Student paired t-test to determine significant differences between different histological stages (Table 2.3).

Table 2.3: Statistical analysis using Student paired t-test to compare pairs of histological groups for each chromosome for overall aneuploidy, overall amplifications and overall deletions. Only significant results (∗) represented by $p<0.05$ are documented.

		Normal/ Normal Specimens	Normal/ Cancer Specimens	PanIN 1	PanIN 2	PanIN 3
Chromosome 1	PanIN 1					
	PanIN 2					
	PanIN 3		p=0.002 ∗amplifications	p=0.0009 ∗amplifications		
	PDAC	p=0.002 ∗aneuploidy			p=0.024 ∗amplifications p=0.014 ∗aneuploidy	

		Normal/ Normal Specimens	Normal/ Cancer Specimens	PanIN 1	PanIN 2	PanIN 3
Chromosome 6	PanIN 1		p=0.031 *amplifications			
	PanIN 2					
	PanIN 3	p=0.049 *deletions p=0.029 *aneuploidy	p=0.044 *aneuploidy			
	PDAC	p=0.028 *deletions p=0.007 *aneuploidy	p=0.0004 *amplifications p=0.043 *aneuploidy	p=0.004 *amplifications	p=0.049 *amplifications	
Chromosome 9	PanIN 1					
	PanIN 2					
	PanIN 3			p=0.033 *amplifications		
	PDAC	p=0.025 *aneuploidy	p=0.0001 *amplifications p=0.001 *aneuploidy	p=0.005 *aneuploidy	p=0.007 *aneuploidy	p=0.048 *amplifications p=0.016 *aneuploidy
Chromosome 18	PanIN 1					
	PanIN 2		p=0.019 *aneuploidy	p=0.039 *amplifications		
	PanIN 3	p=0.027 *aneuploidy	p=0.006 *amplifications	p=0.002 *amplifications p=0.0002 *aneuploidy		
	PDAC	p=0.024 *aneuploidy		p=0.0002 *aneuploidy		

2.3.1.1 Overall aneuploidy

The overall aneuploidy levels for each chromosome probe in a histological lesion resulted from the sum of the deletions percentage and the amplifications percentage corresponding to the lesion. To investigate the overall aneuploidy trend in various histological stages the corresponding results were averaged for each stage and for each chromosome, respectively (Fig. 2.8).

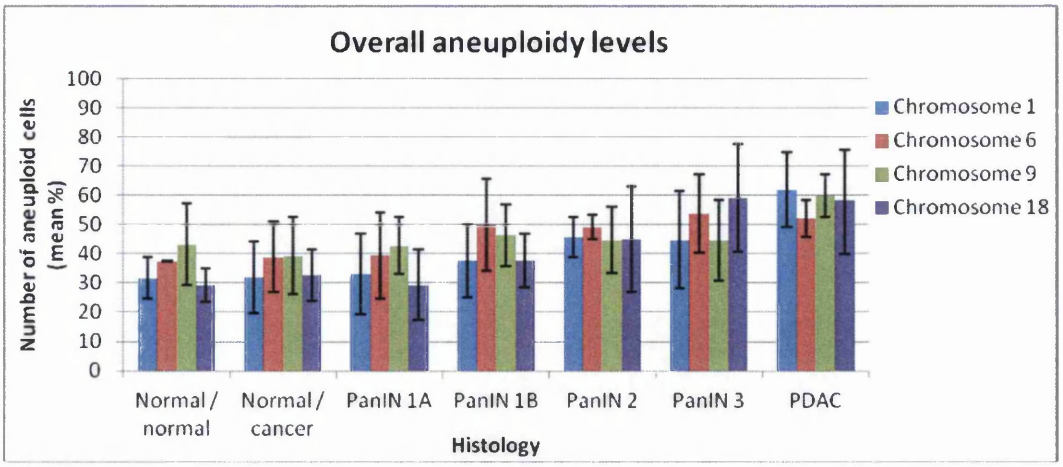

Figure 2.8: Overall number of aneuploid cells (mean%) for chromosomes 1, 6, 9 and 18, respectively, scored in progressive histological stages and demonstrating an increasing trend towards PDAC.

The background level of overall aneuploidy found in normal ducts from the normal specimens was subtracted from the overall aneuplody level found in the normal ducts in the PDAC specimens as well as in PanIN 1, PanIN 2, PanIN 3 and PDAC to reflect the level displayed by the premalignant stages (Fig. 2.9).

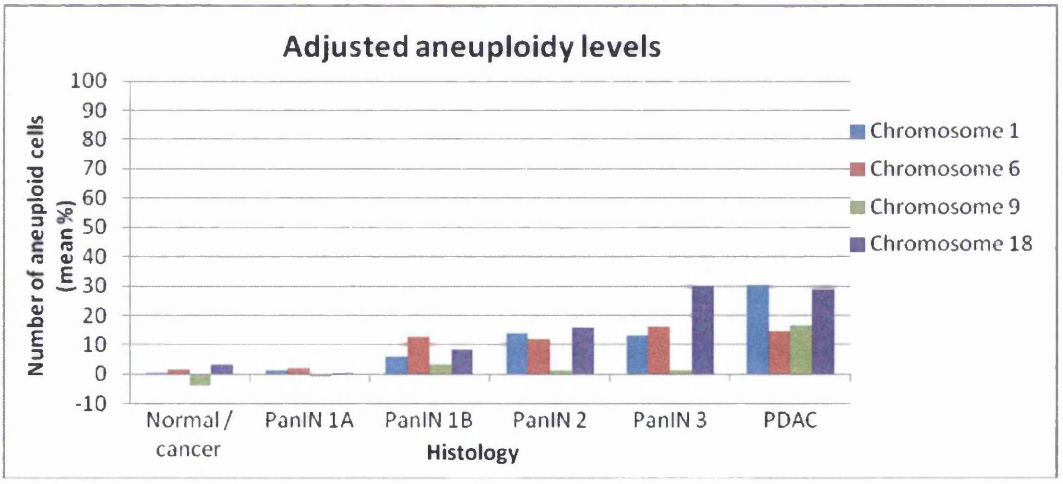

Figure 2.9: Adjusted number of aneuploid cells (mean%) for chromosomes 1, 6, 9 and 18, respectively, scored in progressive histological stages and demonstrating an increasing trend towards PDAC.

The adjusted overall aneuploidy levels showed that, as expected, the levels are very low for all chromosomes in normal ducts and PanIN 1A lesions, displaying negative values as well compared to normal specimens. PanIN 1B lesions showed an increase in the level of overall aneuploidy compared to normal and PanIN 1A stages, while in PanIN 2 the upward trend continued. The PanIN 3 stage seems to reflect the most significant increase for most of the chromosomes analysed and in the last stage, PDAC,

the trend remained constant. For chromosome 1 there was a sharp increase in PDAC, while the levels for chromosome 6 projected an almost linear trend at $12\% \pm 2\%$. The overall chromosome 9 aneuploidy was very low up to the PaIN 3 stage but higher in PDAC. The most consistent upward trend was revealed by the overall aneuploidy levels in chromosome 18, with a marked increase in PanIN 2 compared to the early stages and a further increase in PanIN 3. PDAC displayed similar values compared to PanIN 3.

2.3.1.2 Average aneuploidy

In order to gain insight into the particularities of the histological stages found in the cases included in the current study, the level of average aneuploidy was calculated (Fig. 2.10). This was obtained by averaging the proportion of aneuploid cells across all chromosomes analysed, in ducts with a particular histological stage corresponding to a single specimen. Example: specimen number 3 included 2 normal ducts, 2 ducts with PanIN 1B, one duct with PanIN 2 and one duct with PanIN 3. The average aneuploidy in this specimen for normal ducts was the average between the 2 normal ducts across chromosomes 1, 6, 9 and 18, for PanIN 1B, the average between the 2 ducts with PanIN 1B and for the lone ducts with PanIN 2 or 3 was the average across the 4 chromosomes in the singular duct.

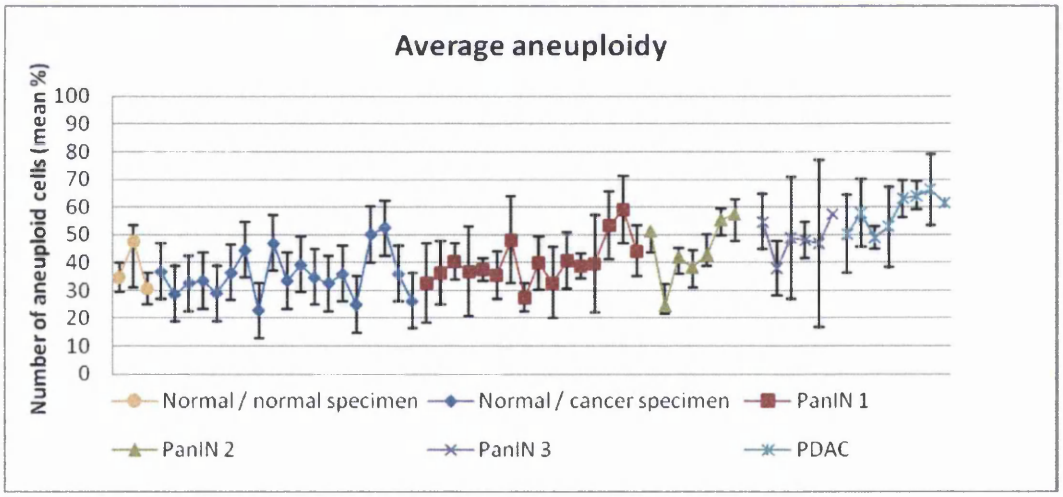

Figure 2.10: The average number of aneuploid cells (mean%) across the histological entities analysed; each vertical bar represents the range of aneuploidy across all chromosomes (mean%); each point on the graph represents a duct with the corresponding histological grade as listed in lower legend.

Each specimen displayed an individual trend between different histological stages, generally starting on a baseline in PanIN 1 and PanIN 2 and increasing in PanIN 3 and PDAC. The specimens with advanced stages (PanIN 3, PDAC) had a higher level of average aneuploidy compared to specimens containing only early stages (PanIN 1,

PanIN 2). There was a noticeable wide range of scores for aneuploidy in the PanIN 3 lesions for the different chromosome probes. The average aneuploidy in PDAC was significantly higher compared to all the other stages (p=0.002 vs normal ducts from normal specimens, p=0.013 vs PanIN 2, p=0.028 vs PanIN 3). Also, the levels seen in PanIN 3 were significantly higher when compared to the normal ducts (p=0.001) and to the levels in PanIN 1 (p=0.025). Even at the PanIN 2 stage there was a significant increase when compared to the normal ducts (p=0.036). This confirmed that aneuploidy in all the chromosomes investigated in this study increased with the histological stage.

2.3.1.3 Overall amplifications

Amplifications were a significant molecular event in any histological stage and they had not been adjusted in relation to the normal specimens. They were less likely to be influenced significantly by sectioning bias and were more common in the advanced premalignant stages (Fig. 2.11).

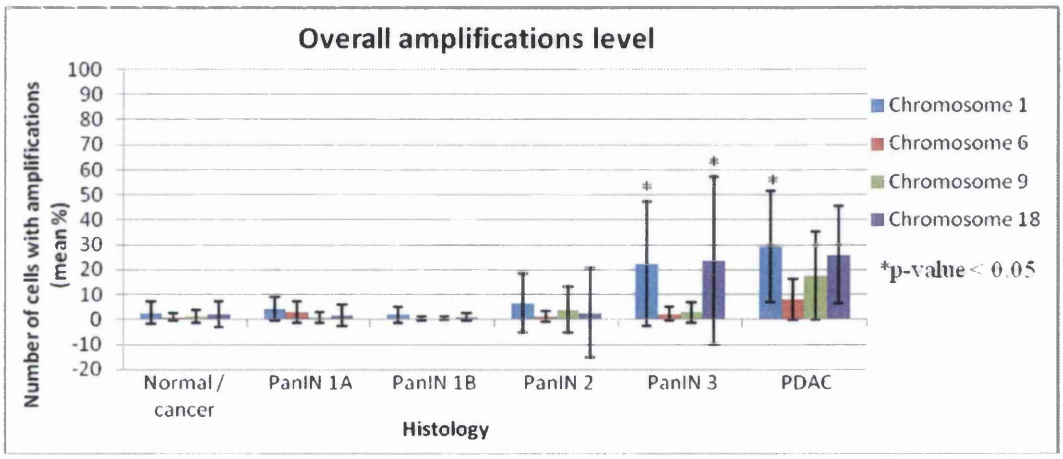

Figure 2.11: Overall number of cells with amplifications (%) for chromosomes 1, 6, 9 and 18, respectively, scored in progressive histological stages; stationary trend in normal/cancer - PanIN 1B; increase particularly in PanIN 2 - PanIN 3 for chromosomes 1 and 9 and in PanIN 3 - PDAC for chromosomes 6 and 18.

The trend for amplifications displayed a positive trend consistent across all the chromosomes investigated. The average levels in PanIN 1 across all probes reached 0.79% (range 0-13.72%) while in PanIN 3 was calculated at 12.69% (range 0.14-76.62%) and in PDAC at 20.14% (range 0.59-63.02%).

The levels seen for chromosome 6 were significantly lower (p=0.013) than for the other chromosomes but the trend was the same. Chromosome 1 showed a significant increase coresponding to PanIN 3 stage (PanIN 3 vs PanIN 1, p=0.0009) and PDAC (PDAC vs PanIN 2, p=0.024), in a similar fashion to chromosome 18 (PanIN 3 vs PanIN 1, p=0.002). The amplifications score for chromosome 9 reached the maximum value in PDAC while in the other stages remained low.

Each of the chromosomes included in the study: 1, 6, 9 and 18, displayed an individual trend in overall aneuploidy as well as deletions and amplifications. Generically, all of them showed a positive trend in chromosome abnormalities as the histological stage approaches the PDAC stage, as shown previously, but further analysis revealed specific characteristics for each probe.

2.3.1.4 Average amplifications

The levels of amplifications calculated as an average across all chromosome probes for each histological type in each specimen included in the study (Fig. 2.12) remained close to zero in the early stages including PanIN 2 (range 0-5.99%, one outlier value at 27.53% in a PanIN 2 duct close to tumoural glands). This was also reflected in the statistical analysis using the Student's paired t-test which showed no significant difference between the various early stages.

A change in the amplifications levels and trend became apparent at the PanIN 3 stage where there was a significant increase when comparing the advanced stage with the values found in the normal ducts from PDAC specimens (p=0.001) and PanIN 1 (p=0.002). A similar pattern was seen in the values calculated for PDAC where the Student's paired t-test returned significant results for differences between PDAC and normal ducts in normal specimens (p=0.18) and PDAC and PanIN 2 (p=0.018).

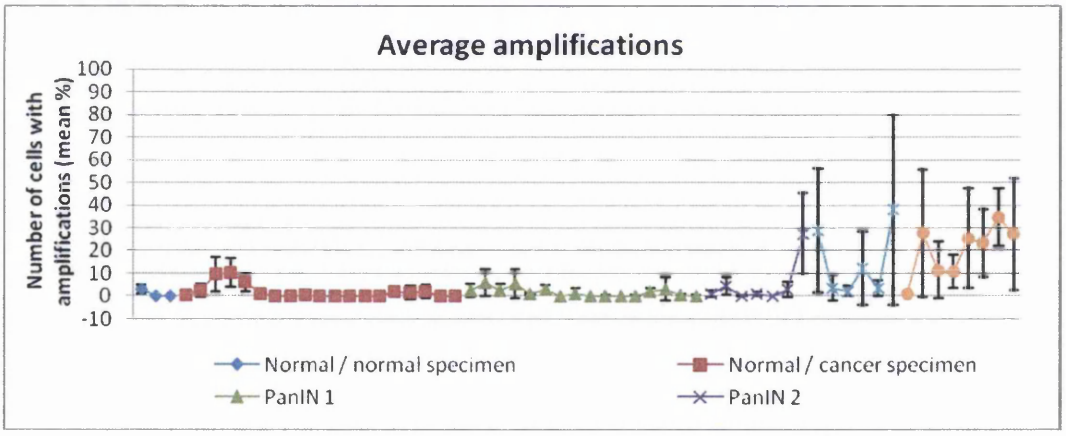

Figure 2.12: The average number of cells with amplifications (mean%) across the histological entities analysed; each vertical bar represents the range of amplifications across all chromosomes (mean%); each point on the graph represents a duct with the corresponding histological grade as listed in lower legend.

The range of values found in the initial stages clustered around the calculated average displaying minimal variations. In contrast, at PanIN 3 and PDAC the values showed a much wider range, supporting the theory that each tumour clone carries individual patterns of aneuploidy, specifically reflected in the levels of amplifications.

2.3.1.5 Overall deletions

There was a high level of deletions in all histological stages, mainly in the early stages: normal duct, PanIN 1 and PanIN 2 (Fig. 2.13). In the advanced premalignant stages (PanIN 3) and in PDAC, the deletions did not prevail in the overall aneuploidy in all chromosomes investigated. In those lesions, amplifications typically appeared more significant than deletions, signaling a shift in the process of carcinogenesis.

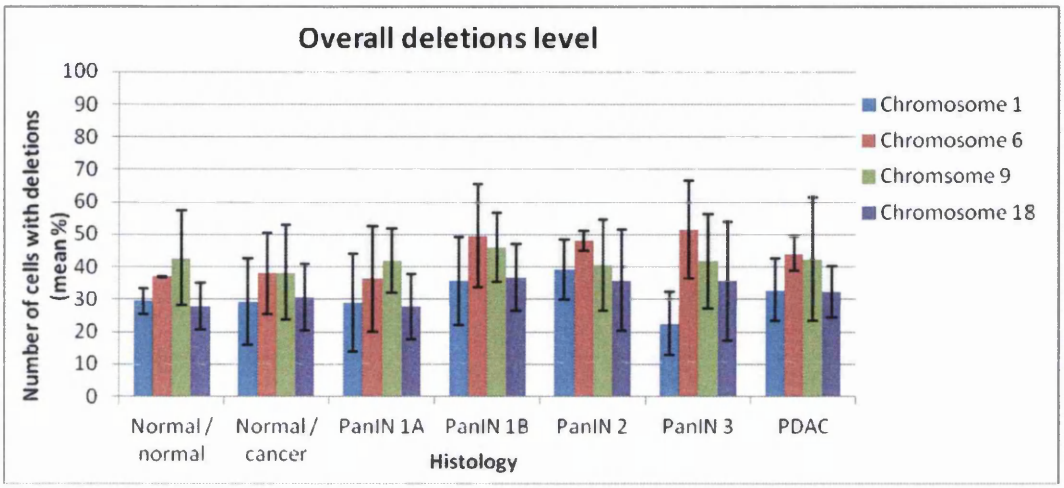

Figure 2.13: Overall number of cells with deletions (mean%) for chromosomes 1, 6, 9 and 18, respectively, scored in progressive histological stages and demonstrating a relatively stationary trend towards PDAC.

The percentage of deletions found in normal ducts from normal specimens was considered as background level, as before for overall aneuploidy, and used to adjust the level of deletions in the precancerous stages and PDAC (Fig. 2.14).

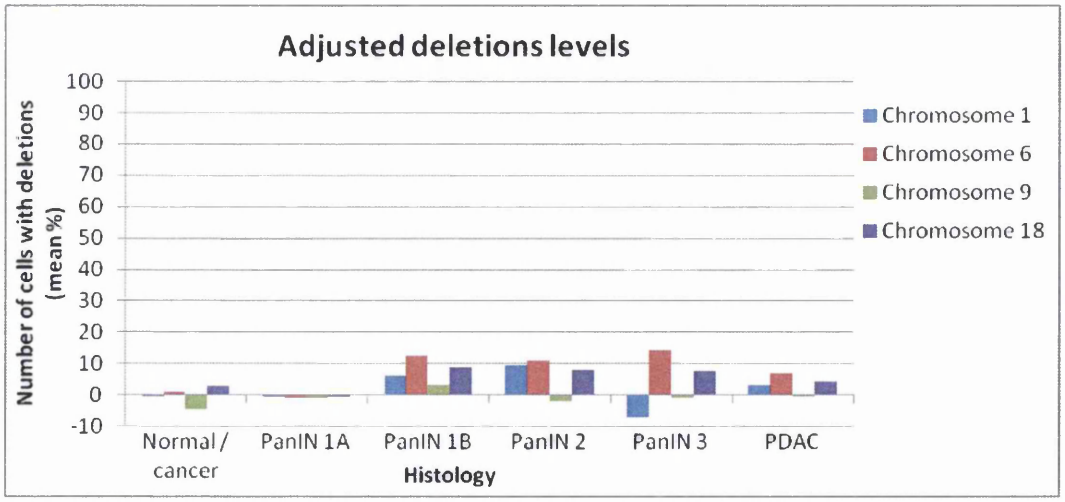

Figure 2.14: Adjusted number of cells with deletions (mean%) for chromosomes 1, 6, 9 and 18, respectively, scored in progressive histological stages.

The percentage of deletions in normal ducts and PanIN 1A were comparable to the results from the normal ducts in normal specimens suggesting that this type of chromosomal abnormality was not significant in the early stages. Generically, the percentage increased in advanced stages but there was no uniform positive trend. For chromosome 1 the level of deletions reached a negative value when adjusted against the normal specimens, reflecting sectioning bias and confirming that deletions were not a hallmark of the carcinogenesis in this scenario. For chromosome 6 the trend increased up to 14% in PanIN 3 while, comparatively, the level for chromosome 9 in the same histology was at –0.99%. For chromosome 18 the adjusted level of deletions was consistently around 8% in PanIN 1B, PanIN2 and PanIN 3, reflecting a different trend compared to the other chromosomes.

2.3.1.6 Average deletions

The average level of deletions found in each type of histology from the specimens included in the study displayed a variable trend between different specimens but remained within a set pattern across all stages. The range of values was also stable throughout the various stages (range 19.53% (PanIN 3)-52.66% (PanIN 2)) (Fig. 2.15).

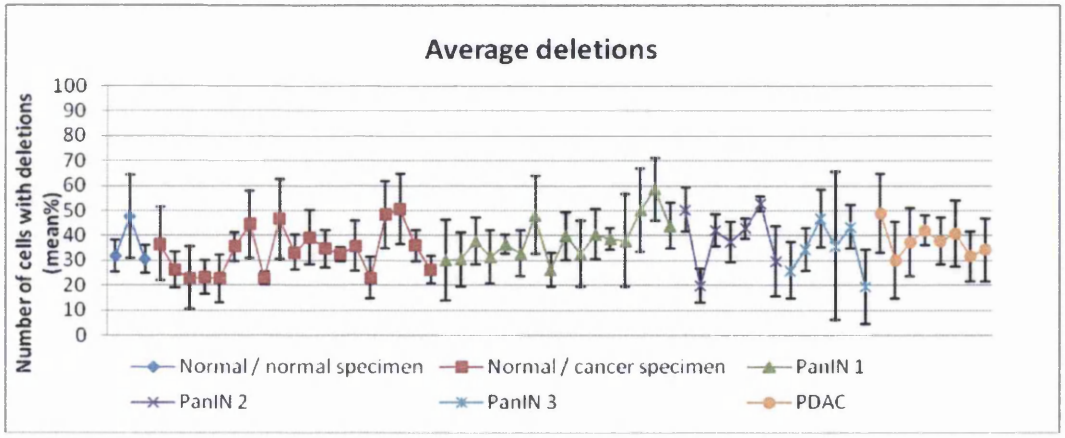

Figure 2.15: The average number of cells with deletions (mean%) across the histological entities analysed; each vertical bar represents the range of deletions across all chromosomes (mean%); each point on the graph represents a duct with the corresponding histological grade as listed in lower legend.

Statistical analysis using the Student's paired t-test confirmed that the average level of deletions did not change significantly between the different histological stages.

2.3.1.7 Chromosome 1

Aneuploidy in chromosome 1 increased with the histological stage, reaching the maximum value in PDAC. Amplifications followed a clear positive trend up to a maximum

in PDAC. For deletions, the levels were variable in different histological stages, with a maximum in the PanIN 2 stage (Fig. 2.16). The mean level of deletions in each of the different histological stages was high (29.15% in normal ducts from PDAC specimens, 28.89% in PanIN 1A, 35.72% in PanIN 1B, 39.18% in PanIN 2, 22.29% in PanIN 3 and 32.73% in PDAC). Despite the fact that deletions were subject to bias, the trend in different histological stages still provided valuable insight into tumour progression. The level of amplifications in normal ducts was 2.63%, in PanIN 1A 4.19%, in PanIN 1B 1.98% and in PanIN 2 6.51%, while in PanIN 3 it reached 22.39% and in PDAC 29.23%.

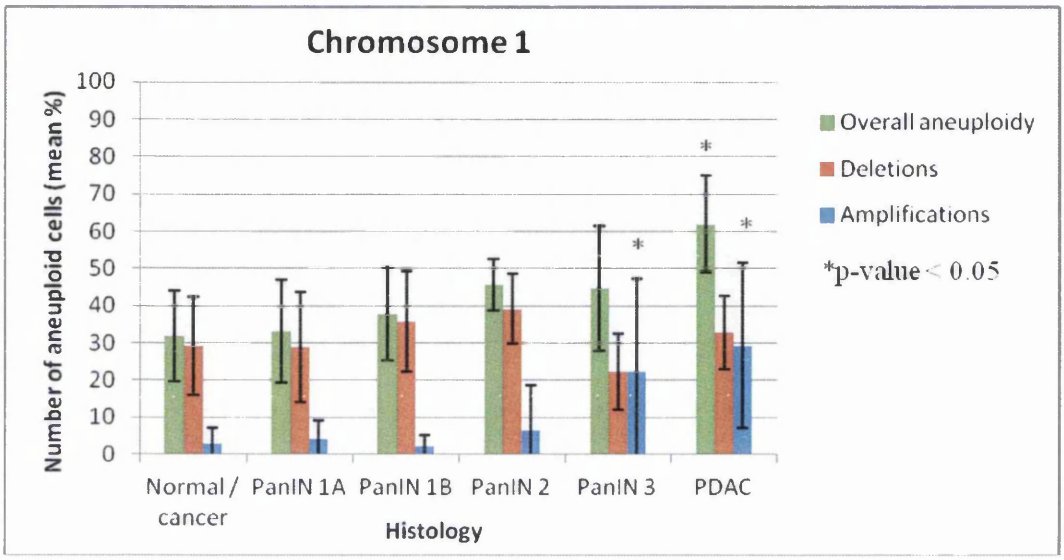

Figure 2.16: Overall number of aneuploid cells, cells with deletions and cells with amplifications (mean%) displayed by chromosome 1 in progressive histological stages; increasing trend towards PDAC for overall aneuploidy and amplifications; * indicates stages with statistically significant differences (p-value<0.05) compared with preceding stages

Basic statistical analysis using Student's paired t-test confirmed significant differences in the levels of overall aneuploidy between PDAC and normal specimens (p=0.002) as well as between PDAC and PanIN 2 stage (p=0.014) and PDAC and PanIN 3 stage (p=0.041). Significant differences were also found in the levels of amplifications between PanIN 3 and normal ducts from PDAC specimens (p=0.001), between PanIN 3 and PanIN 1 (p=0.0009) and between PDAC and PanIN 2 (p=0.024). PanIN 3 appears to be a significant stage where chromosome 1 has a high level of amplifications.

Chromosome 1 showed a significant level of aneuploidy in PDAC as well, particularly amplifications, as confirmed by advanced statistical analysis using one-way ANOVA analysis comparing PDAC to normal ducts in normal specimens (p=0.043, 95% CI=0.59-47.89).

2.3.1.8 Chromosome 6

The levels of overall aneuploidy in chromosome 6 followed a different trend compared to chromosome 1 (Fig. 2.17). They were relatively high in the normal ducts from PDAC specimens (mean 38.87%, range 24.70-68.05%), PanIN 1A (mean 39.37%, range 17.77-66.66%) and PanIN 1B (mean 49.94%, range 30.97-82.60%) and showed no increase in PanIN 2 (mean 49.15%, range 43.21-56.20%) or the advanced stages: PanIN 3 (mean 53.75%, range 37.76-79.03%) and PDAC (mean 52.05%, range 43.80-62.12%). The overall aneuploidy for chromosome 6 was mainly represented by deletions. In virtually all histological stages the levels of deletions followed a similar trend as the levels of overall aneuploidy.

The levels of amplifications for chromosome 6 remained low in PanIN 1 (mean 3.03%, range 0-11.18%), PanIN 2 (mean 1.07%, range 0-5.51%) and even PanIN 3 (mean 2.21%, range 0-7.69%) but displayed a sharp increase in PDAC (mean 7.92%, range 0.59-24.40%).

Statistical analysis (Student's paired t-test) demonstrated a significant increase in the level of overall aneuploidy in PanIN 3 and PDAC when compared with normal ducts from normal specimens (p=0.029, p=0.044 respectively) and normal ducts from PDAC specimens (p=0.007, p=0.043 respectively). The levels of amplifications in PDAC displayed a significant increase compared to normal ducts from PDAC specimens (p=0.0004), PanIN 1 (p=0.004) and PanIN 2 (p=0.049). Also, the level of deletions in PDAC was significantly higher compared to normal ducts from normal specimens (p=0.028).

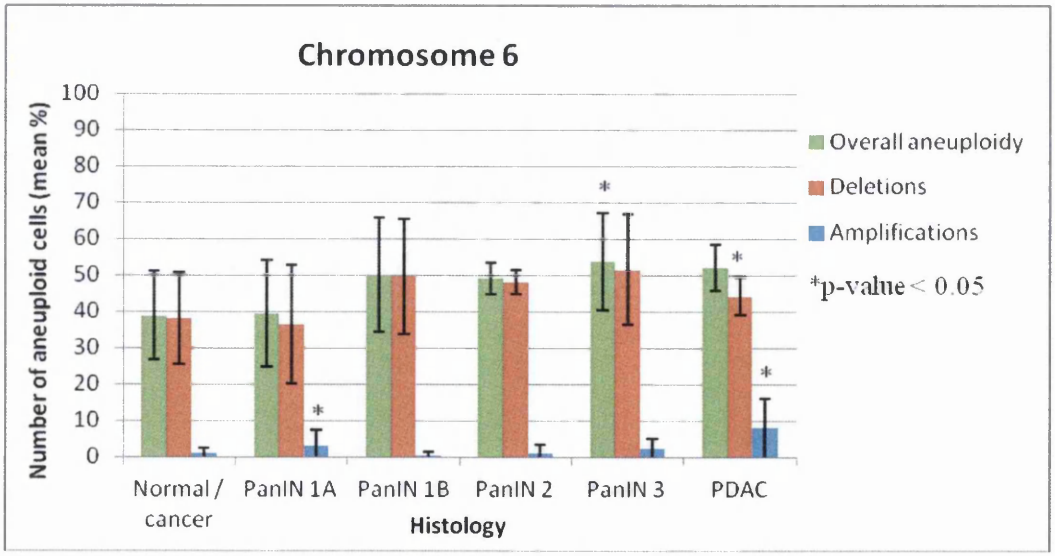

Figure 2.17: Overall number of aneuploid cells, cells with deletions and cells with amplifications (mean%) displayed by chromosome 6 in progressive histological stages; increasing trend towards PDAC for amplifications; $*$ indicates stages with statistically significant differences (p-value<0.05) compared with preceding stages.

The advanced analysis using the one-way ANOVA mean comparison test showed no significant overall difference between histological stages in deletions levels. However, Dunnett T3 test comparing means in each stage with all the other stages revealed a significant difference between PanIN 2 and normal ducts from normal specimens (p=0.004, 95%CI=4.67-17.13) as well as between PDAC and normal ducts from normal specimens (p=0.035, 95%CI=0.52-15.42). For amplifications, the ANOVA mean comparison test showed a significant overall difference between groups (p=0.002) but no similar results were seen when applying the Dunnett T3 test to the data.

2.3.1.9 Chromosome 9

The levels of overall aneuploidy concerning chromosome 9 remained stable in all histological stages including PanIN 3 and then increase in PDAC (Fig. 2.18). In the same premalignant stages the aneuploidy was mainly represented by deletions which reached a relatively high level in every stage in PDAC specimens: normal ducts (mean 38.26%, range 14.59-74.66%), PanIN 1A (mean 41.96%, range 30.30-64.46%), PanIN 1B (mean 45.96%, range 25.47-60.38%), PanIN 2 (mean 40.66%, range 22.94-60.33%) and PanIN 3 (mean 41.75%, range 20.71-59.64%). In PDAC the levels were comparable to the levels in the premalignant stages (mean 42.40%, range 13.88-72.14%).

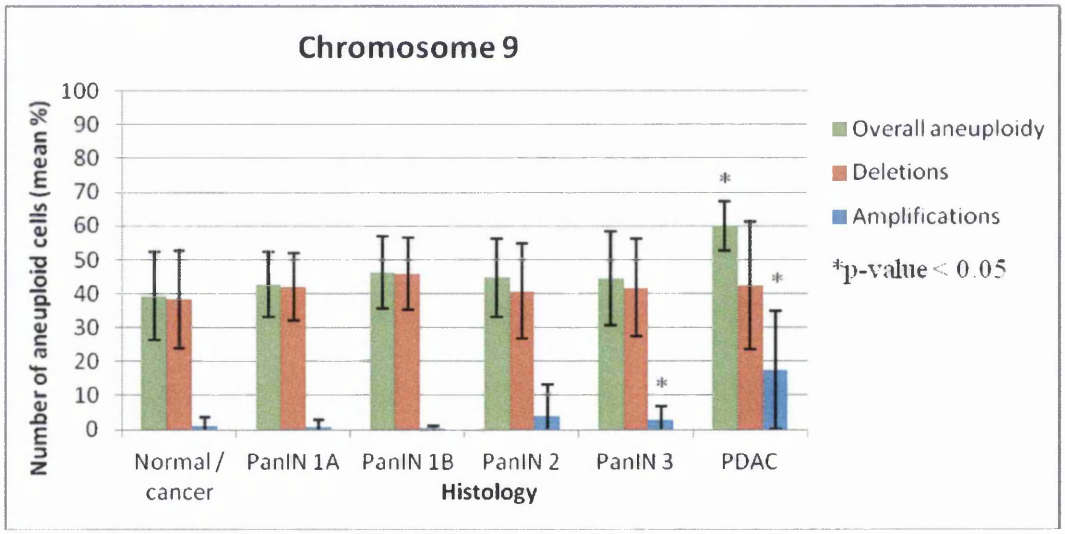

Figure 2.18: Overall number of aneuploid cells, cells with deletions and cells with amplifications (mean%) displayed by chromosome 9 in progressive histological stages; increasing trend towards PDAC for overall aneuploidy and amplifications; * indicates stages with statistically significant differences (p-value<0.05) compared with preceding stages.

The levels of amplifications for chromosome 9 displayed an increase in PanIN 2 (mean 3.98%, range 0-25.08%) compared to normal ducts (mean 1.02%, range 0-

10.04%), PanIN 1A (mean 0.72%, range 0-6.51%) and PanIN 1B (mean 0.38%, range 0-2.29%). In PanIN 3 the levels did not follow the positive trend (mean 2.77%, range 0.23-11.94%) but there was a sharp increase in PDAC (mean 17.54%, range 1.28-48.61%).

Statistical comparison using Student's t-test illustrated the significant difference that the levels of overall aneuploidy display in the cancerous stage compared to all the precursor stages: normal ducts in normal specimens (p=0.025), normal ducts in PDAC specimens (p=0.001), PanIN 1 (p=0.005), PanIN 2 (p=0.007) and PanIN 3 (p=0.016). For amplifications, a significant increase is noted in PDAC compared to PanIN 3 (p=0.033) and normal ducts from PDAC specimens (p=0.0001). Also, at PanIN 3 level the amplifications marked a significant increase compared to the level of amplifications in PanIN 1 (p=0.048). No significant difference was seen in the level of deletions when comparing the various histological stages.

Further statistical analysis using one-way ANOVA mean comparisons test showed no significant difference in the levels of deletions between various histological stages or when each of them was compared to normal ducts from normal specimens. For amplifications, the one-way ANOVA mean comparison test showed a significant difference between groups (p<0.001) and in particular, between PDAC and the normal ducts from normal specimens (p=0.002, 95%CI=6.79-34.06).

2.3.1.10 Chromosome 18

The overall aneuploidy for chromosome 18 in the advanced histological stages (PanIN 3, PDAC) reached higher levels compared to the overall aneuploidy in the initial stages (PanIN 1, PanIN 2) (Fig. 2.19). There was a marked increase between PanIN 2 and PanIN 3 stage while the levels in PDAC retained a similar value to PanIN 3. Most of the pancreatic ductal cells scored in PanIN 3 and PDAC lesions were aneuploid cells (mean 59.12% and 58.17%, respectively). Overall aneuploidy was mainly represented by deletions in the early stages (PanIN 1) but starting with the PanIN 2 stage the amplifications levels increased until in PanIN 3 and PDAC they were at a significantly higher level and contributed to aneuploidy in a comparable percentage as the deletions. There was a slight positive trend in the levels of deletions between PanIN 1A (mean 27.73%, range 17.5-48.03%) and PanIN 1B (mean 36.75%, range 17.05-51.73%), but the trend did not continue in the later stages, displaying a slight decrease in PanIN 2 (mean 35.80%, range 15.17-55.31%) that continued in PanIN 3 (mean 35.72%, range 8.57-54.35%) and PDAC (mean 32.30%, range 20.44-42.53%).

Meanwhile, for amplifications, the levels were initially very low in PanIN 1A (mean 1.57%, range 0-13.72%) and 1B (mean 0.88%, range 0-3.80%), then showed a minimum increase in PanIN 2 (mean 2.67%, range 0-48.69%) and then a marked increase in PanIN 3 (mean 23.39%, range 0.39-76.62%) remaining at a comparable

value in PDAC (mean 25.86%, range 1.74-55.24%). The wide range of values for the levels of amplifications in PanIN 2, PanIN 3 and PDAC suggested that different cell clones drive individual trends in the chromosomal number anomalies seen in chromosome 18. The levels of amplifications seen in all stages carried biological significance for the carcinogenesis process especially as reflected in the levels found in PanIN 3 (mean 23.39%), and PDAC (mean 25.86%).

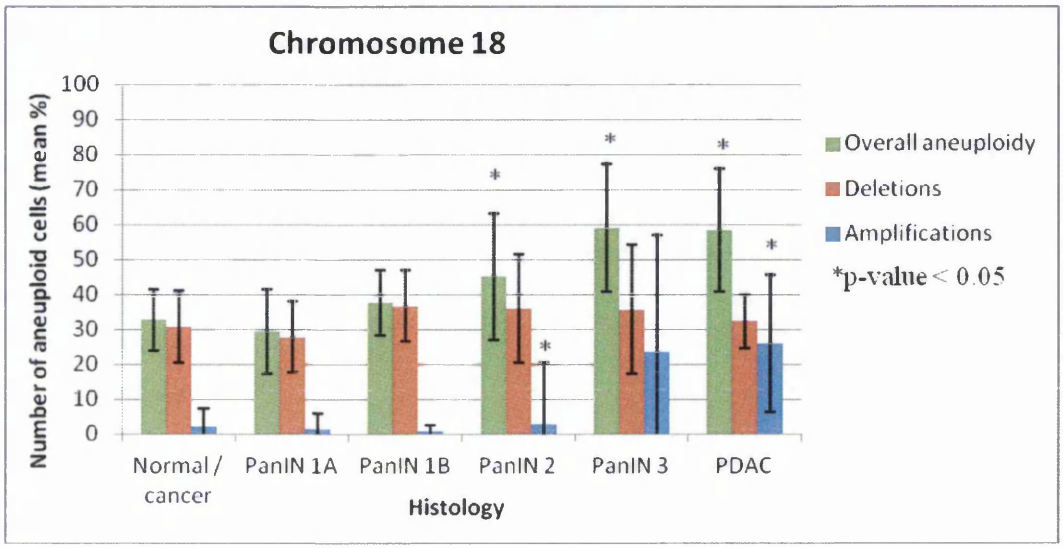

Figure 2.19: Overall number of aneuploid cells, cells with deletions and cells with amplifications (mean%) displayed by chromosome 18 in progressive histological stages; increasing trend towards PDAC for overall aneuploidy and amplifications; * indicates stages with statistically significant differences (p-value<0.05) compared with preceding stages.

The initial statistical analysis with Student's paired t-test showed a significant positive trend of the overall aneuploidy in later stages compared to normal ducts or earlier stages: PanIN 2 vs. normal ducts from PDAC specimens (p=0.019), PanIN 3 vs. normal ducts from normal specimens (p=0.027) and PanIN 1 (p=0.0002), PDAC vs. normal ducts from normal specimens (p=0.024) and PanIN 1 (p=0.0002). For amplifications, a significant increase was noted in PanIN 2 and PanIN 3 compared to earlier stages: PanIN 2 vs. PanIN 1 (p=0.039), PanIN 3 vs. normal ducts from PDAC specimens (p=0.006) and vs. PanIN 1 (p=0.002).

Further statistical analysis using one-way ANOVA mean comparison test showed no significant difference in the levels of deletions when comparing the different histological stages in turn or each stage with the others. For amplifications, there was a significant difference between histological lesions (p=0.001) but further detailed analysis failed to reveal the critical stage where the difference becomes significant.

2.3.2 Case studies

In order to illustrate the individual patterns of aneuploidy in different specimens we selected several specimens which displayed a combination of different histological stages relevant for this concept. In those cases the analysis of overall aneuploidy as well as chromosomal gains and losses provided insight into how these changes may develop in the progression of individual tumours. In the majority of cases, though, one or two histological stages distinct from the PDAC tissue were predominant.

Patient 7 This PDAC specimen contained normal ducts, ducts with PanIN 2, PDAC and a lymph node metastasis. The levels of overall aneuploidy across all chromosomal probes (1, 6, 9 and 18) increased from a baseline value in the normal ducts to a maximal value in the areas with PDAC and metastasis (Fig. 2.20). Chromosome 9 displayed a marked difference between the levels in normal ducts and those in PDAC and metastasis (31.58%, 34.90% respectively). A similar trend was seen for chromosome 18: 13.44% and 42.80% difference between normal ducts and PDAC and metastasis, respectively. Meanwhile, for chromosome 1 and 6, the values generated a slight upward trend towards the advanced stages (14.50%, 5.47% difference between normal and PDAC ducts, respectively).

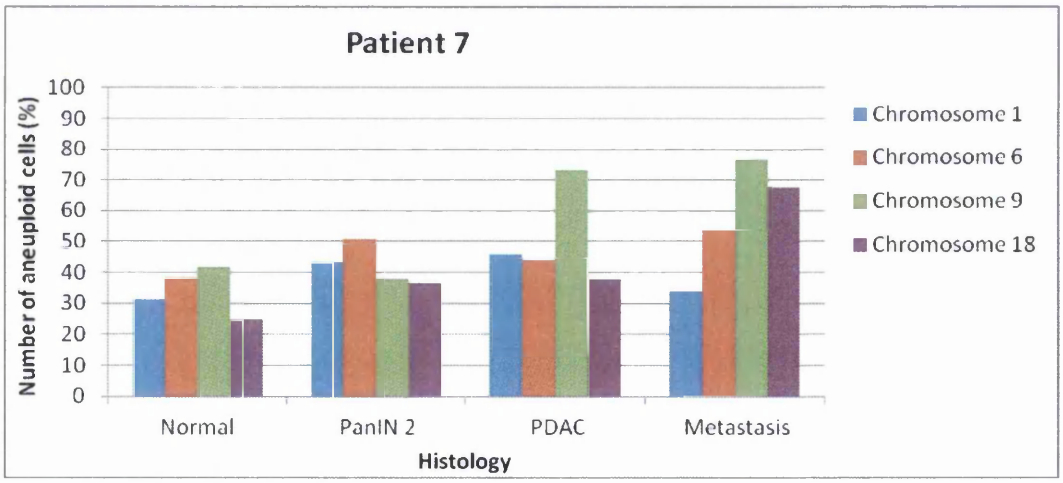

Figure 2.20: Different histological stages from the same PDAC specimen (normal, PanIN 2, PDAC and lymph node metastasis) display various levels of overall aneuploidy.

Deletions accounted for the main percentage of the overall aneuploidy in all histological stages and for all chromosomal probes investigated. Meanwhile, amplifications marked the carcinogenesis process with low values compared to deletions but with increased molecular significance. The levels increased from zero in the normal ducts to 4.26% for chromosome 1, 1.94% for chromosome 6, 0.77% for chromosome 9 and 0.27% for chromosome 18 in the metastatic tissue (Fig. 2.21).

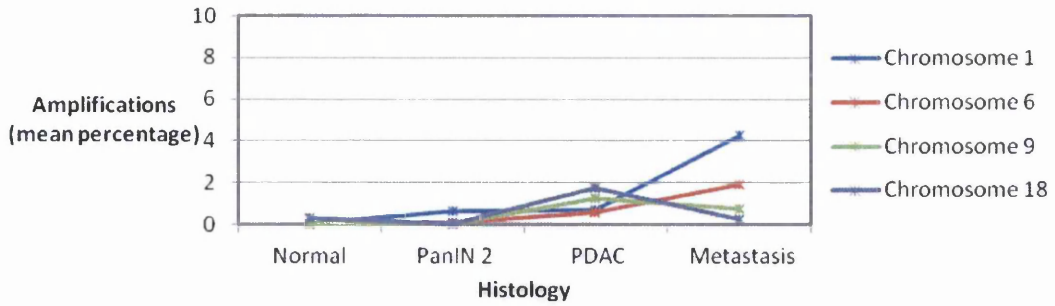

Figure 2.21: Different histological stages from the same PDAC specimen (normal, PanIN 2, PDAC and lymph node metastasis) display various levels of amplifications.

The trends in chromosomal gains and losses seen in this specimen highlighted the role of amplifications and how different chromosomes displayed individual aneuploidy variations along the carcinogenesis process.

Patient 16 This PDAC specimen contained pancreatic ducts with normal tissue, PanIN 1B and PanIN 3. The levels of overall aneuploidy and amplifications are illustrated in Fig. 2.22 Chromosome 1 and 6 followed a marked positive trend in overall aneuploidy between normal ducts and PanIN 3 (28.78% and 48.52% difference, respectively). Meanwhile, chromosome 9 and 18 appeared to follow a counterintuitive trend, with decreasing levels in PanIN 3 compared to PanIN 1B (−16.45%, −7.81% difference respectively). This illustrated that carcinogenesis is a highly diverse process that generates chromosomal abnormalities in a random fashion.

A marked increase was detected when comparing the level of amplifications for chromosome 1 and 18 in PanIN 1B and PanIN 3 (32.16% and 9.92% difference, respectively). Meanwhile, no chromosome 6 amplifications could be confidently identified in any histological entity from this particular specimen. Interestingly, chromosome 9 showed virtually no increase in the level of amplifications between PanIN 1B and PanIN 3 (0.59% difference) (Fig. 2.23).

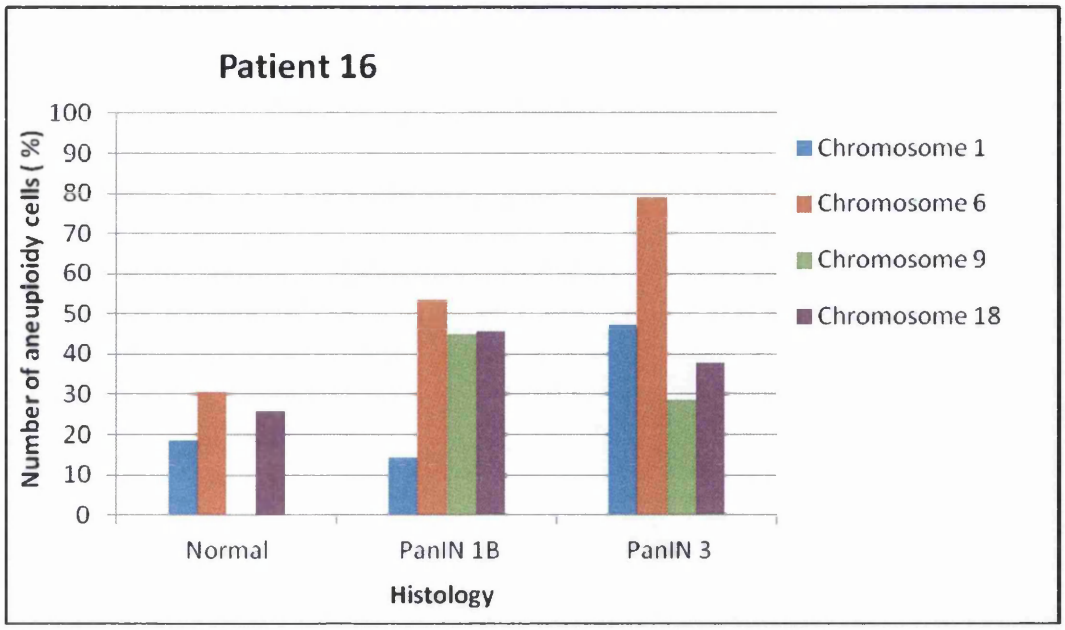

Figure 2.22: Different histological stages from the same PDAC specimen (normal, PanIN 1B and PanIN 3) display various levels of overall aneuploidy.

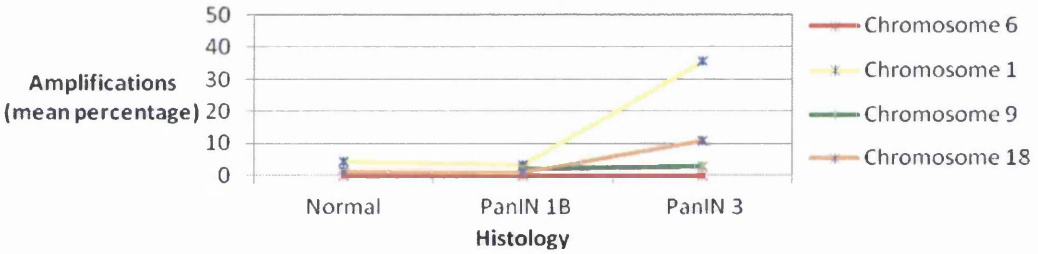

Figure 2.23: Different histological stages from the same PDAC specimen (normal, PanIN 1B and PanIN 3) display various levels of amplifications.

Patient 19 In another PDAC case included in this case series the trends in the levels of aneuploidy in different histological stages showed that the overall aneuploidy in the early stages was higher than that documented in the late stages. The scoring for this PDAC specimen was done on two normal pancreatic ducts, two PanIN 1B lesions, one PanIN 2 and one PanIN 3.

The average aneuploidy across all chromosome probes in the normal ducts was 52.45%, 58.98% in the PanIN 1B lesions, while in the PanIN 2 and PanIN 3 it reached 55.41% and 46.89%, respectively. The overall trend followed a negative curve towards the advanced pre-malignant stage (Fig. 2.24).

Most of the overall aneuploidy was represented by deletions, while the amplifications maintained a low profile across the chromosome probes. Chromosomes 6 and

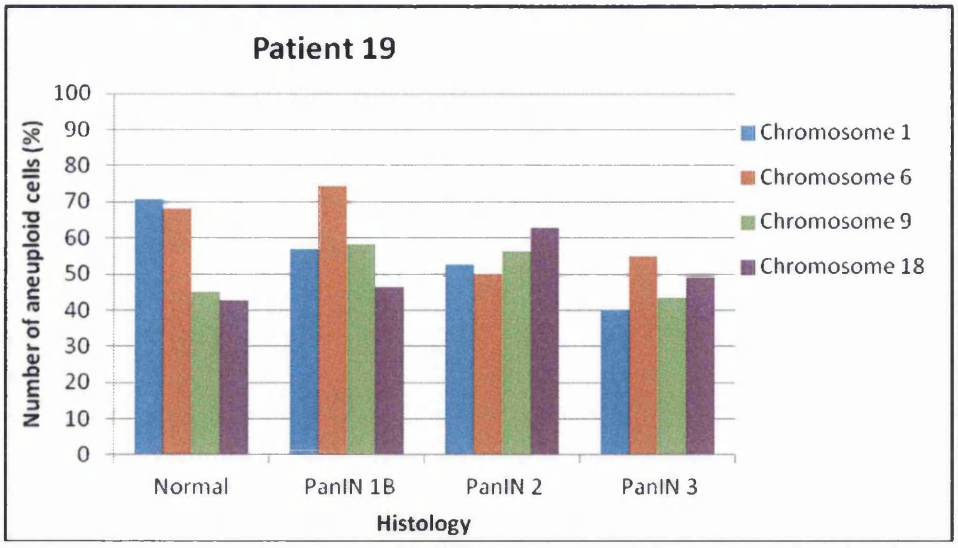

Figure 2.24: Different histological stages from the same PDAC specimen (normal, PanIN 1B, PanIN 2 and PanIN 3) display various levels of overall aneuploidy.

9 showed stationary levels across all histological stages in this specimen (range 0-1.38%, range 0-2.16% respectively) with the highest values seen in the normal ducts, while the PanIN 3 lesion displayed minimal scores (0.14%, 0.92% respectively). There was a different trend in the levels of amplifications for chromosome 1: a high value in the normal ducts (7.27%), a decrease in PanIN 1B (6.61% difference) sustained in PanIN 2 (4.68% difference compared to normal) followed by an increase in PanIN 3 (4.15% difference compared to PanIN 2). For chromosome 18, the highest score was found in the PanIN 2 (7.53%), while the score in PanIN 3 was lower (5.74%) and only 0.89% in PanIN 1B and 0% in the normal ducts (Fig. 2.25).

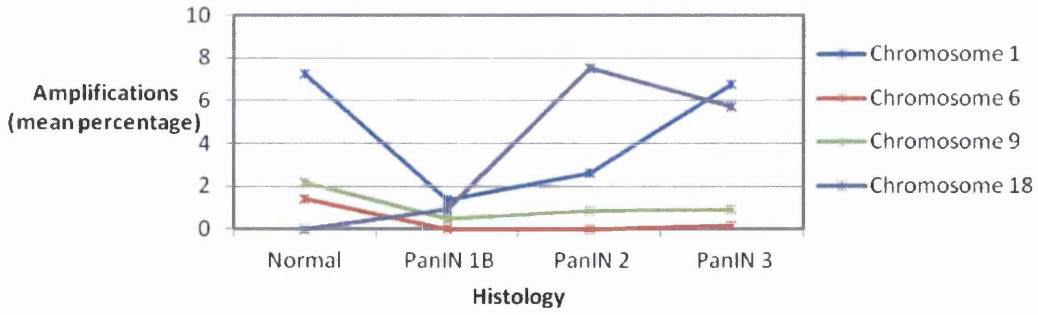

Figure 2.25: Different histological stages from the same PDAC specimen (normal, PanIN 1B, PanIN 2 and PanIN 3) display various levels of amplifications.

The heterogeneity in the chromosomal changes in this specimen as well as the reverse trend in overall aneuploidy suggested that in some malignant clones the initial expansion of aneuploidy is a self-limiting process as the carcinogenesis advances.

2.4 Discussion

2.4.1 Average aneuploidy

In general, the level of aneuploidy in a tumour is closely related to type, stage and histological grade. Individual patterns in different cases with the same type of tumour confirm that aneuploidy develops in relation to individual genetic guidelines and pathways. Thus, it can be considered a trademark process in evaluating individual stages in carcinogenesis.

The scoring for aneuploidy in normal pancreatic ducts from PDAC specimens revealed a high level of aneuploidy (range 18.42-74.66%) that appeared contradictory as the ducts were selected from an area away from the main tumour and macroscopically classified as not involved in the tumoural process. Several normal pancreatic ducts from normal pancreatic specimens (multiple congenital cysts, lympho-epithelial cyst, peritoneal pseudocyst) were included to support the evaluation of the background aneuploidy level. The limitations in this approach were that pancreatic surgery for non-cancerous diseases is very rare and even then it is likely that the disease process involved precludes the confident identification of normal ducts. The normal ducts included were selected from specimens with benign disease with no chromosomal changes.

The aneuploidy scoring in the normal ducts from the normal specimens revealed comparable results (range 25.28-59.40%) to the scoring in the normal ducts from the PDAC specimens, prompting the conclusion that the high level of background aneuploidy in the PDAC specimens is not related entirely to the proximity to the tumour. Potential alternate explanations relate to sectioning bias (when the level of sectioning cuts accross the nuclei and causes the chromosome pair to be fragmented, generating a false low chromosome count), scoring bias (tissue architecture in the normal ducts allows good visualisation of the nuclei with significantly less overlapping compared to advanced stages, thus leading to more aneuploid nuclei being included in the scoring) or tissue bias (pancreatic tissue displaying a relatively high level of aneuploidy unrelated to a cancerous process).

The vast majority of the available studies focused on chromosomal aberrations used region-specific FISH probes to uncover amplifications and/or deletions relevant to the genes located on the respective region. For example, Ghadimi et al. 1999 used FISH to validate their findings revealed by comparative genomic hybridization (CGH) and spectral karyotyping (SKY) on pancreatic cancer cell lines: consistent chromosomal gains for chromosomes 1q, 5, 7, 8, 10, 11, 12q, 16p, 18q11-12, and 20 and losses for chromosomes 9p, 18q, and Xp (Gambini BM et al., 1999). Another study using CGH and SKY on pancreatic cancer lines reported frequent chromosomal gains for chromosomes 3q, 8q, 11q, 17q and 20 and losses for chromosomes 6q, 8p, 17p and 18

(Griffin CA et al., 2007).

Our study showed that, as expected, the average level of amplifications seen across all chromosome probes remains low in the early premalignant stages (PanIN 1, PanIN 2) but increases significantly in the PanIN 3 and PDAC level. Also, the range of values in the advanced stages is wider indicating that different tumour clones display individual patterns of aneuploidy best reflected in the levels of amplifications.

The average level of deletions in the specimens included was more difficult to interpret accurately mainly because of sectioning bias but it is acknowledged that, generically, they play a contributing role to carcinogenesis.

2.4.2 Amplifications

The most significant part of the results was reflected by the levels of amplifications. All chromosome probes included in this study displayed aneuploidy in the form of amplifications, but chromosome 1 showed the highest levels in PDAC (29.23%). For PanIN 3, the highest level was seen in chromosome 18 (23.39%), while chromosome 1 displayed a similar value (22.39%). In the other premalignant stages the levels remained low for all chromosome probes. Also, each chromosome displayed amplifications in an increasing pattern towards the last stages of carcinogenesis.

Most of the cells displaying amplifications showed more than three chromosomal copies typically for both probes used for hybridization. Some areas of the pancreatic ducts with PanIN 2 or PanIN 3 were particularly dense in aneuploid cells with amplifications suggesting that those cells derived from the same clone in the carcinogenesis process.

The areas with overlapping of the nuclei have been excluded to avoid overscoring for amplifications, so potentially the true levels in the tissue could be higher than the levels documented in the study.

Studies have shown that FISH analysis on ERCP brushings from the pancreatobiliary system can twice the sensitivity of a positive diagnosis for malignancy compared to positive routine cytology alone by detecting chromosomal gains (Kipp BR et al., 2004, Moreno Luna LE at al., 2006).

2.4.3 Chromosome 1

Chromosome 1 is the largest human chromosome, representing approximately 8% of the total cellular DNA (US NLM, 2012).

In our study, chromosome 1 displayed a high level of amplifications in the PanIN 3 stage of carcinogenesis. The deletions proportion increased towards the last stages and, despite the bias involved in their analysis, they suggest an accumulation of anomalies as the carcinogenesis advances. PanIN 3 and PDAC display levels of amplifications

significantly higher than the earlier stages which may suggest that in advanced stages chromosome 1 has a significant role in defining the tumour genotype.

Hilgers et al. identified loss of heterozygosity (LOH) on the chromosomal arm 1p in 50% of pancreatic cancers evaluated, suggesting the presence of a tumour suppresor gene on that locus (Hilgers et al., 1999).

2.4.4 Chromosome 6

Between 5.5% and 6% of total cellular DNA is found on chromosome 6. Several oncogenes have been located on the short arm (6p) which is frequently duplicated in cancers (US NLM, 2011).

The levels of overall aneuploidy in chromosome 6 follow a different trend compared to chromosome 1, displaying a stable relatively high value in all histological stages. The levels of deletions constitute the main chromosome abnormality. This suggests that deletions in chromosome 6 numbers are a significant molecular event in pancreatic carcinogenesis, despite tissue sectioning bias. The levels of amplifications in chromosome 6 are overall low in all specimens, only significantly increasing in PDAC compared to the other histological stages. Advanced statistical analysis confirmed a significant increase in deletions in PanIN 2 and PDAC compared to normal specimens.

2.4.5 Chromosome 9

Chromosome 9 represents approximately 4.5% of the total cellular DNA (US NLM, 2012).

The chromosome 9 aneuploidy levels are mainly represented by deletions, similar to the pattern seen for chromosome 6, but at a lower value. The level of amplifications for chromosome 9 remains low in all premalignant stages except for PanIN 2 where it shows a minimal increase. There is a marked increase in amplifications corresponding to the PDAC stage which highlights the significance of the chromosomal gains in this stage when compared with all the other stages. Amplifications appear to be the main chromosome number anomaly affecting chromosome 9 in pancreatic carcinogenesis in the specimens included in this study.

2.4.6 Chromosome 18

Chromosome 18 represents 2.5% of the total cellular DNA and carries the tumour suppressor gene SMAD4 on locus18q21.1 (US NLM, 2012).

Chromosome 18 displays significantly higher levels of overall aneuploidy in PanIN 3 and PDAC compared to the early stages (PanIN 1, PanIN 2). The marked increase in

the levels of amplifications in PanIN 3 demonstrates the central role that amplifications play in the abnormal profile of chromosome 18 in pancreatic carcinogenesis in the specimens included in this study. There is a wide range of values for amplifications displayed in PanIN 2, PanIN 3 and PDAC suggesting that different cell clones drive individual trends in the chromosomal number anomalies in this case. Also, PanIN 2 appears to represent a critical stage in the trend of anomalies in chromosome 18 but that was not confirmed on a one-way ANOVA mean comparison test.

A study using comparative genomic hybridization (CGH) to screen 33 pancreatic ductal adenocarcinomas for genomic alterations found that chromosome 18 was the chromosome altered preferentially. The tumours investigated in the study displayed frequent chromosomal losses involving 18q, 10p, 8p, 13q (Schlege C, 2000). Similar findings regarding chromosome 18 were reported in an earlier attempt to establish the most consistent chromosomal abnormalities in PDAC, using fluorescence in situ hybridization as the design method (Griffin C et al., 1995). This is in contrast with the pattern we found for chromosome 18: amplifications were predominant in the specimens with PDAC.

Meanwhile, a study including 20 primary pancreatic non-endocrine tumours and 9 metastases reported a different set of results, using chromosome banding after short-term culture. They found that the main karyotypic imbalances were chromosome losses in 18, Y and 21 and gains of 7, 2, and 20, partial or whole-arm losses of 1p, 3p, 6q, 8p, 9p, 15q, 17p, 18q, 19p, and 20p, and partial or whole-arm gains of 1q, 3q, 5p, 6p, 7q, 8q, 11q, 12p, 17q, 19q, and 20q (Gorunova L, 1998).

One small study aiming to test the utility of FISH in evaluating chromosomal alterations in PDAC showed losses for chromosome 8, 17 (four out of 10 cases for both), 20 (three out of 10 cases) and 18 (two out of 10 cases) alongside gains for chromosomes 7 and 18 in one tumour (Adsay N et al., 1999).

2.4.7 Case studies

PDAC specimens with different histological stages were selected and the levels of overall aneuploidy and amplifications were analysed by simple comparison. In one specimen, the trends followed a predictive upward curve from normal ducts to PanIN 2, PDAC and lymph node metastasis. For amplifications this carries a marked significance at molecular level as it highlights how carcinogenesis disrupts normal cellular division resulting in tumour growth and metastasis. In another specimen, the trends followed the expected increase only for chromosome 1 and 6 from PanIN 1B to PanIN 3. The levels of overall aneuploidy seen in chromosome 9 and 18 followed a downward trend between the same histological stages. Amplifications in the same specimen increased towards PanIN 3 only for chromosome 1 and 18, while the trend was stationary for chromosome 9 and a zero value was recorded for chromosome 6 across all

histological stages.

The trends of aneuploidy and chromosomal gains, in particular, seen in different PDAC specimens illustrate the random pattern of chromosomal abnormalities in various histological stages as the carcinogenesis progresses in the specimens included in this study.

Different tumour genomes involve different types of genetic instability. The link between chromosomal aberrations and prognosis has been shown for a variety of tumours like prostate cancer (Paris P.L. et al., 2004), breast cancer (Callagy G et al., 2005), gastric cancer (Weiss MM et al., 2004) and lymphoma (Martinez-Climent JA et al., 2003, Rubio-Moscado F et al., 2005). This area of research needs expanding with studies to validate the observational statistical results.

2.4.8 Survival analysis

Overall, the survival of the patients included in this study was 12 months on average, ranging from 3 months to 18 months, which is consistent with the data from the literature (NCI, 2009). There was a significant increase in survival where the tumour size was less than 4 cm (p=0.041) but the sample size was relatively small. For the same reason, there were limitations towards a more in depth analysis including aneuploidy levels. However, a noteworthy observation was made about an apparent correlation between relatively high levels of average aneuploidy in tumour areas and decreased survival. In one case with 64.04% average aneuploidy across all the investigated chromosomes the survival was only 7 months. Similarly, 57.81% average aneuploidy was associated with a survival of 6 months, 52.72% with 9 months, while 48.72% average aneuploidy was noted in a case with 20 months survival. All the described cases received postoperative chemotherapy and the tumour size ranged between 4 and 6 cm, which is an important factor for survival as mentioned previously. The average levels of amplifications seen in the actual tumour areas did not correlate significantly with survival but it was noted that the cases with a high level (10.73%, 23.33% and 27.66%) had a relatively shorter survival (9, 7 and 6 months, respectively) compared to a case with 1.07% average amplifications which survived for 13 months.

In the cases displaying PanIN 3 lesions the survival analysis was equally difficult due to the small sample size and confounding factors like tumour size, local invasion and postoperative chemoradiotherapy. Nevertheless, it is worth noting that a high level of average aneuploidy (57.41%) was associated with a 6 months survival while a relatively lower level of aneuploidy (38.04%) was associated with a 10 months survival. The same observation does not apply to the average levels of amplifications in PanIN 3 where in one case a level of 37.87% was associated with a 6 months survival while a level of 3.58% was seen in a case with 10 months survival and 2.14% in a case with 3 months survival. Overall, the levels of aneuploidy appear to have a link with survival but a more detailed analysis in a larger sample size would be needed to confirm that.

2.5 Conclusion

The levels of aneuploidy found in the specimens included in this study pertinent to chromosomes 1, 6, 9 and 18 reinforced the fact that aneuploidy is a significant event in pancreatic carcinogenesis. The significant increase in the PanIN 3 premalignant stage indicates that this stage accumulates the genetic anomalies inexorably leading to the fully established stage of adenocarcinoma. The amplifications are the most relevant anomaly and mainly chromosomes 1, 9 and 18 were affected by this type of missegregation while chromosome 6 displayed predominantly deletions.

Further investigations into a larger panel of chromosomes and with extension to other parameters (proteomics, metabolics) could add to the already established grounds for personalized genetic therapy.

The recognized causes for aneuploidy are: chromosomal instability and aneugens (exogens that cause aneuploidy). In pancreatic carcinogenesis the chromosomal instability appears to have the main role in aneuploidy while there is no direct evidence that aneugens are involved. The current study confirms this hypothesis which leads to the question what causes the instability and whether the mitotic checkpoint remains intact during carcinogenesis. The next chapter was designed as an attempt to investigate the Mad2 and BubR1 mitotic checkpoint proteins in the PanIN premalignant lesions.

Chapter 3

Mad2 and BubR1

3.1 Introduction

Mad2 and BubR1 are two important proteins involved in controlling the cell cycle as part of the spindle assembly checkpoint. The genes that control these proteins are part of the genetic pathways involved in controlling the cell cycle and so genetic defects at this level can lead to chromosomal instability and carcinogenesis (Jallepalli P et al., 2001). Mad2 mutations have been shown in breast and bladder cancer (Percy et al., 2000, Hernando et al., 2001) while BubR1 mutations are associated with colon cancer (Weaver BA et al., 2006, Cahill DP et al., 1998).

Immunohistochemistry (IHC) is a method of investigating the presence and location of proteins in tissue sections. It is based on the antibody-antigen reaction. This reaction can be visualized using chromogenic or fluorescent detection. The chromogenic detection uses an enzyme conjugated to the antibody which produces a colour precipitate at the site of the protein. The fluorescent detection method uses a fluorophore which is conjugated to the antibody and can be visualized using fluorescence microscopy (Buchwalow IB et al., 2010). As the antibody is highly specific for the target protein, it represents a valid method for detecting the protein of interest. Thus, it is widely used in diagnostic, prognostic and research fields. It is relevant in diagnosing tumours of unknown origin, in investigating prognostic markers in cancer by identifying relevant enzymes, tumour-specific antigens, tumour suppressor genes, oncogenes and tumour proliferation markers and in predicting the response to therapy in breast and prostate cancer. It is also used to confirm infectious agent in tissue with antimicrobial antibodies. It has a role in investigating neurodegenerative disorders, brain trauma and muscle disease. In genetics it can be used to establish the function of specific proteic gene products involved in various genetic pathways (Duraiyan J et al., 2012).

3.2 Materials and method

3.2.1 Sample characteristics

A panel of 20 normal ducts, 18 ducts with PanIN 1, 6 ducts with PanIN 2, 7 ducts with PanIN 3, 4 ducts with PDAC and one lymph node metastasis was selected out of the sample used to score aneuploidy.

The sample was formed by 15 patients, male:female ratio 1:1.5, average age 70 years.

The inclusion criteria involved sectioning feasibility (further sectioning was not possible in the specimens where the ducts with PanINs were peripheral), the presence of progressive histological stages in the same specimen, relatively high or low levels of aneuploidy. The exclusion criteria involved inability to obtain further sections. Also, the time limitations for this pilot study did not allow the inclusion of all available specimens or of other relevant proteins.

Table 3.1: Patient demographics selected for the immunohistochemistry study. The patient ranking is not consecutive as it reflects the ranking in the aneuploidy study where the sample has been sourced.

Patient no.	Age	Sex	Diagnosis	Date of surgery	Tumour size (cm)	Histology	TNM	Stage	Survival (months)
1	64	M	IPMN	20/02/2009	n/a	normal duct, PanIN 1, PanIN 2	n/a	n/a	n/a
2	72	M	pancreatic cancer	30/12/2010	3.7	normal duct, PanIN 1	pT3N1	IIB	12
6	69	M	pancreatic cancer	28/10/2010	n/a	normal duct, PanIN 1	pT3N1	IIB	10
7	80	M	pancreatic cancer	01/07/2011	4	normal duct, PanIN 2, invasive cancer, lymph node with metastasis	pT3N1M1	IV	13

TNM - tumour staging system; **IPMN** - intraductal pancreatic mucinous neoplasm; **PanIN** - pancreatic intraepithelial neoplasia

Patient no.	Age	Sex	Diagnosis	Date of surgery	Tumour size (cm)	Histology	TNM	Stage	Survival (months)
9	75	M	pancreatic cancer	15/07/2011	4.6	normal duct, PanIN 1, PanIN 2	pT3N1	IIB	18
10	65	F	pancreatic cancer	24/06/2011	3.3	normal duct, PanIN 1	pT3N1	IIB	14
11	70	M	pancreatic cancer	17/06/2011	4.1	normal duct, PanIN 1, PanIN 3	pT3N1	IIB	3
12	81	M	pancreatic cancer	14/07/2011	2	normal duct, PanIN 1	pT3N0	IIA	15
14	58	M	pancreatic cancer	13/10/2011	4.7	normal duct, PanIN 1, PanIN 2	pT3N1	IIB	4
16	67	F	pancreatic cancer	14/10/2011	3.5	normal duct, PanIN 1	pT3N0	IIA	10

TNM - tumour staging system; **IPMN** - intraductal pancreatic mucinous neoplasm; **PanIN** - pancreatic intraepithelial neoplasia

Patient no.	Age	Sex	Diagnosis	Date of surgery	Tumour size (cm)	Histology	TNM	Stage	Survival (months)
17	62	F	chronic pancreatitis	07/10/2011	3.7	normal duct, PanIN 1	n/a	n/a	n/a
20	74	F	pancreatic cancer	24/11/2011	n/a	normal duct, PanIN 1	pT2N0	IB	18
23	82	M	pancreatic cancer	24/02/2012	4	invasive cancer	pT3N1	IIB	20
24	70	M	pancreatic cancer	01/03/2012	4.9	invasive cancer	pT3N1	IIB	9
25	63	F	benign peritoneal pseudocyst	26/01/2012	n/a	normal duct	n/a	n/a	n/a

TNM - tumour staging system; **IPMN** - intraductal pancreatic mucinous neoplasm; **PanIN** - pancreatic intraepithelial neoplasia

3.2.2 Optimization

The antibodies used were the MAD2L1 Rabbit anti-Human Polyclonal (aa3-13) antibody (1mg/ml, Lifespan Biosciences) for Mad2 and BUB1B/BubR1 Rabbit anti-Human Polyclonal Antibody (0.5mg/ml Lifespan Biosciences) for BubR1. The Mad2 antibody was optimized using human cerebral tissue while the BubR1 antibody was optimized using human endometrial tissue, as per manufacturer instructions. This was performed in the Graduate Entry Postgraduate Laboratory, Singleton Hospital ABMU Health Board. The Ventana automated immunohistochemistry protocol was used (Ventana Medical Systems, Tucson, AZ). All the steps in the optimization process as well as the supervision of the automated method was done by the senior staff in the Pathology Laboratory as per laboratory protocol.

Several readjustments were needed to ensure adequate staining as assessed by two independent reviewers.

An optimal dilution of 1:200 was obtained for Mad2 and 1:100 for BubR1 which enabled adequate staining on PDAC tissue.

The formalin-fixed paraffin embedded (FFPE) archival tissue sections from tissue blocks obtained after elective surgical resection for malignant or benign pancreatic disease were stored in the Histopathology Department, Morriston Hospital, ABMU Health Board Swansea. Immunostaining was performed on close serial sections cut from the same paraffin block used for the aneuploidy study so that the same duct could be analysed.

The 4 μm thick FFPE sections were kept at 37°C for 1 hour prior to the staining treatment.

The selected sections were then introduced in an automated system used for immunohistochemistry (Ventana Medical Systems, Tucson, AZ). The protocol used an indirect biotin-avidin system coupled to an enzyme product to allow visualization of the bound antibody. The detection kit used secondary antibodies to locate the bound primary antibody and was followed by the binding of an avidin enzyme conjugate to the biotin. The complex could then be visualized using a precipitating enzyme generated product. All the reagents, antibodies and stains were introduced in the corresponding slots in the carousel of the automated system. The slides to be analyzed were labeled with slide barcode labels generated by the automated protocol and introduced in their respective carousel. The automated system then ran the process to a set automated protocol. At the end of each workday an instrument cleaning procedure was performed. Biannual calibration was ensured. A negative control was run from each tissue block by excluding the application of the primary antibody.

3.3 Results

Each set of sections was accompanied by a hematoxylin and eosin stained section to allow identification of the relevant histopathological structures. This was compared with the sections used for IHC and thus the areas of interest were marked (Fig 3.1 - 3.2).

The scoring protocol included a score for the intensity of the staining and a score for the distribution of the staining. The Mad2 antibody produced predominantly nuclear staining, whereas the BubR1 antibody showed both cytoplasmic and nuclear staining. This has been shown in the literature in cases of PDAC and it seems to be related to the altered permeability of the nuclear membrane as a result of the carcinogenesis process (Burum-Auensen et al., 2007).

The scoring was performed for nuclear staining only and involved a score of 0 to 3 as per following:

- For intensity:
  - 0 = no staining
  - 1 = weak staining
  - 2 = moderate staining
  - 3 = strong staining
- For distribution:
  - 0 = no cells stained
  - 1 = less that 30% of cells stained
  - 2 = 30-60% cells stained
  - 3 = over 60% cells stained

The intensity and distribution of staining for the two different proteins varied between different histological stages for the same protein and also between the two proteins in the same specimen (Fig. 3.3).

The final score for each specimen was obtained by multiplying the intensity score by the distribution score.

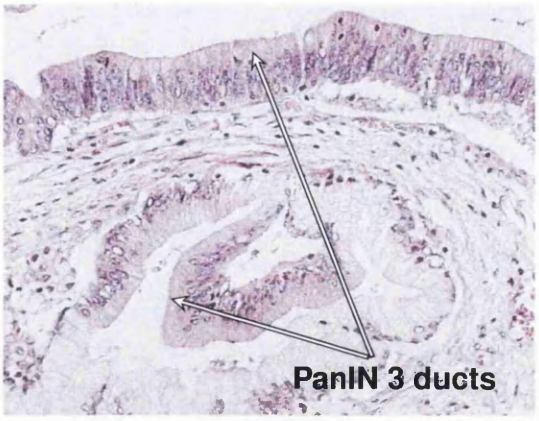

(a) Haematoxylin-eosin (HE) section x10 showing the multilayered ductal cells with some desquamation from the top layer and mucin accumulation at the apical pole.

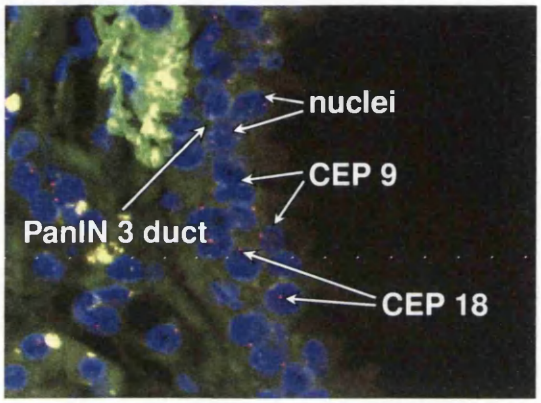

(b) FISH section x60 seen with DAPI filter showing a fragment of the duct with CEP 9 green signals, CEP 18 orange signals, DAPI blue cells nuclei and non-specific cytoplasmic uptake.

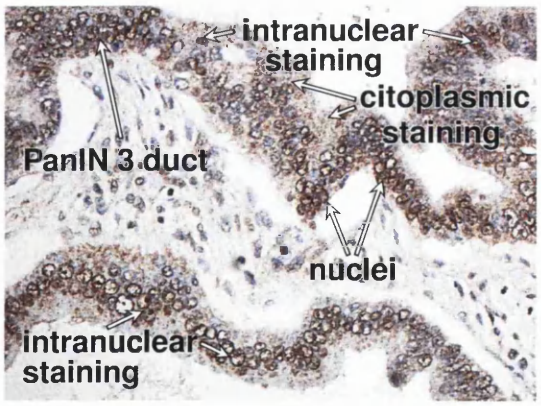

(c) Photomicrograph of the duct after immunostaining using Mad2 antibody with brown antibody predominantly intranuclear staining and blue nucleoplasm staining.

Figure 3.1: Tissue section with PanIN 3; PanIN 3 ducts highlighted on the HE section; the chromosomal probes CEP 9 and CEP 18 highlighted on the FISH section; the Mad2 score 6 staining highlighted on the IHC section.

(a) Haematoxylin-eosin (HE) section $\times 10$ showing the duct with areas of multilayered cells with mucin accumulation at the apical pole

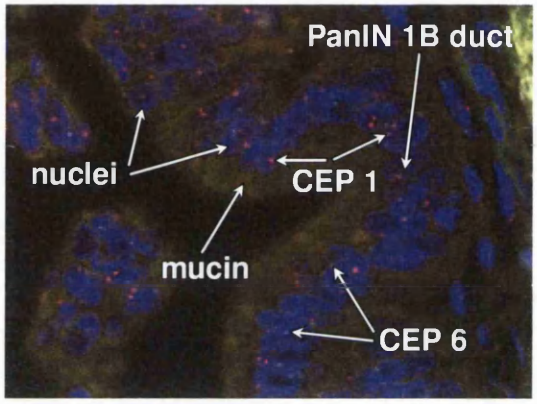

(b) FISH section $\times 60$ seen with DAPI filter showing a fragment of the duct with CEP 6 green signals, CEP 1 orange signals, DAPI blue cells nuclei and non-specific cytoplasmic uptake in the stromal layer

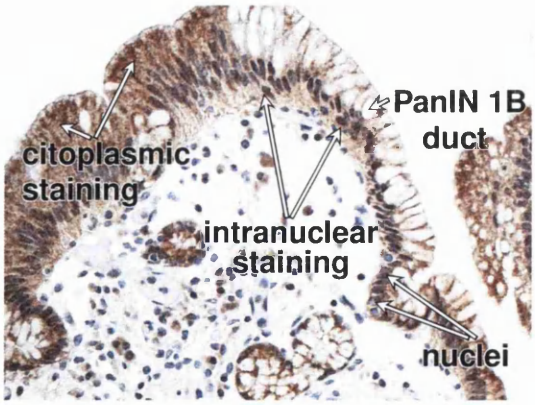

(c) Photomicrograph of the duct after immunostaining using BubR1 antibody with brown antibody intranuclear and cytoplasmic staining and blue nucleoplasm staining.

Figure 3.2: Tissue section with PanIN 1B; PanIN 1B duct highlighted on the HE section; the chromosomal probes CEP 1 and CEP 6 highlighted on the FISH section; the BubR1 score 4 staining highlighted on the IHC section.

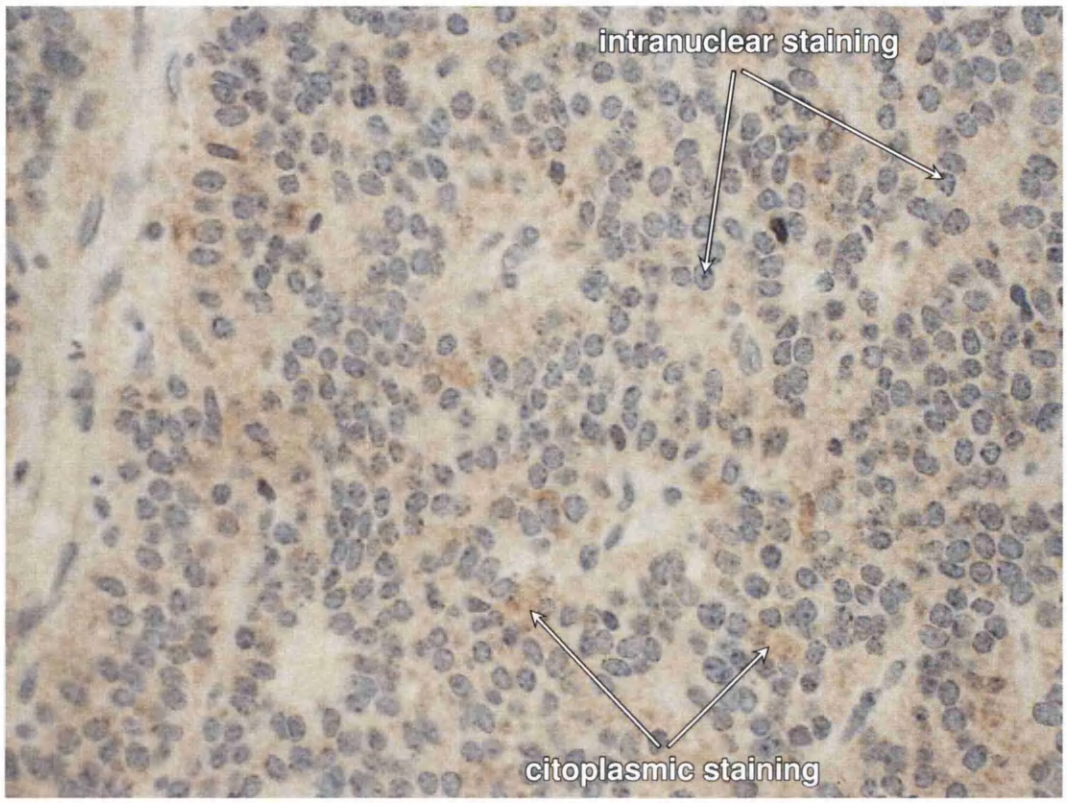

(a) BubR1

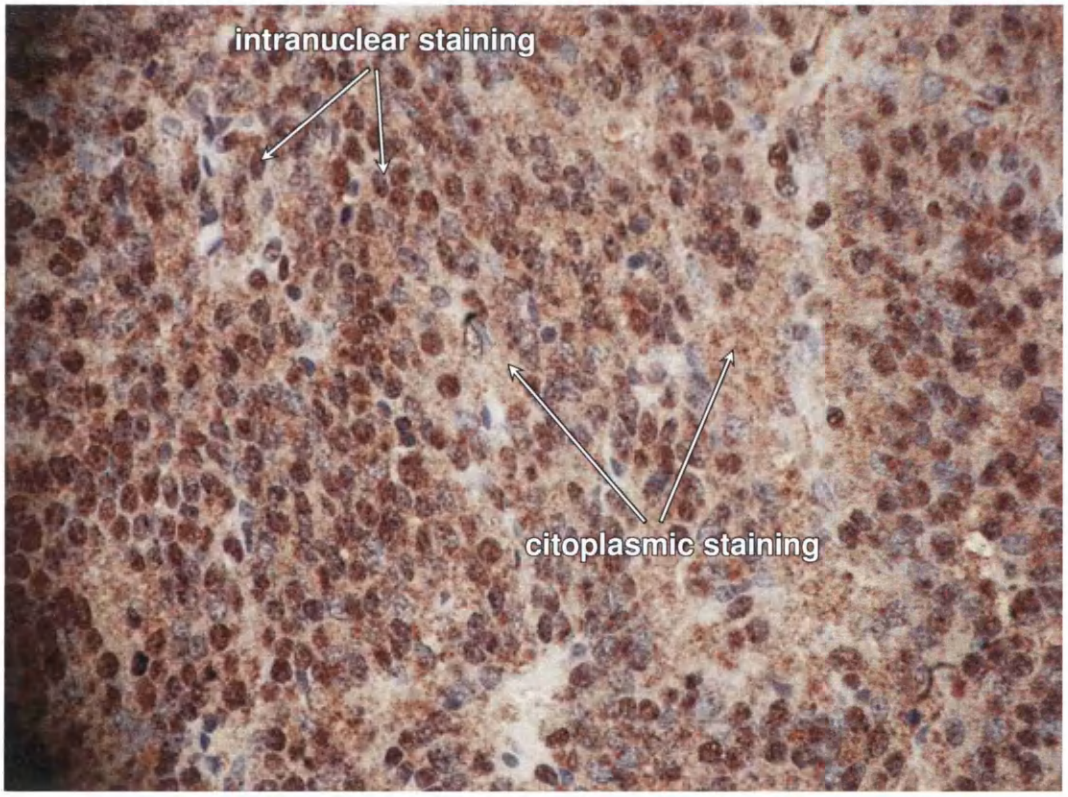

(b) Mad2

Figure 3.3: Photomicrograph $\times 40$ with immunostaining for BubR1 (score 2) and Mad2 (score 6), respectively, in the same specimen displaying pancreatic ductal adenocarcinoma

3.3.1 Statistical analysis

For analysis, the final scoring results were divided into overall and average protein levels.

They were then analysed using IBM SPSS Statistics version 2011. A Student paired t-test was used to compare the results for groups of two different histological stages and a Linear Mixed-Effect model was used to determine potential correlations with the aneuploidy data as well as specimen characteristics. Significance was attributed to a p-value less than 0.05. Several case studies were included to illustrate individual patterns in different tumours.

3.3.1.1 Protein levels (cohort and average values)

The detailed plotting of all values for the Mad2 protein levels in different histological stages followed a non-linear trend, similar to the average values included further on in this chapter. A median score of 6.00 was seen in all histological stages. The levels in normal ducts and in the areas with PDAC were similar, with most of the values positively skewed compared to the median. The levels found in PanIN 1 and PanIN 2 were below the median while PanIN 3 displayed values very different compared to the median (Fig. 3.4).

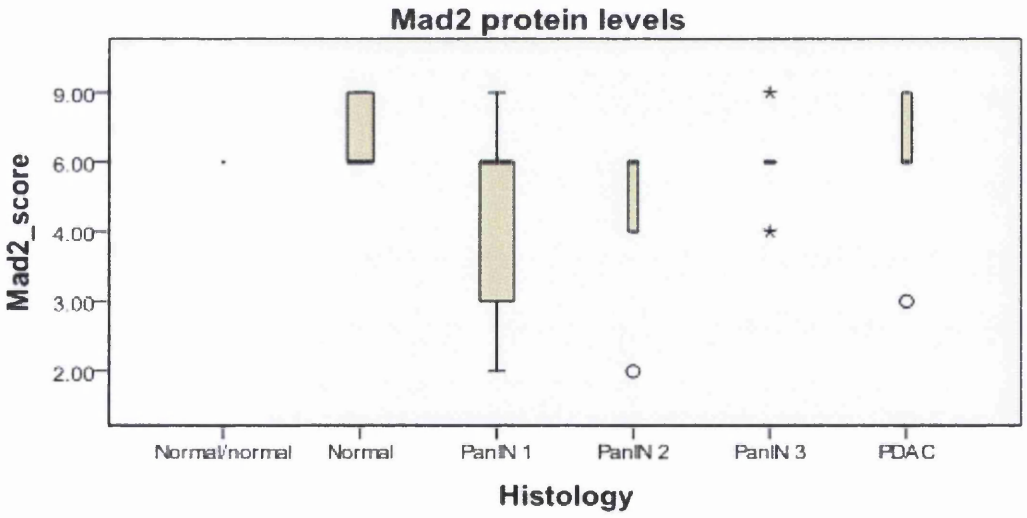

Figure 3.4: Box plot illustrating the levels of the mitotic checkpoint protein Mad2 in progressive histological stages scored by nuclear immunostaining; the median is represented by the thick horizontal line; outlier values are marked by ○ and ★ respectively

The detailed plotting of the values obtained for BubR1 showed a different trend compared to the values for Mad2 (Fig. 3.5). The median values for each histological

stage were variable and a score of zero (no staining seen), was found in some samples in all premalignant stages (normal, PanIN 1, PanIN 2 and PanIN 3). Noticeably, the values seen in PDAC were higher than all the other stages, as individual values as well as a median value (median=4.00, compared to median=3.00 in normal ducts and PanIN 3 and median=2.00 in PanIN 1 and PanIN 2). Also, most histological stages displayed outlier values on either side of the median.

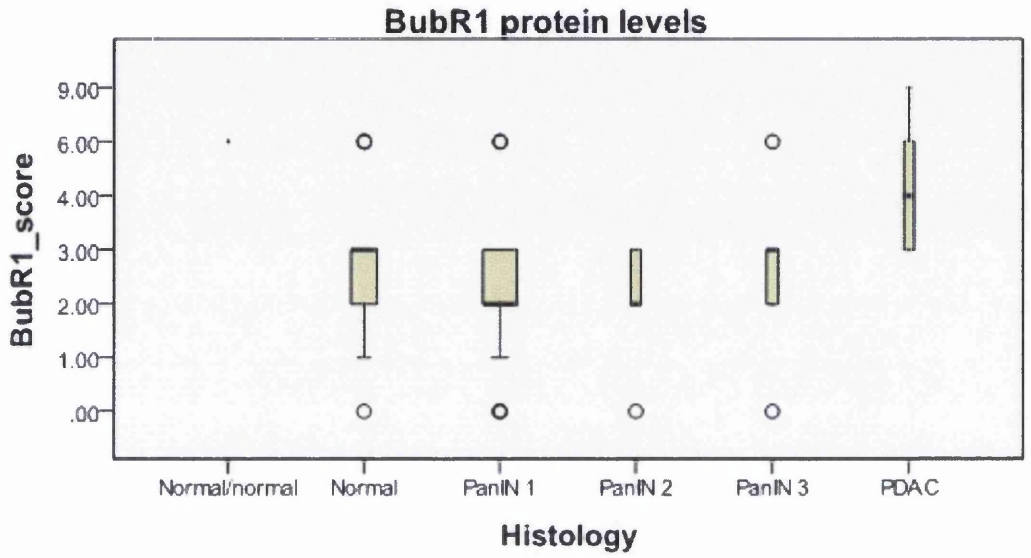

Figure 3.5: Box plot illustrating the levels of the mitotic checkpoint protein BubR1 in progressive histological stages scored by nuclear immunostaining; the median is represented by the thick horizontal line; outlier values are marked by ○

For a basic comparison of the scores in different histopathological stages, the average score for each histopathological stage (i.e. normal ducts, PanIN 1, PanIN 2, PanIN 3 and PDAC) was calculated for Mad2 and BubR1 and the results included in a bar graph (Fig. 3.6).

The average score for Mad2 across all histopathological stages showed disorganized variability. The levels in the normal ducts (average score 6.473) nearly reached the maximum average score across all stages (average maximum score 6.75, in PDAC).

The average score in PanIN 1 (A and B) showed a negative trend compared to the average score in the normal ducts (14.18% difference) but was higher than the score in PanIN 2 (16% difference). The average score in PanIN 3 displayed a 24.03% increase compared to PanIN 2 and a 9.56% increase compared to PanIN 1. Similarly, the average score in PDAC reached the maximum of all scores and was higher than the average score in PanIN 1 (17.69% increase) and PanIN 2 (30.86% increase), but was still similar to the score seen in normal tissue. No statistically significant difference was found between the scores in different histological stages.

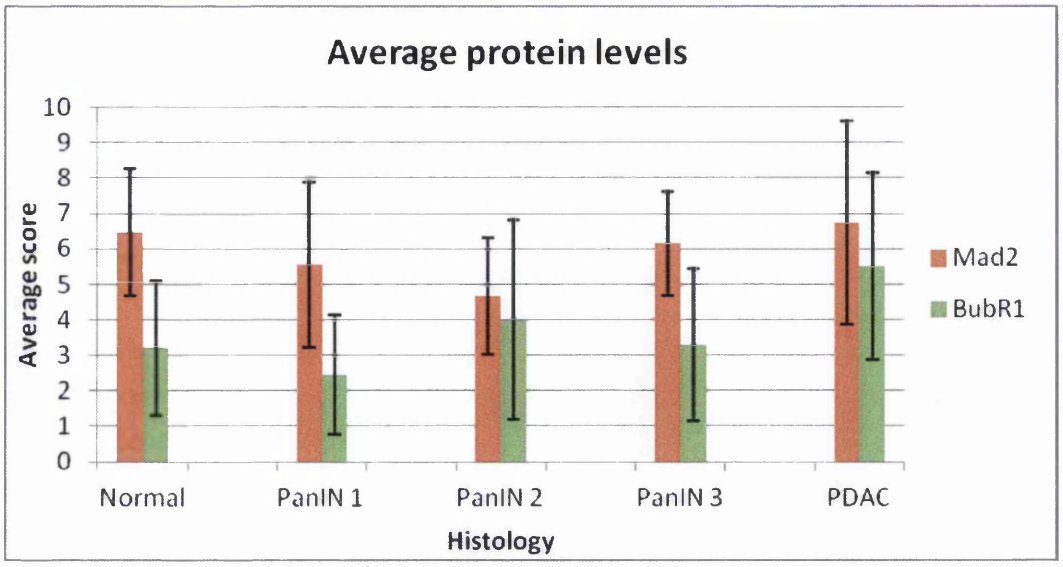

Figure 3.6: The average levels of proteins Mad2 and BubR1 scored by nuclear immunostaining in progressive histological stages

The average scores associated with BubR1 varied between different histological stages. The average score seen in the normal ducts was 3.2 and 2.44 in the ducts with PanIN 1 (23.61% difference). An increase was seen in PanIN 2 compared to PanIN 1 (38.88% difference) and the normal ducts (20% difference). Then the average scores registered a slight decrease in PanIN 3 compared to PanIN 2 (17.85% difference) but then increased significantly in PDAC compared to the normal ducts (p=0.050) and PanIN 1 (p=0.007).

The display of the levels of both proteins in relation to histological stages showed more distinctly the differences between their trends (Fig. 3.7).

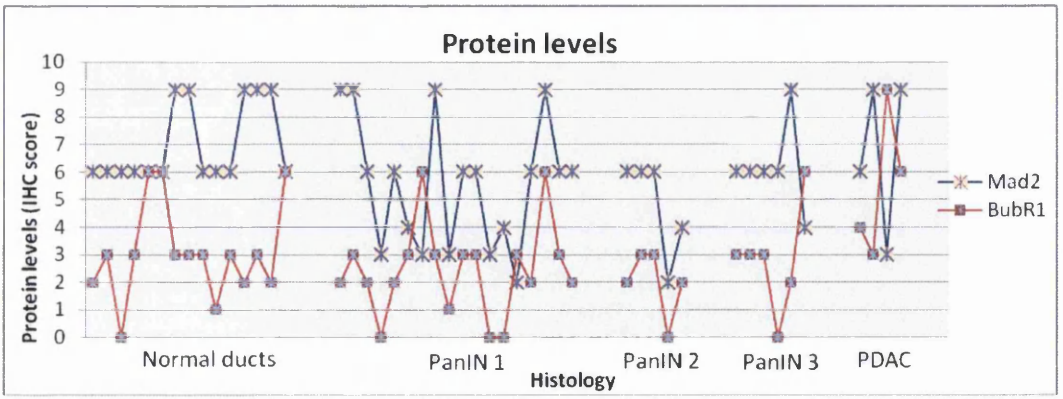

Figure 3.7: The combined levels of Mad2 and BubR1 in all the histological stages

Thus, in the normal ducts, in the ducts with PanIN 3 and in the areas with PDAC, the levels of Mad2 and BubR1 generated a trend that is almost the mirror image of each other. In the ducts with PanIN 1 and the ducts with PanIN 2 the trend was similar

between the two proteins. Overall, the scores for BubR1 were lower than the scores for Mad2 in all premalignant stages, while in PDAC they showed disparate trends.

A total of 18 specimens with ducts classed as PanIN 1 (A and B) which displayed a wide range of aneuploidy were selected in order to investigate any observational trend patterns in the IHC scores related to different extremes of aneuploidy levels. 9 specimens displayed a relatively low level of average overall aneuploidy across chromosomes 1, 6, 9 and 18 (up to 39% average overall aneuploidy) while the remaining 9 displayed a relatively high level (above 39% average overall aneuploidy).

The corresponding scores for Mad2 and BubR1 were plotted against the average overall aneuploidy levels to investigate whether there is any similarity in their trends (Fig. 3.8). This showed that in both groups the levels of Mad2 and BubR1 followed individual trends, not consistently mirrored by the average aneuploidy. This could be generated by the fact that the average aneuploidy across all chromosomes included in the study blends together highly different individual trends in chromosomal anomalies and that the levels of Mad2 and BubR1 followed a different trend.

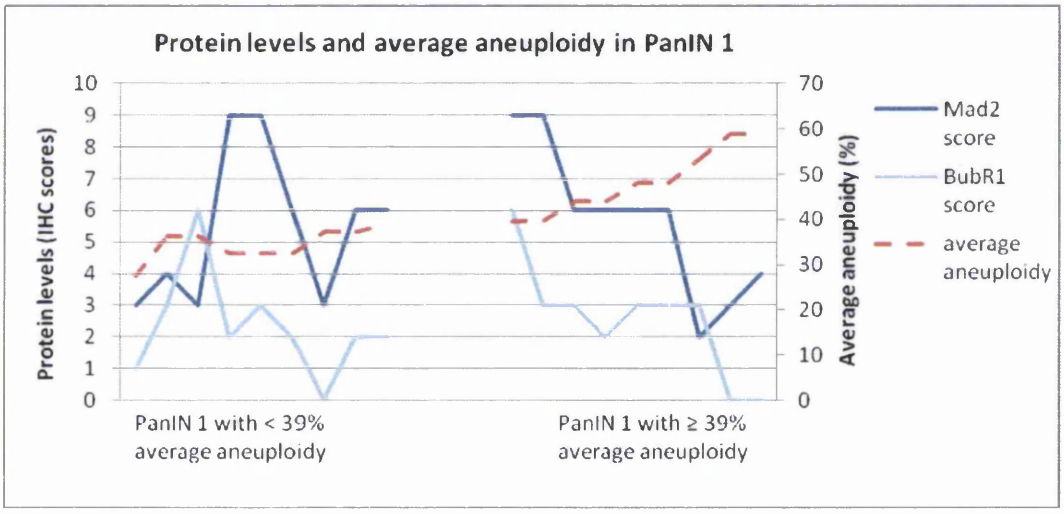

Figure 3.8: The trends in the immunohistochemistry scores for Mad2 and BubR1 (values on the primary vertical axis) and in the average overall aneuploidy (percentages on the secondary vertical axis) in the specimens with PanIN 1 in individual patients with relatively low levels of average overall aneuploidy (<39%, to the left of the plot area) and in the specimens with PanIN 1 with relatively high levels of average overall aneuploidy (≥39%, to the right of the plot area)

In the ducts with PanIN 1 the average aneuploidy was represented by deletions as the level of amplifications was on average much lower (0-3.21%) and so the correlations demonstrated earlier were not reflected in this particular set of data.

3.3.1.2 Correlations

An analysis was conducted to study the interaction between the levels of proteins (Mad2, BubR1) and general patient data, specimen level data and chromosome data. The patient level data consisted of background characteristics such as patient sex, age and tumour size. The specimen level data included a classification of histology, while the chromosome data contained measurements of aneuploidy, amplification and deletion levels for chromosomes 1, 6, 9 and 18.

As a consequence of the complex interactions between these variables and the unbalanced and hierarchical nature of the data set it was felt that simple correlations would not provide a robust tool for making these measurements. In place of this Linear Mixed-Effect models (LMM) were fitted in SPSS. LMMs are comparison models used to compare data from different categories with large a number of independent variable. Among the independent variables only the amplification data failed a Kolmogorov-Smirnov test of normality and was therefore log transformed in order to qualify for inclusion. The key dependent variables representing the protein levels (Mad2, BubR1) failed a Kolmogorov-Smirnov test, and could not be transformed. However, this failure appeared to be as a result of their discrete structure and as they exhibited neither strong asymmetry nor long tails it was felt that the method would be sufficiently robust.

The first stage of the analysis was to identify which of the background variables correlated with the protein and chromosome levels so that their effect could be included in any tests of correlation. A LMM was fitted in each case, with the optimal model chosen using AIC/BIC criteria rather than the p-values of the individual terms. Table 3.2 shows the chosen parameters included in the optimal models for each variable. These are potential confounders and should be included in any test of correlation to compensate for their impact. Only one of the two associations involving protein levels was significant, with the groups of PanIN 3 and PDAC associated with significantly reduced Mad2 levels (p=0.025).

Table 3.2: The parameters included in the optimal models for each variable in the LMM model

Variable	Histology	Sex	Age	Tumour Size
Mad2	1	—	—	—
BubR1	—	—	—	1
Ploid1	—	1	—	—
Ploid6	—	—	—	—
Ploid9	1	—	1	—
Ploid18	1	—	—	—
Amp1	1	—	—	—
Amp6	1	1	1	—
Amp9	1	—	—	—
Amp18	—	—	—	—
Del1	1	1	—	1
Del6	—	—	—	—
Del9	—	—	1	—
Del18	—	—	—	1

A LMM was then built to measure the residual correlation between protein levels and all of the chromosome markers in turn, after allowing for the effects of all correlates of either variable. The statistically significant associations are shown in Table 3.3.

Given the large number of tests we conducted there is a serious danger of false positive results due to multiple testing. None of these results would be likely to survive a conservative correction for multiple testing (such as Bonferroni), although it is arguable whether such a correction is necessary, or even appropriate. As a consequence of these points and of the distribution of certain key variables we should be cautious in our interpretation of the findings.

Table 3.3: The statistically significant associations obtained from the LMM model

Dependent Variable	Independent Variable	p-value	Estimate (95% CI)		Other variables included in model
Mad2	Amp1	0.011*	−0.83	[−1.45,−0.20]	Histology
BubR1	Amp1	0.058	0.47	[−0.02,0.96]	Histology, Tumour size
BubR1	Amp6	0.008**	1.80	[0.55,3.05]	Histology, Sex, Age, Tumour size
BubR1	Del1	0.024*	−0.06	[−0.12,−0.01]	Histology, Sex, Tumour Size

*$p < 0.05$; **$p < 0.01$

3.3.2 Case studies

We selected several specimens with a variety of progressive histological stages in order to provide insight into the characteristics of individual tumours and also into the relevant changes at chromosomal and mitotic checkpoint protein levels.

For the purpose of illustrating this, examples were included in this analysis, similar to the case studies in the chapter on aneuploidy.

The first case study is based on a specimen that displayed normal ducts, ducts with PanIN 1B, ducts with PanIN 2 and ducts with PanIN 3. The levels of amplifications, deletions and overall aneuploidy were scored as described in the aneuploidy chapter and then the levels of the Mad2 and BubR1 proteins were scored by immunohistochemistry. In this particular case, the values for the parameters described do not follow intuitive or correlated trends (Fig. 3.9).

The average percentages for overall aneuploidy and deletions across chromosomes 1, 6, 9 and 18 displayed a slight negative curve starting with PanIN 1B and through to PanIN 3 while the average percentages for amplifications described a slight positive curve in the same histological stages. These trends were not consistently reflected by the trends for the levels of Mad 2 and BubR1: BubR1 showed no uptake in the ducts with PanIN 1B, PanIN 2 or PanIN 3 (but generated a score of 1 in the normal ducts, hence excluding technical bias) while Mad2 reflected the overall trends seen in the average Mad2 levels: high score in the normal ducts, decreasing then in the PanIN 1B, PanIN 2 and increasing sharply in PanIN 3.

The second case study involved a specimen with normal ducts, ducts with PanIN 2, areas with PDAC and an adjacent lymph node metastasis. The trends for the average

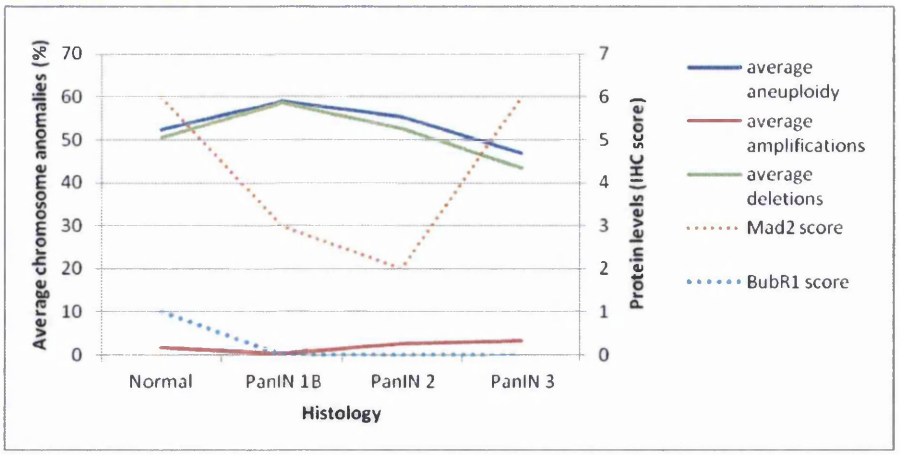

Figure 3.9: The trends for average aneuploidy, average amplifications and average deletions (percentages on the primary Y axis) and for the immunostaining scores for the Mad2 and BubR1 protein levels (values on the secondary Y axis) in the first case study

overall aneuploidy, amplifications and deletions across chromosomes 1, 6, 9 and 18 were plotted against the trends for the scores for the Mad2 and BubR1 protein levels (Fig. 3.10).

Here, the trends for the average overall aneuploidy (mainly consisting of deletions) and for the average amplifications displayed a positive curve, starting in the normal ducts and continuing in the ducts with PanIN 2, with the top values seen in PDAC and the lymph node metastasis. In contrast, the scores for Mad2 were high in the normal ducts, decreased in PanIN 2 and remained stable in PDAC and lymph node metastasis. The scores for BubR1 followed a mirroring trend, with higher values in one normal duct and lesser values for the other histological stages.

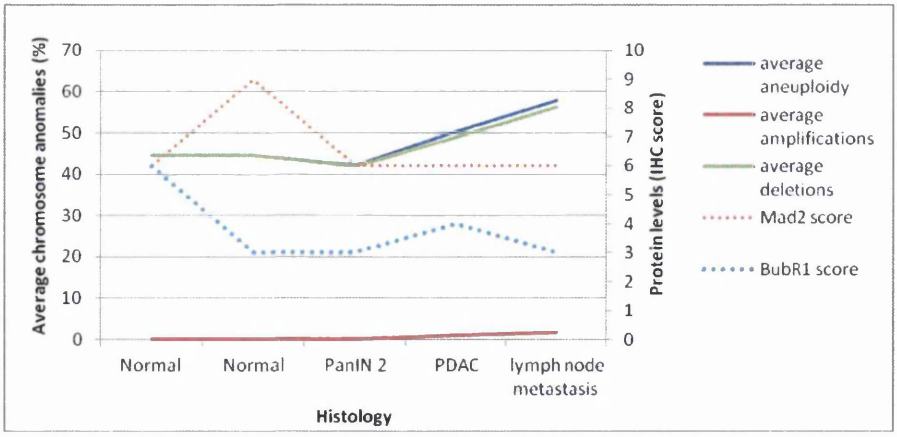

Figure 3.10: The trends for average aneuploidy, average amplifications and average deletions (percentages on the primary Y axis) and for the immunostaining scores for the Mad2 and BubR1 protein levels (values on the secondary Y axis) in the second case study

3.4 Discussion

3.4.1 Correlations

Overall, the peak average levels for Mad2 and BubR1 were seen in PDAC. However, the trend for Mad2 revealed similarly high levels in the normal ducts from PDAC specimens while for the other histological stages the trend appeared random. Meanwhile, the levels for BubR1 showed a fairly consistent upward trend with low average levels in the normal ducts and comparatively high levels in PDAC.

Advanced statistical model analysis revealed correlations between the levels of Mad2 and BubR1 and aneuploidy but the results need cautious interpretation because of the multiple incongruent variables included in the model.

Wu et al. 2004, used the Western Blot method to quantify the levels of Mad2 and cyclin B1 and flow cytometry for cell cycle distribution and DNA ploidy in a panel of gastric cancers. They found that even though increased levels of Mad2 were found in 74% of tumours there was no association with the ploidy status or the clinicopathological characteristics of the sample.

3.4.2 BubR1 as a potential indicator of aneuploidy

Amplifications are significant molecular events in carcinogenesis and the positive correlation with one of the major checkpoint protein levels reinforces the link between the function of the spindle assembly checkpoint and the incidence of chromosomal abnormalities (Bharadwaj et al., 2004).

Shin et al. found that BubR1 was down regulated in colon adenocarcinomas and that the decrease of the BubR1 protein levels was potentially linked to chromosomal instability in their study (Shin et al., 2003).

Gladhaug et al. used immunohistochemistry on tissue microarrays to investigate the levels of spindle checkpoint proteins Aurora A, Mad 2 and BubR1 in resected adenocarcinomas localized in the head of the pancreas. Their results showed that the expression of the mentioned proteins was not associated with ploidy status. Any level of BubR1 was shown to be sufficient to predict poor prognosis (p=0.006) while Aurora A and Mad2 expressions were not related to prognosis. Also, BubR1 expression was found to independently predict a poor prognosis (Gladhaug IP et al., 2010).

Baker et al. reached the conclusion that increased levels of BubR1 are protective against aneuploidy and potentially extend the healthy lifespan in several tissues by correcting mitotic checkpoint impairment and microtubule-kinetochore attachment defects. They used transgenic mice to illustrate that sustained high levels of BubR1 potentially preserve genomic integrity and reduce tumorigenesis (Baker et al., 2013).

In the present study further investigations into potential correlations between the

levels of Mad2 and, particularly, BubR1 were deemed unsuitable due to sample design and limitations in applying suitable statistical tests.

3.4.3 Caveats: low vs high aneuploidy, case studies

The Mad2 and BubR1 protein levels failed to show a correlating trend with the levels of average aneuploidy in two distinct groups of specimens with PanIN 1 ducts: one with relatively low levels of average overall aneuploidy (<39%) and the other with relatively high levels of average overall aneuploidy ($\geqslant$39%). This may be related to the early premalignant stage or to the fact that in this stage the overall aneuploidy is mainly represented by deletions and no significant direct correlation was found with the Mad2 and BubR1 protein levels.

The case studies represented two specimens with a variety of histological stages and thus different levels of overall aneuploidy. They did not reveal any correlations between the levels of overall aneuploidy and the levels of the Mad2 and BubR1 proteins. This could be related to individual characteristics and heterogeneity of the tumours but also an indication of the complexity of the molecular changes that occur in carcinogenesis.

3.4.4 Separate findings

Incidentally, it was noted that the Mad2 and BubR1 protein levels in the normal acinar cells and islets of Langerhans in the normal pancreatic specimens displayed a similar level as the cells in an endocrine tumour (Fig. 3.11 - 3.12). This observation was based on seeing the different patterns of Mad2 and BubR1 staining and immunostaining of a small sample of endocrine tumours following this. The interest comes from the fact that endocrine tumours have a much better prognosis than ductal adenocarcinomas. The next step would be to compare Mad2 and BubR1 levels with tumour size and Ki-67 proliferation rate which are the main prognostic factors, and this forms the design for a separate research project.

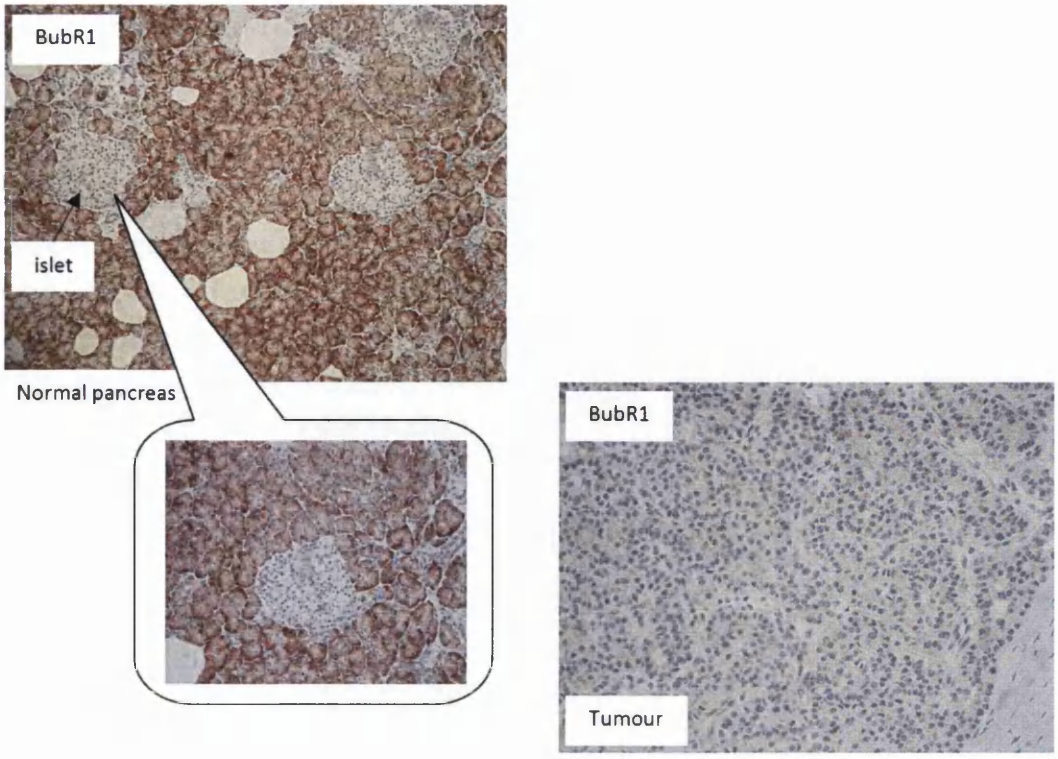

Figure 3.11: Immunostaining for BubR1 levels in the islet endocrine cells in a normal pancreatic tissue displays a similar intensity to an endocrine tumour specimen

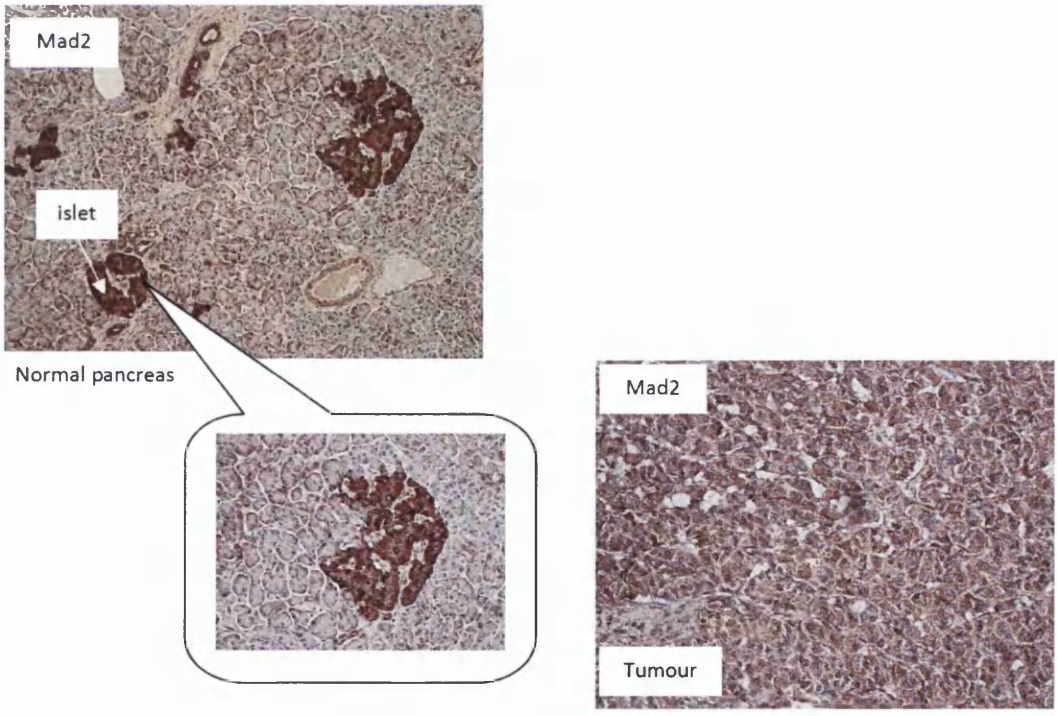

Figure 3.12: Immunostaining for Mad2 levels in the islet endocrine cells in a normal pancreatic tissue displays a similar intensity to an endocrine tumour specimen

3.5 Conclusion

The levels of mitotic checkpoint proteins Mad2 and BubR1 demonstrated up-regulation in the final stage of carcinogenesis but failed to characterize a defined premalignant stage where the trend would increase significantly. Limitations related to sample size precluded further statistical testing regarding correlations and significance for progress and survival. However, the advances in diagnostic and therapeutic methods open the field for in depth characterization of the tumorigenesis in pancreatic adenocarcinoma.

Chapter 4

General Discussion

Pancreatic carcinogenesis is an intricate process which has been investigated with perseverance due to the rapid natural progress of the disease. The current pilot study aimed to discover links between the aneuploidy levels in progressive premalignant histological stages of PanIN and the characteristics of the respective tumour as well as data on the mitotic checkpoint proteins Mad2 and BubR1. We used FISH to score the aneuploidy levels displayed by chromosomes 1, 6, 9 and 18 and found that the most significant abnormalities were the amplifications and that the overall aneuploidy levels increase significantly in the late premalignant stage of PanIN 3 and in ductal adenocarcinoma for all the chromosomes analysed. Also, in view of the recognized intercorrelations between aneuploidy and anomalies in the mechanisms controlling the cell cycle, we proceeded with selecting one group of specimens with relevant levels of aneuploidy and subjected them to IHC treatment to see if the levels of expression for Mad2 and BubR1 reflect a similar pattern to aneuploidy. We found that it was difficult to establish a clear correlation, most likely due to the small number of specimens and the large panel of variables.

FISH is a widely used method of investigating chromosomal anomalies and the extended methods of SKY (spectral karyotyping) and CISH (chromogenic in situ hybridization) allow detailed mapping of specific normal or abnormal DNA sequences, in either interphase or metaphase, or global changes in individual chromosomes. For the present study, only a snapshot of four chromosomes was included because of time limitations and the specimens were scored only by one investigator.

Among other methods used alongside FISH are comparative genomic hybridization (CGH), loss of heterogosity (LOH) studies, flow cytometry, microarrays analysis. The advantage of these methods is that they are highly specific for genetic mutations which allows a detailed mapping of the mutations in a tumour specimen. The disadvantage is that they have less specificity for aneuploidy. Using CGH in this study may have returned a more detailed profile of the gene mutations corresponding to each of the premalignant stage included but less information about the specific aneuploidy levels.

The aneuploidy levels found in this study were mainly represented by deletions which are predominantly related to sectioning bias. Nevertheless, the most relevant anomalies were the amplifications which increased significantly in PanIN 3 and ductal adenocarcinoma.

Similarly, a study on breast cancer showed that aneuploidy is present in a third of cases with atypical hyperplasia, in a larger proportion of intraductal carcinomas and in the majority of cases with invasive carcinoma (Shackney S et al., 1995).

In prostate intraepithelial neoplasia, chromosome missegregation occurs alongside point mutations, driving the carcinogenesis to the stage of prostate cancer (Qian J et al., 1999).

In Barrett's oesophagus, most of cell populations are diploid, but in some cases aneuploidy arises in one population and it can then spread to a large area, persisting for a long period of time before the progression to invasive adenocarcinoma (Reid BJ et al., 1996).

A study investigating the potential implications of aneuploidy for improved screening for colorectal cancer in ulcerative colitis patients found that the evaluation of DNA ploidy in correlation to laminin-5 (basement membrane protein) positivity and increased cyclin A expression in aneuploid lesions appeared to be the strongest predictor for malignant change in an individual patient (Habermann JK et al., 2012).

Other studies looking at the genetic changes in pancreatic carcinogenesis found that the most significant events took place mostly at the PanIN 2 stage (p16 inactivation, MUC1 overexpression) (Koostra JBM et al., 2008, Maitra A et al., 2003). Our study found that there was a significant increase in the level of overall aneuploidy and in the level of amplifications at the PanIN 3 stage. The levels in the PanIN3 stage were similar to the levels found in the ductal adenocarcinoma.

The progress in molecular research in pancreatic carcinogenesis is leading the road to individualized genetic therapy. Also, the quest for biomarkers with high specificity and sensitivity is a high priority. In this context, aneuploidy could play a role as a clinical tool contributing to a panel of biomarkers used to determine the genetic imprint of a particular tumour. The standardized methods of scoring aneuploidy are already allowing its use in breast cancer to determine the Her2 status which then guides the therapy. Likewise, aneuploidy is an indicator of progression in Barrett's oesophagus, uroepithelial tumours and myeloproliferative diseases (Reid BJ et al., 1996, Qian J et al., 1999, Nolte M et al., 1996, Chapman PB et al., 2011).

The large panel of molecular changes in pancreatic carcinogenesis have been investigated in the hope of discovering more therapeutic targets. Unfortunately, the complexity of the molecular changes has imposed limitations on the use of specific therapeutic targets.

The most useful molecular change could potentially be a marker easily measurable

and with an accurate sensitivity and specificity for carcinogenesis.

The abnormal expression of the mitotic checkpoint protein BubR1 is linked to aneuploidy as one of the mechanisms of chromosomal instability. This protein can be easily assessed using immunohistochemistry which is widely available as a standard method in the histopathology departments.

Tang Y-C et al. 2011 investigated the potential targeting of aneuploid cells in tumours with specific drugs as part of new cancer therapies. They found that the 17-N-allylamino-17-demethoxygeldanamycin (17-AAG), an antibiotic derivative which inhibits the heat shock protein 90 (Hsp90) and the 5-Aminoimidazole-4-carboxamide ribonucleotide (AICAR), an analog of adenosine which stimulates the AMP-dependent-protein-kinase activity (AMPK), showed increased selectivity against mouse embryonic fibroblasts with trisomy. Also, the two mentioned molecules showed some selectivity against cells with chromosomal instability related to specific alterations in BubR1 and Cdc20. These results were demonstrated also in colorectal cancer cell lines and only for AICAR in a subset of lung tumour cell lines, showing that the findings are highly specific to certain subsets of tumour cell lines. The potential application, in view of the authors, is that once these results would be confirmed by in vivo studies, cancer cells could be treated with drugs that increase aneuploidy by impacting on chromosome alignment or the mitotic checkpoint, in sinergy with drugs that act against the proteotoxic and energy stress induced by aneuploidy.

The ductal premalignant stages are characterized by progressive cellular changes which help differentiate between the different stages. In the early stages there is a progressive accumulation of mucin while in the late premalignant stages there is desquamation of the cells in the top cellular layer. The macroscopic changes are accompanied by the corresponding molecular changes at every stage. The differences between PanIN 1A and 1B are often subtle but PanIN 1B has more similarities with PanIN 2. PanIN 3 can be difficult to differentiate from the adenocarcinoma invading the ducts so, in order to ensure a confident grading, the ducts with PanIN 3 need to be away from the tumour.

The patients included in the aneuploidy study had a survival period of 12 months, on average, ranging between 3 and 18 months. From an observational perspective it appeared that a tumour size less than 4 cm was correlated with a better survival while a high level of amplifications in the PanIN3 or PDAC areas, with a poorer prognosis. However, a robust detailed analysis was not performed due to the small sample size and large panel of compounding variables.

No correlation was noted between the Mad2 and BubR1 protein levels and survival but again the small sample size needs to be taken into account as well as the fact that the scoring was limited to histological lesions rather than the entire tumour.

The results from this study need to be considered in the context and limitations of

the study. The conclusions are not imposing but the small numbers and the limited follow-up period are contributing to the limitations. More follow-up, in the form of disease-free survival rather than deceased or not type of data would enlarge the picture about how the aneuploidy in premalignant stages associated with a tumour may influence progress and survival.

A recent pilot study found that the progression-free survival period was longer than expected in 27% of the selected patients with refractory cancers who were treated using targets identified by molecular profiling with IHC, FISH and microarray analysis (Von Hof et al., 2010). Prospective clinical trials are currently being designed to include a genotypic arm where genetic profiling is the selection criteria in view of validating useful novel biomarkers (Schmid RM, 2013).

Future work related to the current study would include extending the period of clinical follow-up to allow for better survival analysis, including more specimens with PanIN 2 and PanIN 3 lesions which represent a significant step in carcinogenesis, expanding the panel of molecular markers investigated i.e include more chromosomes, investigate relevant genetic pathways alongside the numerical anomalies, include a larger panel of protein markers. Obtaining specimens of normal pancreatic tissue from other centres would expand the negative control group allowing for more in depth analysis. Also, pancreatic juice analysis using mass spectrometry would potentially demonstrate correlated components linked to carcinogenesis. A separate project is planned to investigate the Mad2 and BubR1 levels in pancreatic endocrine tumours and correlate them with tumour size and Ki-67 proliferation rate which are the main prognostic factors. The prognosis for pancreatic endocrine tumours is better than for pancreatic adenocarcinoma and the study could reveal what impact the levels of Mad2 and BubR1 have on it.

Chapter 5

Conclusion

Aneuploidy is a significant progressive molecular event in pancreatic carcinogenesis and by investigating it alongside other parameters like mitotic checkpoint proteins Mad2 and BubR1 it could add to the molecular signature of individual tumours.

Chapter 6

List of illustrations

Chapter 7

Bibliography

Adsay NV, Dergham ST, Koppitch FC, Dugan MC, Mohamed AN, Vaitkevicius VK, Sarkar FH. 1999. Utility of fluorescence in situ hybridization in pancreatic ductal adenocarcinoma. *Pancreas* 18(2), 111-116.

Adsay NV, Fukushima N, Furukawa H, Hruban RH, Klimstra DS. 2010. Intraductal neoplasms of the pancreas. In: Bosman FT, CarneiroF, Hruban RH, Theise N (eds).*WHO Classification of tumours of the digestive system. World Health Organisation Classification of tumours* IARC, Lyon, pp 304-313.

Aguirre AJ, Brennan C, Bailey G, Sinha R, Feng B, Leo C, Zhang Y, Zhang J, Gans JD, Bardeesy N, Cauwels C, Cordon-Cardo C, Redston MS, DePinho RA, Chin L.2004. High-resolution characterization of the pancreatic adenocarcinoma genome. *PNAS* 101(24), 9067-72.

Almoguera C, Shibata D, Forrester K, Martin J, Arnheim N, Perucho M. 1988. Most human carcinomas of the exocrine pancreas contain mutant c-K-ras genes. *Cell* 53, 549-554.

Babu JR, Jeganathan KB, Baker DJ, Wu X, Kang-Decker N, van Deursen JM. 2003. Rae1 is an essential mitotic checkpoint regulator that cooperates with Bub3 to prevent chromosome missegregation. *J Cell Biol* 160, 341-353.

Baker DJ, Jeganathan KB, Cameron JD, Thompson M, Juneja S, Kopecka A, Kumar R, Jenkins RB, de Groen PC, Roche P, van Deursen JM. 2004. BubR1 insufficiency causes early onset of aging associated phenotypes and infertility in mice. *Nat Genet* 36, 744-749.

Baker D, Dawlaty M, Wijshake T, Jeganathan K, Malureanu L, van Ree J, Crespo-Diaz R, Reyes S, Seaburg L, Shapiro V, Behfar A, Terzic A, van de Sluis B, van Deursen J. 2013. Increased expression of BubR1 protects against aneuploidy and cancer and extends healthy lifespan. *Nature Cell Biol* 15, 96-102.

Bardeesy N, Aguirre AJ, Chu GC, Cheng KH, Lopez LV, Hezel AF, Feng B, Brennan C, Weissleder R, Mahmood U, Hanahan D, Redston MS, Chin L, Depinho RA. 2006. Both p16(Ink4a) and the p19(Arf)-p53 pathway constrain progression of pancreatic adenocarcinoma in the mouse. *Proc Natl Acad Sci USA* 103, 5947-52.

Bartlett JM. 2004. Fluorescence in situ hybridization, technical overview. *Methods in molecular medicine* 97, 77-87.

Bartlett JM, Going JJ, Mallon EA, Watters AD, Reeves JR, Stanton P, Richmond J, Donald B, Ferrier R, Cooke TG. 2001. Evaluating HER2 amplification and overexpression in breast cancer. *J Pathol* 195, 422-428.

Baumgart M, Werther M, Bockholt A, Scheurer M, Rüschoff J, Dietmaier W, Ghadimi BM, Heinmöller E. 2010. Genomic instability at both the base pair level and the chromosomal level is detectable in earliest PanIN lesions in tissues of chronic pancreatitis. *Pancreas* 39(7), 1093-1103.

Bauxbaum JL, Eloubeidi ML. 2010. Molecular and clinical biomarkers of pancreas cancer. *JOP* 11(6), 536-544.

Benson AB. 2007. Adjuvant therapy for pancreatic cancer, one small step forward. *JAMA* 297, 311-313.

Bharadwaj R, Yu H. 2004. The spindle checkpoint, aneuploidy, and cancer. *Oncogene* 23, 2016-27.

Bierie B, Moses HL. 2006. Tumour microenvironment: TGFbeta: the molecular Jekyll and Hyde of cancer. *Nat Rev Cancer* 6, 506-20.

Bockman DE. 2008. Anatomy and fine structure. [Online] In: Beger HG, Warshaw AL, Buchler MW, Kozarek RA, Lerch MM, Neoptolemos JP, Shiratori K, Whitcomb DC, Rau BM Eds. *The Pancreas: An integrated textbook of basic science, medicine, and surgery* (2nd Ed):50-52, Wiley-Blackwell Publishing Ltd [Accessed on June 30, 2014].

Braat H, Bruno M, Kuipers EJ, Peppelenbosch MP. 2012. Pancreatic cancer: promise for personalized medicine? *Cancer Letters* 318, 1-8.

Brand RE, Lerch MM, Rubinstein WS, Neoptolemos JP, Whitcomb DC, Hruban RH, Brentnall TA, Lynch HT, Canto MI. 2007. Advances in counselling and surveillance of patients at risk for pancreatic cancer. *Gut* 56, 1460-9.

Brossens LAA, Oferhaus GJ. 2013. Molecular pathology of pancreatic cancer precursors lesions. In: Simeone DM, Maitra A (eds). *Molecular genetics of pancreatic cancer*pp 27-47. New York: Springer Science Ltd.

Buchwalow IB, Bocker W. 2010. *Immunohistochemistry: Basics and Methods (1st Ed)*pp 27-47. Berlin: Springer Verlah Heidelberg.

Burum-Auensen E, De Angelis PM, Schjølberg AR, Kravik KL, Aure M, Clausen OP. 2007. Subcellular localization of the spindle proteins Aurora A, Mad2 and BubR1 assessed by imunohistochemistry. *J Histochem Cytochem* 55, 477-486.

Cahill DP, Lengauer C, Yu J, Riggins GJ, Willson JK, Markowitz SD, Kinzler KW, Vogelstein B. 1998. Mutations of mitotic checkpoint genes in human cancers. *Nature* 392, 300-303.

Caldas C, Hahn SA, da Costa LT, Redston MS, Schutte M, Seymour AB, Weinstein CL, Hruban RH, Yeo CJ, Kern SE. 1994. Frequent somatic mutations and homozygous deletions of the p16 (MTS1) gene in pancreatic adenocarcinoma. *Nat Genet* 8, 27-32.

Callagy G, Pharoah P, Chin SF, Sangan T, Daigo Y, Jackson L, Caldas C. 2005. Identification and validation of prognostic markers in breast cancer with the complementary use of array-CGH and tissue microarrays. *J Pathol* 205, 388-396.

Cancer Research UK 2014. Pancreatic cancer mortality statistics [Online]. `http://www.cancerresearchuk.org/cancer-info/cancerstats/types/pancreas/mortality/#citationstats` [Accessed June 29, 2014].

Carpelan-Holmstrom M, Nordling S, Pukkala E, Sankila R, Lüttges J, Klöppel G, Haglund C. 2005. Does anyone survive pancreatic ductal adenocarcinoma? A nationwide study re-evaluating the data of the Finnish Cancer Registry. *Gut* 54, 385-387.

Chapman PB, Hauschild A, Robert C, Haanen JB, Ascierto P, Larkin J, Dummer R, Garbe C, Testori A, Maio M, Hogg D, Lorigan P, Lebbe C, Jouary T, Schadendorf D, Ribas A, O'Day SJ, Sosman JA, Kirkwood JM, Eggermont AM, Dreno B, Nolop K, Li J, Nelson B, Hou J, Lee RJ, Flaherty KT, McArthur GA. 2011. Improved survival with vemurafenib in melanoma with BRAF V600E mutation. *N Engl J Med* 364, 2507-16.

Cheville JC, Karnes RJ, Therneau TM, Kosari F, Munz JM, Tillmans L, Basal E, Rangel LJ, Bergstralh E, Kovtun IV, Savci-Heijink CD, Klee EW, Vasmatzis G. 2008. Gene panel model predictive of outcome in men at high-risk of systemic progression and death from prostate cancer after radical retropubic prostatectomy. *J Clin Oncol* 26, 3930-36.

Crippa S, Fernandez-Del Castillo C, Salvia R, Finklestein D, Bassi C, Dominguez I, Muzikansky A, Thayer Sp, Falconi M, Mino-Kenudson M, Capelli P, Lauwers

GY, Partelli S, Pederzoli P, Warshaw AL. 2004. Mucin-producing neoplasms of the pancreas: an analysis of distinguishing clinical and epidemiologic characteristics. *Clin Gastroenterol Hepatol* 8(2):213-219.

Cronin J, McAdam E, Danikas A, Tselepis C, Griffiths P, Baxter J, Thomas L, Manson J, Jenkins G. 2011. Epidermal growth factor receptor (EGFR) is over expressed in high-grade dysplasia and adenocarcinoma of the esophagus and may represent a biomarker of histological progression in Barrett's esophagus (BE). *Am J Gastroenterol* 106, 1-3.

Dai W, Wang Q, Liu T, Swamy M, Fang Y, Xie S, Mahmood R, Yang YM, Xu M, Rao CV. 2004. Slippage of mitotic arrest and enhanced tumor development in mice with BubR1 haploinsufficiency. *Cancer Res* 64, 440-445.

deWilde RF, Hruban RH, Maitra A, Johan G, Offerhaus A. 2012. Reporting precursors to invasive pancreatic cancer: pancreatic intraepithelial neoplasia, intraductal neoplasm and mucinous cystic neoplasm. *Diagnostic Histopathology* 18(1), 17-30.

DiGiuseppe JA, Redston MS, Yeo CJ, Kern SE, Hruban RH. 1995. p53-independent expression of the cyclin-dependent kinase inhibitor p21 in pancreatic carcinoma. *Am J Pathol* 147, 884-888.

de Wilde RF, Aust D, Weitz J, Pilarsky C, Grutzmann R. 2014. Precursor lesions for sporadic pancreatic cancer: PanIN, IPMN, and MCN. *Biomed Res Int* 2014:474905.

Doak SH, Jenkins GJS, Parry EM, Griffiths AP, Shah V, Baxter JN, Parry JM. 2003. Characterisation of the p53 status at the gene, chromosomal and protein level in oesophageal adenocarcinoma. *Br J Cancer* 89, 1729-35.

Dobles M, Liberal V, Scott ML, Benezra R, Sorger PK. 2000. Chromosome missegregation and apoptosis in mice lacking the mitotic checkpoint protein Mad2. *Cell* 101, 635-645.

Duda DG, Sunamura M, Lefter LP, Furukawa T, Yokoyama T, Yatsuoka T, Abe T, Inoue H, Motoi F, Egawa S, Matsuno S, Horii A. 2003. Restoration of SMAD4 by gene therapy reverses the invasive phenotype in pancreatic adenocarcinoma cells. *Oncogene* 22, 6857-64.

Duraiyan J, Govindarajan R, Kaliyappan K, Palanisamy M. 2012. Application of immunohistochemistry. *J Pharm Bioallied Sci* 4(2), S307-S309.

Duffy MJ, Sturgeon C, Lamerz R, Haglund C, Holubec VL, Klapdor R, Nicolini A, Topolcan O, Heinemann V. 2010. Tumor markers in pancreatic cancer: a European Group on Tumor Markers (EGTM) status report. *Ann Oncol* 21, 441-7.

Early Breast Cancer Trialists' Collaborative Group. 1998. Tamoxifen for early breast cancer: An overview of the randomized trials. *Lancet* 351, 1451-67.

Feldman G, Beaty R, Hruban R, Maitra A. 2007. Molecular genetics of pancreatic intraepithelial neoplasia. *J Hepatobiliary Pancreat Surg* 14, 224-232.

Ferlay J, Shin HR, Bray F, Forman D, Mathers C, Parkin DM. 2010. Estimates of worldwide burden of cancer in 2008: GLOBOCAN 2008. *Int J Cancer* 127(12), 2893-917.

Fleisher M, A.M. D, Sturgeon CM, Lamerz R, Witliff JL. 2002. *Tumour markers: physiology, pathobiology, technology and clinical aplications* Chicago: AACC press.

Fujii H, Inagaki M, Kasai S, Miyokawa N, Tokusashi Y, Gabrielson E, Hruban RH. 1997. Genetic progression and heterogeneity in intraductal papillary-mucinous neoplasms of the pancreas. *Am J Pathol* 151, 1447-54.

Ghadimi BM, Schröck E, Walker RL, Wangsa D, Jauho A, Meltzer PS, Reid T. 1999. Specific chromosomal aberrations and amplification of the AIB1 nuclear receptor coactivator gene in pancreatic carcinomas. *Am J Pathol* 154(2), 525-536.

Gaujoux S, Brennan MF, Gonen M, D'Angelica MI, DeMatteo R, Fong Y, Schattner M, DiMaio C, Janakos M, Jarnagin WR, Allen PJ. 2011. Cystic lesions of the pancreas: changes in the presentation and management of 1,424 patients at a single institution over a 15-year time period. *J Am Coll Surg* 212, 590-600; discussion 600-603.

Gemma A, Seike M, Seike Y, Uematsu K, Hibino S, Kurimoto F, Yoshimura A, Shibuya M, Harris CC, Kudoh S. 2000. Somatic mutation of the hBUB1 mitotic checkpoint gene in primary lung cancer. *Genes Chromosomes Cancer* 29, 213-218.

Genetics Home Reference. 2012. U.S National Library of Medicine. `http://ghr.nlm.nih.gov` [Accessed October 13, 2013]

Ghaneh P, Costello E, Neoptolemos JP. 2008. Biology and management of pancreatic cancer. *Postgrad Med J* 84, 478-497.

Gladhaug IP, Westgaard A, Schjølberg AR, Burum-Auensen E, Pomianowska E, Clausen OPF. 2001. Spindle proteins in resected pancreatic head adenocarcinomas: BubR1 is an independent prognostic factor in pancreatobiliary-type tumours. *Histopathology* 56, 345-355.

Goggins M. 2010. Development of Novel Pancreatic Tumor Biomarkers. In: Neoptolemos JP, Urrutia R, Abbruzzese J, Büchler M (eds). *Pancreatic Cancer* pp 1173-1201. New York: Springer Science Ltd.

Gorunova L. 1998. Cytogenetic analysis of pancreatic carcinomas. Intratumor heterogeneity and nonrandom pattern of chromosome aberrations. *Genes Chromosomes Cancer* 23(2), 81-99.

Griffin C, Hruban R, Morsberger L, Ellingham T, Long PL, Jaffee EM, Hauda KM, Bohlander SK, Yeo CJ. 1995. Consistent chromosomal abnormalities in adenocarcinoma of the pancreas. *Cancer Research* 55, 2394-99.

Griffin CA, Morsberger L, Hawkins AL, Haddadin M, Patel A, Ried T, Schrock E, Perlman EJ, Jaffee E. 2007. Molecular cytogenetic characterization of pancreas cancer cell lines reveals high complexity chromosomal alterations. *Cytogenet Genome Rev* 118(2-4), 148-56.

Guerra C, Schumacher A, Canamero M, Grippo P, Verdaguer L, Perez-Gallego L, Dubus P, Sandgren E, Barbacid M. 2007. Chronic pancreatitis is essential for induction of pancreatic ductal adenocarcinoma by K-Ras oncogene in adult mice. *Cancer Cell* 11(3), 291-302.

Habermann JK, Auer G, Ried T, Roblick UJ. 2012. Ulcerative colitis and colorectal cancer: aneuploidy and implications for improved screening. In: Prof. Mustafa Shennak (ed.). *Ulcerative colitis from genetics to complications*spp 111-125, InTech, Available from: http://www.intechopen.com/books/ulcerative-colitis-from-genetics-to-complications/ulcerative-colitis-and-colorectal-cancer-aneuploidy-and-implications-for-improved-screening [Accessed January 3, 2015]

Hahn SA, Seymour AB, Hoque ATMS, Schutte M, da Costa LT, Redston MS, Caldas C, Weinstein CL, Fischer A, Yeo CJ, Hruban RH, Kern SE. 1995. Allelotype of pancreatic adenocarcinoma using xenograft enrichment. *Cancer Res* 55, 4670-75.

Hahn SA, Kern SE. 1995. Molecular genetics of exocrine pancreatic neoplasms. *Surg Clin North Am* 75, 857-869.

Hahn SA, Schutte M, Hoque AT, Moskaluk CA, da Costa LT, Rozenblum E, Weinstein CL, Fischer A, Yeo CJ, Hruban RH, Kern SE. 1996. DPC4, a candidate tumour suppressor gene at human chromosome 18q21.1. *Science* 271, 350-353.

Halling K, Kipp B. 2007. Fluorescence in situ hybridization in diagnostic cytology. *Human Pathology* 38, 1137-44.

Hernando E, Orlow I, Liberal V, Nohales G, Benezra R, Cordon-Cardo C. 2001. Molecular analyses of the mitotic checkpoint components hsMAD2, hBUB1 and hBUB3 in human cancer. *Int J Cancer* 95, 223-227.

Hezel A, Kimmelman AC, Stanger BZ, Bardeesy N, DePinho RA. 2006. Genetics and biology of pancreatic ductal adenocarcinoma. *Genes & development* 20, 1218-49.

Hilgers W, Tang DJ, Sugar AY, Shekher MC, Hruban RH, Kern SE. 1999. High-resolution deletion mapping of chromosome arm 1p in pancreatic cancer identifies a major consensus region at 1p35. *Genes Chromosomes Cancer* 24(4), 351-355.

Hingorani SR, Wang L, Multani AS, Combs C, Deramaudt TB, Hruban RH, Rustgi AK, Chang S, Tuveson DA. 2005. Trp53R172H and KrasG12D cooperate to promote chromosomal instability and widely metastatic pancreatic ductal adenocarcinoma in mice. *Cancer Cell* 7, 469-83.

Hruban RH, Goggins M, Parsons J, Kern SE. 2000. Progression model for pancreatic cancer. *Clin Cancer Res* 6, 2969-72.

Hruban RH, Takaori K, Klimstra DS, Adsay NV, Albores-Saavedra J, Biankin AV, Biankin SA, Compton C, Fukushima N, Furukawa T, Goggins M, Kato Y, Klöppel G, Longnecker DS, Lüttges J, Maitra A, Offerhaus GJ, Shimizu M, Yonezawa S. 2004. An illustrated consensus on the classification of pancreatic intra-epithelial neoplasia and intraductal papillary mucinous neoplasms. *Am J Surg Pathol* 28, 977-987.

Iacobuzio-Donahue CA. 2012. Genetic evolution of pancreatic cancer: lessons learnt from the pancreatic cancer genome sequencing project. *Gut* 61, 1085-94.

Iacobuzio-Donahue CA. 2012. Personalized medicine in pancreatic cancer: prognosis and potential implications for therapy. *J Gastrointest Surg* 16(9), 1651-2.

Iwanaga Y, Chi YH, Miyazato A, Sheleg S, Haller K, Peloponese Jr. JM, Li Y, Ward JM, Benezra R, Jeang KT. 2007. Heterozygous deletion of mitotic arrest-deficient protein 1 (MAD1) increases the incidence of tumors in mice. *Cancer Res* 67, 160-166.

Jallepalli P, Lengauer C. 2001. Chromosome segregation and cancer: cutting through the mystery. *Nature reviews* 1, 109-117.

Jamieson NB, Ross Carter C, McKay CJ, Oien KA. 2011. Tissue biomarkers for prognosis in pancreatic ductal adenocarcinoma: a systematic review and meta-analysis. *Clin Cancer Res* 17, 3316-31.

Jeganathan K, Malureanu L, Baker DJ, Abraham SC, van Deursen JM. 2007. Bub1 mediates cell death in response to chromosome missegregation and acts to suppress spontaneous tumorigenesis. *J Cell Biol* 179, 255-267.

Jover R, Zapater P, Castells A, Llor X, Andreu M, Cubiella J, Balaguer F, Sempere L, Xicola RM, Bujanda L, Reñé JM, Clofent J, Bessa X, Morillas JD, Nicolás-Pérez D, Pons E, Payá A, Alenda C. 2009. The efficacy of adjuvant chemotherapy with 5-fluorouracil in colorectal cancer depends on the mismatch repair status. *Eur J Cancer* 45, 365-373.

Kalitsis P, Earle E, Fowler KJ, Choo KH. 2000. Bub3gene disruption in mice reveals essential mitotic spindle checkpoint function during early embryogenesis. *Genes Dev* 14, 2277-82.

Kanda M, Matthaei H, Wu J, Hong SM, Yu J, Borges M, Hruban RH, Maitra A, Kinzler K, Vogelstein B, Goggins M. 2012. Presence of somatic mutations in most early-stage pancreatic intraepithelial neoplasia. *Gastroenterology* 142(4):730-733.

Kayed H, Kleeff J, Osman T, Keleg S, Büchler MW, Friess H. 2006. Hedgehog signalling in the normal and diseased pancreas. *Pancreas* 32, 119-29.

Kipp BR, Stadheim LM, Halling SA, Pochron NL, Harmsen S, Nagorney DM, Sebo TJ, Therneau TM, Gores GJ, de Groen PC, Baron TH, Levy MJ, Halling KC, Roberts LR. 2004. A comparison of routine cytology and fluorescence in situ hybridization for the detection of malignant bile duct strictures. *Am J Gastroenterol* 99(9), 1675-81.

Koostra JBM, Feldman G, Habbe N, Maitra A. 2008. Morphogenesis of pancreatic cancer: role of pancreatic intraepithelial neoplasia (PanINs). *Langenbeck's Archives of Surgery* 393(4), 561-70.

Lampson MA, Kapoor TM. 2004. The human mitotic checkpoint protein BubR1 regulates chromosome-spindle attachments. *Nature Cell Biology* 7, 93-98.

Leach SD. 2005. Epithelial differentiation in pancreatic development and neoplasia: new niches for nestin and Notch. *J Clin Gastroenterol* 39, S78-82.

Li C, Heidt DG, Dalerba P, Burant CF, Zhang L, Adsay V, Wicha M, Clarke MF, Simeone DM. 2007. Identification of pancreatic cancer stem cells. *Cancer Res* 67, 1030-7.

Liu H, Dibling B, Spike B, Dirlam A, Macleod K. 2004. New roles for the RB tumor suppressor protein. *Curr Opin Genet Dev* 14, 55-64.

Lomberk G, Fernández-Zapico ME, Urrutia R. 2005. When developmental signalling pathways go wrong and their impact on pancreatic cancer development. *Curr Opin Gastroenterol* 21, 555-60.

Loukopoulos P, Shibata T, Katoh H, Kokubu A, Sakamoto M, Yamazaki K, Kosuge T, Kanai Y, Hosoda F, Imoto I, Ohki M, Inazawa J, Hirohashi S. 2007. Genome-wide array-based comparative genomic hybridization analysis of pancreatic adenocarcinoma: Identification of genetic indicators that predict patient outcome. *Cancer Sci* 98, 392-400.

Mahlamaki EH, Hoglund M, Gorunova L, Karhu R, Dawiskiba S, Andren-Sandberg A, Kallioniemi OP, Johansson B. 1997. Comparative genomic hybridization reveals frequent gains of 20q, 8q, 11q, 12p, and 17q, and losses of 18q, 9p, and 15q in pancreatic cancer. *Genes Chromosomes Cancer* 20, 383-391.

Maitra A, Adsa NV, Argani P, Iacobuzio-Donahue C, De Marzo A, Cameron J, Yeo C, Hruban R. 2003. Multicomponent analysis of the pancreatic adenocarcinoma progression model using a pancreatic intraepithelial intraepithelial neoplasia tissue microarray. *Modern Pathology* 16(9), 902-12.

Malumbres M, Barbacid M. 2003. RAS oncogenes: the first 30 years. *Nat Rev Cancer* 3, 459-65.

Mauro LA, Herman JM, Jaffee EM, Laheru DA. 2014. Carcinoma of the pancreas. [Online] In: Niederhuber JE, Armitage JO, Doroshow JH, Kastan MB, Tepper JE. *Abeloff's Clinical Oncology* [5th Ed] 459-65. Philadelphia: Saunders, Elsevier Inc.

Martinez-Climent JA, Alizadeh AA, Seagraves R, Blesa D, Rubio-Moscardo F, Albertson DG, Garcia-Conde J, Dyer MJS, Levy R, Pinkel D, Lossos IS. 2003. Transformation of follicular lymphoma to diffuse large cell lymphoma is associated with a heterogeneous set of DNA copy number and gene expression alterations. *Blood* 101, 3109-17.

Michel LS, Liberal V, Chatterjee A, Kirchwegger R, Pasche B, Gerald W, Dobles M, Sorger PK, Murty VV, Benezra R. 2001. MAD2 haplo-insufficiency causes premature anaphase and chromosome instability in mammalian cells. MAD2 haploinsufficiency causes premature anaphase and chromosome instability in mammalian cells. *Nature* 409, 355-359.

Miyamoto Y, Maitra A, Ghosh B, Zechner U, Argani P, Iacobuzio-Donahue CA, Sriuranpong V, Iso T, Meszoely IM, Wolfe MS, Hruban RH, Ball DW, Schmid RM, Leach SD. 2003. Notch mediates TGF alpha-induced changes in epithelial differentiation during pancreatic tumorigenesis. *Cancer Cell* 3, 565-76.

Montgomery E, Bronner MP, Goldblum JR, Greenson JK, Haber MM, Hart J, Lamps LW, Lauwers GY, Lazenby AJ, Lewin DN, Robert ME, Toledano AY, Shyr Y, Washington K. 2001. Reproducibility of the diagnosis of dysplasia in Barrett's esophagus: a reaffirmation. *Hum Pathol* 32, 368-378.

Moreno Luna LE, Kipp B, Halling KC, Sebo TJ, Kremers WK, Roberts LR, Barr Fritcher EG, Levy MJ, Gores GJ. 2006. Advanced cytology techinques for the detection of malignant pancreatobiliary strictures. *Gastroenterology* 131(4), 1064-72.

Moskaluk CA, Hruban RH, Kern SE. 1997. p16 and K-ras gene mutations in the intraductal precursors of human pancreatic adenocarcinoma. *Cancer Res* 57, 2140-43.

Musacchio A, Hardwick KG. 2002. The spindle checkpoint: Structural insights into dynamic signalling. *Nat Rev Mol Cell Biol* 3, 731-41.

National Cancer Institute. 2009. Surveillance, Epidemiology and End Results Program fact sheets: Pancreas cancer. `http://seer.cancer.gov/statfacts/html/pancreas.html` [Accessed December 13, 2013]

National Comprehensive Cancer Network. 2011. Practice Guidelines in Oncology for Pancreatic Adenocarcinoma - v.1. `http://www.nccn.org` [Accessed July 2, 2014]

Neoptolemos JP, Stocken DD, Bassi C, Ghaneh P, Cunningham D, Goldstein D, Padbury R, Moore MJ, Gallinger S, Mariette C, Wente MN, Izbicki JR, Friess H, Lerch MM, Dervenis C, Olah A, Butturini G, Doi R, Lind PA, Smith D, Valle JW, Palmer DH, Buckels JA, Thompson J, McKay CJ, Rawcliffe CL, Buchler MW; European Study Group for Pancreatic Cancer. 2010. Adjuvant chemotherapy with fluorouracil plus folinic acid vs gemcitabine following pancreatic cancer resection: a randomized controlled trial. *JAMA* 304, 1073-81.

Nolte M, Werner M, Ewig M, von Wasielewski R, Link H, Diedrich H, Georgii A. 1996. Megakaryocytes carry the fused bcr-abl gene in chronic myeloid leukaemia: a fluorescence in situ hybridization analysis from bone marrow biopsies. *Virchows Arch* 427, 561-565.

Nomoto S, Haruki N, Takahashi T, Masuda A, Koshikawa T, Fujii Y, Osada H. 1999. Identification of frequent impairment of the mitotic checkpoint and molecular analysis of the mitotic checkpoint genes, hsMAD2 and p55CDC, in human lung cancers. *Oncogene* 18(30), 4295-300.

Ottehnhof NA, de Wilde RF, Maitra A, Hruban RH, Offerhaus GJ. 2011. Molecular Characteristics of pancreatic ductal adenocarcinoma. *Patholog Res Int* 2011, article ID 620601, 16 pages

Paris PL, Andaya A, Fridlyand J, Jain AN, Weinberg V, Kowbel D, Brebner JH, Simko J, Watson VJE, Volik S, Albertson DG, Pinkel D, Alers JC, van der Kwast TH, Vissers KJ, Schroder FH, Wildhagen MF, Febbo PG, Chinnaiyan AM, Pienta KJ, Carroll PR, Rubin MA, Collins C, van Dekken H. 2004. Whole genome scanning identifies genotypes associated with recurrence and metastasis in prostate tumors. *Hum Mol Genet* 13, 1303-13.

Percy MJ, Myrie KA, Neeley CK, Azim JN, Ethier SP, Petty EM. 2000. Expression and mutational analyses of the human MAD2L1 gene in breast cancer cells. *Genes Chromosomes Cancer* 29, 356-362.

Perera D, Tilston V, Hopwood JA, Barchi M, Boot-Handford RP, Taylor SS. 2007. Bub1 maintains centromeric cohesion by activation of the spindle checkpoint. *Dev Cell* 13, 566-579.

Perez EA, Romond EH, Suman VJ, Jeong JH, Davidson NE, Geyer CE Jr, Martino S, Mamounas EP, Kaufman PA, Wolmark N. 2011. Four-year follow-up of trastuzumab plus adjuvant chemotherapy for operable human epidermal growth factor receptor 2-positive breast cancer: Joint analysis of data from NCCTG N9831 and NSABP B-31. *J Clin Oncol* 29, 3366-73.

Perry N, Broeders M, de Wolf C, Tornberg S, Holland R, Von Karsa L. 2006. European guidelines for quality assurance in breast cancer screening and diagnosis. pp 306-308, 4th ed.

Prasad NB, Biankin A, Fukushima N, Maitra A, Dhara S, Elkahloun AG, Hruban RH, Goggins M, Leach SD. 2005. Gene expression profiles in pancreatic intraepithelial neoplasia reflect the effects of Hedgehog signalling on pancreatic ductal epithelial cells. *Cancer Res* 65, 1619-26.

Qian J, Jenkins RB, Bostwick DG. 1999. Genetic and chromosomal alterations in prostatic intraepithelial neoplasia and carcinoma detected by fluorescence in situ hybridization. *Eur Urol* 35, 479-483.

Rane SG, Lee JH, Lin HM. 2006. Transforming growth factor-beta pathway: role in pancreas development and pancreatic disease. *Cytokine Growth Factor Rev* 17, 107-19.

Rao CV, Yang YM, Swamy MV, Liu T, Fang Y, Mahmood R, Jhanwar-Uniyal M, Dai W. 2005. Colonic tumorigenesis in BubR1+/- ApcMin/+ compound mutant mice

is linked to premature separation of sister chromatids and enhanced genomic instability. *Proc Natl Acad Sci USA* 102, 4365-70.

Redston MS, Caldas C, Seymour AB, Hruban RH, da Costa L, Yeo CJ, Kern SE. 1994. p53 mutations in pancreatic carcinoma and evidence of common involvement of homocopolymer tracts in DNA microdeletions. *Cancer Res* 54, 3025-33.

Rehman AO, Wang CY. 2006. Notch signalling in the regulation of tumor angiogenesis. *Trends Cell Biol* 16, 293-300.

Reid BJ, Barrett MT, Galipeau PC, Sanchez CA, Neshat K, Cowan DS, Levine DS. 1996. Barrett's oesophagus: ordering the events that lead to cancer. *Eur J Cancer Prevention* 5(2), 57-65.

Ribic CM, Sargent DJ, Moore MJ, Thibodeau SN, French AJ, Goldberg RM, Hamilton SR, Laurent-Puig P, Gryfe R, Shepherd LE, Tu D, Redston M, Gallinger S. 2003. Tumour microsatellite-instability status as a predictor of benefit from fluorouracil-based adjuvant chemotherapy for colon cancer. *N Engl J Med* 349, 247-257.

Ried T, Schröck E, Ning Y, Wienberg J. 1998. Chromosome painting: a useful art. *Hum Mol Genet* 7, 1619-26.

Riediger H, Keck T, Wellner U, zur Hausen A, Adam U, Hopt UT, Makowiec F. 2009. The lymph node ratio is the strongest prognostic factor after resection of pancreatic cancer. *J Gastrointest Surg* 13, 1337-44.

Rubio -Moscardo F, Climent J, Siebert R, Piris MA, Martín-Subero JI, Nieländer I, Garcia-Conde J, Dyer MJS, Terol MJ, Pinkel D, Martinez-Climent JA. 2005. Mantel cell lymphoma genotypes identified with CGH to BAC microarrays define a leukemic subgroup of disease and predict patient outcome. *Blood* 105, 4445-54.

Sandberg AA, Ishihara T, Miwa T, Hauschka TS. 1961. The in vivo chromosome constitution of marrow from 34 human leukemias and 60 non-leukemic controls. *Cancer Res* 21, 678-689.

Sato M, Sekido Y, Horio Y, Takahashi M, Saito H, Minna JD, Shimokata K, Hasegawa Y. 2000. Infrequent mutation of the hBUB1 and hBUBR1 genes in human lung cancer. *Jpn J Cancer Res* 91, 504-509.

Sato M, Fukushima N, Hruban RH, Goggins M. 2008. CpG island methylation profile of pancreatic intraepithelial neoplasia. *Mod Pathol* 21(3):238-244.

Schlege C. 2000. Identification of frequent chromosomal aberrations in ductal adenocarcinoma of the pancreas by comparative genomic hybridization (CGH). *J Path* 191(1), 27-32.

Schmid RM. 2013. The evasive pancreatic cancer – reasons for (still) losing the battle. Oral presentation at The 45th Annual Meeting of the European Pancreatic Club, Zurich

Schutte M, Hruban RH, Geradts J, Maynard R, Hilgers W, Rabindran SK, Moskaluk CA, Hahn SA, Schwarte-Waldhoff I, Schmiegel W, Baylin SB, Kern SE, Herman JG. 1997. Abrogation of the Rb/p16 tumour-suppressive pathway in virtually all pancreatic carcinomas. *Cancer Res* 57, 3126-30.

Schwarte-Waldhoff I, Volpert OV, Bouck NP, Sipos B, Hahn SA, Klein-Scory S, Lüttges J, Klöppel G, Graeven U, Eilert-Micus C, Hintelmann A, Schmiegel W. 2000. Smad4/DPC4-mediated tumor suppression through suppression of angiogenesis. *Proc Natl Acad Sci USA* 97, 9624-9.

Seufferlein T, Bachet JB, Van Cutsem E & Rougier P, on behalf of the European Society of Medical Oncology Guidelines Working Group. 2012. Pancreatic adenocarcinoma: ESMO-ESDO Clinical Practice Guidelines for diagnosis, treatment and follow-up. *Ann Onc* 123(S7), vii33-vii40.

Seymour AB, Hruban RH, Redston M, Caldas C, Powell SM, Kinzler KW, Yeo CJ, Kern SE. 1994. Allelotype of pancreatic adenocarcinoma. *Cancer Res* 54, 2761-64.

Shedden K, Taylor JM, Enkemann SA, Tsao MS, Yeatman TJ, Gerald WL, Eschrich S, Jurisica I, Giordano TJ, Misek DE, Chang AC, Zhu CQ, Strumpf D, Hanash S, Shepherd FA, Ding K, Seymour L, Naoki K, Pennell N, Weir B, Verhaak R, Ladd-Acosta C, Golub T, Gruidl M, Sharma A, Szoke J, Zakowski M, Rusch V, Kris M, Viale A, Motoi N, Travis W, Conley B, Seshan VE, Meyerson M, Kuick R, Dobbin KK, Lively T, Jacobson JW, Beer DG. 2008. Gene expression-based survival prediction in lung adenocarcinoma: A multi-site, blinded validation study. *Nat Med* 14, 822-827.

Shackney SE, Singh SG, Yakulis R, Smith CA, Pollice AA, Petruolo S, Waggoner A, Hartsock RJ. 1995. Aneuploidy in breast cancer: A fluorescence in situ hybridization study. *Cytometry (Communications in Clinical Cytometry)* 22, 282-291.

Sherr CJ. 2004. Principles of tumor suppression. *Cell* 116, 235-46.

Shi C, Hruban RH. 2012. Intraductal papillary mucinous neoplasm. *Hum Pathol* 43(1):1-16.

Shin HJ, Baek KH, Jeon AH, Park MT, Lee SJ, Kang CM, Lee HS, Yoo SH, Chung DH, Sung YC, McKeon F, Lee CW. 2003. Dual roles of human BubR1, a mitotic checkpoint kinase, in the monitoring of chromosomal instability. *Cancer Cell* 4, 483-497.

Silk AD, Zasadil LM, Holland AJ, Vitre B, Cleveland DW, Weaver BA. 2013. Chromosome missegregation rate predicts whether aneuploidy will promote or suppress tumours. *Proc Natl Acad Sci USA* 110(44), E4134-E4141.

Sipos B, Frank S, Gress T, Hahn S, Klöppel G. 2009. Pancreatic intraepithelial neoplasia – revisited and updated. *Pancreatology* 9, 45-54.

Skoulidis F, Cassidy LD, Pisupati V, Jonasson JG, Bjarnason H, Eyfjord JE, Karreth FA, Lim M, Barber LM, Clatworthy SA, Davies SE, Olive KP, Tuveson DA, Venkitaraman AR. 2010. Germline Brca2 heterozygosity promotes Kras(G12D)-driven carcinogenesis in a murine model of familial pancreatic cancer. *Cancer Cell* 18, 499-509.

Sotillo R, Hernando E, Diaz-Rodriguez E, Teruya-Feldstein J, Cordon-Cardo C, Lowe SW, Benezra R. 2007. Mad2 overexpression promotes aneuploidy and tumorigenesis in mice. *Cancer Cell* 11, 9-23.

Speicher MR, Carter NP. 2005. The new cytogenetics: blurring the boundaries with molecular biology. *Nat Rev Genet* 6, 782-792.

Steinberg W. 1990. The clinical utility of the CA 19-9 tumor associated antigen. *Am J Gastroenterol* 85, 350-5.

Sugio K, Molberg K, Albores-Saavedra J, Virmani AK, Kishimoto Y, Gazdar AF. 1997. K-ras mutations and allelic loss at 5q and 18q in the development of human pancreatic cancers. *Int J Pancreatol* 21, 205-217.

Tanaka M, Fernandez-del Castillo C, Adsay V, Chari S, Falconi M, Jang, J, Kimura W, Levy P, Bishop Pitman M, Schmidt CM, Shiizu M, Wolfgang CL, Yamaguchi K, Yamao K. 2012. International consensus guidelines 2012 for the management of IPMN and MCN of the pancreas. *Pancreatology* 12:183-197.

Tang Y-C, Williams BR, Siegel JJ, Amon A. 2011. Identification of aneuploidy-selective antiproliferation compounds. *Cell* 144(4), 499-512.

Thayer SP, di Magliano MP, Heiser PW, Nielsen CM, Roberts DJ, Lauwers GY, Qi YP, Gysin S, Fernández-del Castillo C, Yajnik V, Antoniu B, McMahon M, Warshaw AL, Hebrok M. 2003. Hedgehog is an early and late mediator of pancreatic cancer tumorigenesis. *Nature* 425, 851-6.

The Royal College of Physicians and Royal College of Radiologists. 2013. Evidence-based indications for the use of PET-CT in the UK. London: RCP, RCR.

Thompson S, Bakhoum S, Compton D. 2010. Mechanisms of chromosomal instability. *Curr Biol* 20, 285-295.

Van Cutsem E, Köhne CH, Hitre E, Zaluski J, Chang Chien CR, Makhson A, D'Haens G, Pintér T, Lim R, Bodoky G, Roh JK, Folprecht G, Ruff P, Stroh C, Tejpar S, Schlichting M, Nippgen J, Rougier P. 2009. Cetuximab and chemotherapy as initial therapy for metastatic colorectal cancer. *N Engl J Med* 360, 1408-17.

Van Laethem JL, Verslype C, Iovanna JL, Michl P, Conroy T, Louvet C, Hammel P, Mitry E, Ducreux M, Maraculla T, Uhl W, Van Tienhoven G, Bachet JB, Maréchal R, Hendlisz A, Bali M, Demetter P, Ulrich F, Aust D, Luttges J, Peeters M, Mauer M, Roth A, Neoptolemos JP, Lutz M. 2012. New strategies and designs in pancreatic cancer research: consensus guidelines report from an European expert panel. *Ann Onc* 23(3), 570-576.

Varetti G, Musacchion A. 2008. The spindle assembly checkpoint. *Curr Biol* 18(14), R591-595.

Vogelstein B, Lane D, Levine AJ. 2000. Surfing the p53 network. *Nature* 408, 307-310.

Von Hoff DD, Stephenson JJ Jr, Rosen P, Loesch DM, Borad MJ, Anthony S, Jameson G, Brown S, Cantafio N, Richards DA, Fitch TR, Wasserman E, Fernández C, Green S, Sutherland W, Bittner M, Alarcon A, Mallery D, Penny R. 2010. Pilot study using molecular profiling of patients' tumors to find potential targets and select treatments for their refractory cancers. *J Clin Oncol* 28(33), 4877-83.

Weaver BA, Cleveland DW. 2006. Does aneuploidy cause cancer? *Curr Opin Cell Biol* 18, 658-667.

Weaver BA, Silk AD, Montagna C, Verdier-Pinard P, Cleveland DW. 2007. Aneuploidy acts both oncogenically and as a tumor suppressor. *Cancer Cell* 11, 25-36.

Weiss MM., Kuipers EJ, Postma C, Snijders AM, Pinkel D, Meuwissen SGM, Albertson D, Meijer GA. 2004. Genomic alterations in primary gastric adenocarcinomas correlate with clinicopathological characteristics and survival. *Cell Oncol* 26, 307-317.

Wilentz RE, Geradts J, Maynard R, Offerhaus GJ, Kang M, Goggins M, Yeo CJ, Kern SE, Hruban RH.1998. Inactivation of the p16 (INK4A) tumor-suppressor gene in pancreatic duct lesions: loss of intranuclear expression. *Cancer Res* 58(20):4740-4744.

Wilentz RE, Iacobuzio-Donahue CA, Argani P, McCarthy DM, Parsons JL, Yeo CJ, Kern SE, Hruban RH. 2000. Loss of expression of Dpc4 in pancreatic intraepithelial neoplasia: evidence that Dpc4 inactivation occurs late in neoplastic progression. *Cancer Res* 60, 2002-26.

Williams L, Jenkins GJ, Doak SH, Fowler P, Parry EM, Brown TH, Griffiths AP, Williams JG, Parry JM. 2005. Fluorescence In Situ Hybridisation (FISH) analysis of chromosomal aberrations in gastric tissue: the involvement of Helicobacter pylori. *Br J Cancer* 92, 1759-66.

Williams L, Somasekar A, Davies DJ, Cronin J, Doak SH, Alcolado R, Williams JG, Griffiths AP, Baxter JN, Jenkins GJ. 2009. Aneuploidy involving chromosome 1 may be an early predictive marker of intestinal type gastric cancer. *Mutat Res* 669, 104-111.

Williams NA, Bulstrode C, O'Connell PR Ed. 2013. *Bailey & Love Short Practice of Surgery* (26th Ed):1128-29, Abdingdon: CRC Press, Tayloy and Francis Ltd.

Winter JM, Cameron JL, Campbell KA, Arnold MA, Chang DC, Coleman J, Hodgin MB, Sauter PK, Hruban RH, Riall TS, Schulick RD, Choti MA, Lillemoe KD, Yeo CJ. 2006. 1423 pancreaticoduodenectomies for pancreatic cancer: a single-institution experience. *J Gastrointest Surg* 10, 1199-1210;discussion 1210-11.

Wolfgang CL, Herman JM, Laheru DA, Klein AP, Erdek MA, Fishman EK, Hruban RH. 2013. Recent progress in pancreatic cancer. *CA Cancer J Clin* 63, 318-348.

Wu C, Chi C, Huang T. 2004. Elevated level of spindle checkprotein MAD2 correlates with cellular mitotic arrest, but not with aneuploidy and clinicopathological characteristics in gastric cancer. *World J Gastro* 10(22), 3240-44.

Yachida S, Jones S, Bozic I, Antal T, Leary R, Fu B, Kamiyama M, Hruban RH, Eshleman JR, Nowak MA, Velculescu VE, Kinzler KW, Volgelstein B, Iacobuzio-Donahue CA. 2010. Distant metastasis occurs late during the genetic evolution of pancreatic cancer. *Nature* 467, 1114-17.

Yamaguchi H, Shimizu M, Ban S, Koyama I, Hatori T, Fujita I, Yamamoto M, Kawamura S, Kobayashi M, Ishida K, Morikawa T, Motoi F, Unno M, Kanno A, Satoh K, Shimosegawa T, Orikasa H, Watanabe T, Nishimura K, Ebihara Y, Koike N, Furukawa T.2009. Intraductal tubulopapillary neoplasms of the pancreas distinct from pancreatic intraepithelial neoplasia and intraductal papillary mucinous neoplasms. *Am J Surg Pathol* 33(8):1164-1172.

Yamano M, Fujii H, Takagaki T, Kadowaki N, Watanabe H, Shirai T. 2000. Genetic progression and divergence in pancreatic carcinoma. *Am J Pathol* 156(6), 2123-33.

Yu H. 2002. Regulation of APC-Cdc20 by the spindle checkpoint. *Curr Opin Cell Biol* 14, 706-14.

Yu H. 2006. Structural activation of Mad2 in the mitotic spindle checkpoint: the two-state Mad2 model versus the Mad2 template model. *J Cell Biol* 173(2), 153-157.

Yu J, Li A, Hong SM, Hruban RH, Goggins M. 2012. MicroRNA alterations of pancreatic intraepithelial neoplasias. *Clin Cancer Res* 18(4):981-992.

Yuen , Karen Wing Yee. 2010. Chromosome instability (CIN), aneuploidy and cancer. Encyclopedia of Life Sciences, Chichester: John Wiley & Sons Ltd.

Zamboni G, Fukushima N, Hruban RH, Klimstra DS, Adsay NV, Furukawa H. 2010. Mucinous cystic neoplasms of the pancreas. In: Bosman FT, Carneiro F, Hruban RH, Theise N (eds).*WHO Classification of tumours of the digestive system. World Health Organisation Classification of tumours* IARC, Lyon, pp 300-303.